

# California Climate Risk: Evaluation of Climate Risks for California Department of Water Resources

A Collaborative Study of the Hydrosystems Research Group, University of  
Massachusetts, Amherst, and the California Department of Water Resources  
Division of Integrated Water Management

Inception Report

7 February 2017

# Contents

---

Executive Summary.....	viii
Introduction .....	1
Climate Change in California.....	1
Observed Trends.....	2
Projections.....	5
Atmospheric Rivers.....	7
Drought.....	7
Previous Studies.....	8
Relevant Studies Conducted to Date.....	8
Studies and Other Efforts in Progress as of December 2015.....	9
Academic studies of climate change impact on the water resources of California.....	9
Methodology .....	11
Description of Study Area.....	13
Description of Weather Generator.....	15
Development of New Climatological Sequences.....	16
Application of Climate Shifts.....	18
Details on Approach to Climate Change Factors.....	19
Description of SAC SMA Hydrologic Model.....	21
Hamon Evapotranspiration Calculation.....	22
In-grid Routing: Nash-Cascade Unit Hydrograph.....	22
River Channel Routing: Linearized Saint-Venant Equation.....	23
Water Resources System Model.....	23
Generation of Inputs to CalLite.....	24
Model Verification.....	34
Weather Generator Performance.....	34
Hydrologic Model Performance.....	36
System Model Performance.....	37
Risk Assessment Results.....	39
Exposure.....	39
Sensitivity.....	40
Vulnerability and Risk.....	40
Performance Metric 1: Oroville Storage.....	42

Performance Metric 2: Net Delta Outflow .....	46
Performance Metric 3: Annual SWP Deliveries .....	52
Performance Metric 8: Annual SWP Delivery Shortages.....	54
Summary .....	56
Other Considerations and Next Steps.....	57
References .....	58
Appendix.....	64

## Figures

Figure 1. Trend in annual mean temperature for the region contributing flow to the California Department of Water Resources system, 1915-2011. ....	2
Figure 2. Monthly trends in annual mean temperature for the region contributing flow to the DWR system, 1915-2011. ....	3
Figure 3. Trend in annual mean precipitation for the region contributing flow to the DWR system, 1915-2011. ....	4
Figure 4. Monthly trend in annual mean precipitation for the region contributing flow to the DWR system, 1915-2011. ....	4
Figure 5. Precipitation in the Shasta watershed 1915-2011 from <i>Livneh et al.</i> [2013]. ....	5
Figure 6. Mid-Century Conditional Climate Probability Density. Cyan dots represent GCMs run with RCP 8.5; yellow dots represent GCMs runs with RCP 6.0; turquoise dots represent GCMs run with RCP 4.5; Green dots represent GCMs runs with RCP 2.5. ....	6
Figure 7. Modeling Workflow for Climate Change Vulnerability Assessment. ....	12
Figure 8. California Central Valley System and Rim Sub-basins. Table inset shows the percent contribution of each river to the total delta outflow. Fifteen percent of the total delta outflow is contributed by unshaded areas within the red outline. ....	13
Figure 9. State, Federal, and Local water infrastructure from the California Water Plan [2013] Volume 3, pg 7-6. ....	15
Figure 10. Wavelet power spectrum for average annual precipitation for the Central Valley catchment (1950-2003). ....	17
Figure 11. Exploration of differential rate of change in precipitation (left) and temperature (right) between early-mid-20 <sup>th</sup> century (1920-1960) and the end of the 20 <sup>th</sup> century (1980-2011). Hollow triangles show changes in high-elevation (>2000 m) grid cells of the <i>Maurer et al.</i> [2002] dataset, and solid dots show changes in low-elevation (<2000 m) grid cells. ....	19
Figure 12. CMIP5 Projected temperature change: 1971-2000 vs 2036-2065. ....	20
Figure 13. CMIP5 Projected precipitation change: 1971-2000 vs 2036-2065. ....	20
Figure 14. Schematic of distributed hydrologic model. ....	22
Figure 15. CalLite schematic. ....	24
Figure 16. Maps of three calibration sets for the application of SAC-SMA-DS to the CVS. ....	26
Figure 17. Pearson correlation coefficients of two historical local inflows (I_BRANANIS and I_MDOTA) with historical 12 rim inflows. ....	28
Figure 18. Quantile mapping procedure applied to example California sub-basin. ....	30
Figure 19. Input variables with strong correlation to San Joaquin Water Year Type classification-historical observed data shown. ....	31
Figure 20. AD_Wilkins: Correlation with Shasta flow. ....	32
Figure 21. AD_SACAME historical behavior. ....	33
Figure 22. Estimates of Sea Level Rise by Degree C. ....	34
Figure 23. Performance of WARM Weather Generator WARM – Annual Precipitation. ....	35
Figure 24. Validation of CalLite stress test modeling workflow for Total North of Delta Storage. Top: Scatterplot fit of annual averaged validation trace values to default trace values. Bottom: Default (blue) and validation (red) trace monthly Total North of Delta Storage showing perfect fit before 1950 and differences after 1950. ....	37

Figure 25. Validation of CalLite stress test modeling workflow for Delta Outflow. Top: Scatterplot fit of annual averaged validation trace values to default trace values. Bottom: Default (blue) and validation (red) trace monthly Delta Outflow showing perfect fit before 1950 and differences after 1950..... 38

Figure 26. Validation of CalLite stress test modeling workflow for SWP Annual Deliveries. Top: Scatterplot fit of annual averaged validation trace values to default trace values. Bottom: Default (blue) and validation (red) trace monthly SWP deliveries showing perfect fit before 1950 and differences after 1950. .... 39

Figure 27. Response Surface – April 1<sup>st</sup> Oroville Storage..... 42

Figure 28. Response Surface – April 1<sup>st</sup> Oroville Storage, with GCM “cloud” ..... 43

Figure 29. Shift in April 1<sup>st</sup> Oroville storage, Current to Mid-Century Conditions ..... 44

Figure 30. Response Surface – September 1<sup>st</sup> Oroville Storage without (left) and with (right) GCM “cloud” ... 45

Figure 31. Shift in September 1<sup>st</sup> Oroville Storage, Current to Mid-Century Conditions..... 46

Figure 32. Response Surfaces –Net Delta Outflow ..... 47

Figure 33. Response Surfaces –Net Delta Outflow with GCM “cloud” ..... 48

Figure 34. Shift in Winter Net Delta Outflow, Current to Mid-Century Conditions..... 49

Figure 35. Shift in Spring Net Delta Outflow, Current to Mid-Century Conditions..... 50

Figure 36. Shift in Summer Net Delta Outflow, Current to Mid-Century Conditions ..... 51

Figure 37. Shift in Fall Net Delta Outflow, Current to Mid-Century Conditions ..... 52

Figure 38. Response Surface – Annual SWP Deliveries without (left) and with (right) GCM “cloud” ..... 53

Figure 39. Shift in SWP Annual Deliveries, Current to Mid-Century Conditions..... 54

Figure 40. Response Surface – Annual SWP Delivery Shortage without (left) and with (right) GCM “cloud” .... 55

Figure 41. Shift in Annual SWP Delivery Shortage, Current to Mid-Century Conditions..... 56

Figure 42. CDF of annual streamflow of a subsample of wavelet (WARM) and non-wavelet (ARMA) weather-generated traces (no temp/precip change) relative to observed historical and paleo record cdfs..... 64

Figure 43. CDF of annual streamflow of a subsample of all weather-generated traces (no temp/precip change) relative to observed historical and paleo record cdfs ..... 65

## Tables

Table 1. Decision relevant metrics.....	12
Table 2. Hydrologic Sequences with 15 Year Wavelet Signal .....	17
Table 3. Range of Temperature and Precipitation Changes Explored .....	18
Table 4. Twelve Major Rim Inflows to the CalLite Model .....	25
Table 5. R Squared Correlations for 31 most important inputs.....	27
Table 6. Pairs of rim flows and local inflows determined by correlation. Blue bold text in parentheses represent the values of Pearson’s correlation coefficient and red bold text represent contribution of local inflows to the total system inflows.....	29
Table 7. Sea Level Rise Discretization within CalLite 3.0 .....	34
Table 8. Statistics of the 12 WARM Weather Generator Runs Selected for Drought Characteristics .....	36
Table 9. Hydrologic model performance by sub-basin .....	36
Table 10. Conditional Climate Probability Density of each Climate Change Shift, 1970-2000 to 2035-2065 ....	40

## Abbreviations

AD	accretion/depletion parameters within CalLite
ARMA	auto-regressive moving average model
WARM	Wavelet ARMA model
CalLite	a simplified, faster version of CalSim
CalSim	the DWR and USBR California water resources simulation model
CALVIN	CALifornia Value Integrated Network, a hydro-economic optimization model of California's statewide water supply system
cdf	cumulative distribution function
CMIP	Coupled Model Intercomparison Project
CVP	Central Valley Project
CVS	California Central Valley System
CWP	California Water Plan
DWR	California Department of Water Resources
ENSO	El Niño Southern Oscillation
GCM	General Circulation Model
IPCC	Intergovernmental Panel on Climate Change
MAF	million acre-feet
NOAA	National Oceanic and Atmospheric Administration
NWS	National Weather Service
pdf	probability density function
PDO	Pacific Decadal Oscillation
RCP	Representative Concentration Pathways
SAC-SMA-DS	a distributed version of the Sacramento Soil Moisture Accounting hydrologic model
SWE	Soil water equivalent
SWP	State Water Project
USBR	United States Bureau of Reclamation
WRIMS	Water Resource Integrated Modeling System

## Executive Summary

---

This Inception Report introduces a joint endeavor of the California Department of Water Resources (DWR) and the University of Massachusetts, Amherst (UMass), to improve planning for the uncertain effects of climate change on DWR's system by integrating vulnerability-based analysis with traditional risk-based assessment methods. This report summarizes progress made during approximately two years of informal partnership during which the team defined research goals, established an experimental approach, developed and validated a workflow of modeling tools, tried and abandoned a number of alternative experimental designs, refined the strategy for data visualization, and produced preliminary assessments of the vulnerability of the DWR water system to climate change.

The report begins with a review of historical and projected climate change in California, which includes description of a number of explorations by the DWR-UMass team into climate trends and projections within the California Central Valley System (CVS), specifically. The next section of the report summarizes previous work accomplished by the academic community, the government, and the community of water resources practitioners evaluating climate change related risks to the DWR system.

With that background in place, the report moves to an explanation of the methodology developed for this study (illustrated in Figure ES1), and provides details on each sub-step of the process. It is explained that, whereas these previous studies have tested the response of some aspect of the California water system to climate traces different from the historical, the decision scaling approach adopted for this study allows systematic assessment of the vulnerability of the entire (interconnected and complex) DWR water system to a wide range of potential future climate conditions, and quantification of the significance of climate shift relative to natural (and climate-change-amplified) variability. The climate response function that results from the decision scaling approach identifies the range of climate changes within which the performance of the system is acceptable, and the critical amount of climate change beyond which violations of water system performance will occur. An important benefit of this approach is the ability to assign formal probability estimates to the vulnerability space, which allows discussion of risk and opportunity (each a function of impact and likelihood) in water system investment.

DWR's vulnerability assessment for long-term and persistent hydrologic impacts of climate change focuses on impacts to the operation of the State Water Project (SWP), including ecological conditions that dictate operating rules. DWR owns and operates the SWP for flood control, maintenance of environmental and water quality conditions, water supply, hydropower, and recreation. Thus, analysis of SWP performance under climate changed conditions yields an array of impact metrics across all of these areas of concern.

This study has adopted CalLite 3.0, a simplified, faster version of the water system model used by DWR (CalSim-II), to simulate the coordinated operations of the Central Valley Project (CVP) and SWP under a wide range of climate possibilities. This study uses a weather generator to develop time series of plausible alternative precipitation and temperature, which are then sampled systematically in order to explore a wide range of climate change characteristics. An advanced hydrologic model (in this case SAC-SMA-DS) translates descriptors of fundamental meteorological drought into measures of available water at Earth's surface. The estimates of available water from the hydrologic model become the key inputs to a water system model (CalLite 3.0), which simulates the complex interactions of water supply, water demand, regulatory compliance, and operational choices and produces measures of water system performance such as water deliveries, reservoir storage, and river flow volume. In the case of CalLite 3.0, a number of additional inputs, beyond river flows that could not be directly provided by the hydrologic model, are required. This

requirement necessitated an additional pre-processing routine (quantile mapping and water year typing) that involves incorporation of anthropogenic co-factors in the operation of water system infrastructure.

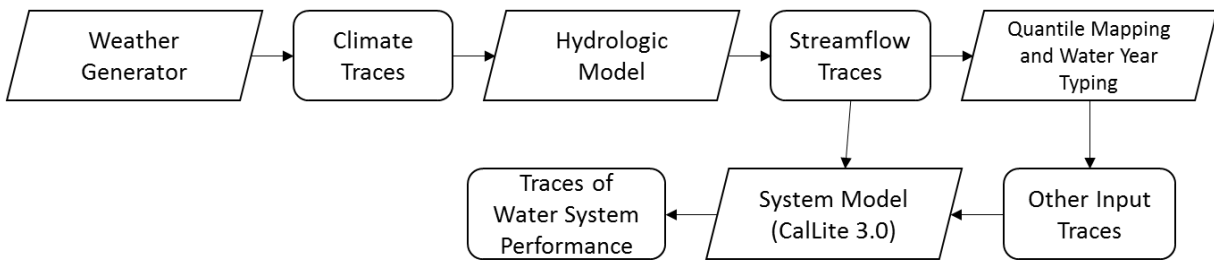


**Figure ES1. Modeling Workflow for Climate Change Vulnerability Assessment**

When simulated repeatedly, the resulting workflow (Figure ES1) allows the exploration of climate change impact in response to a wide range of meteorological input. Table ES1 lists the decision-relevant metrics used for the DWR climate vulnerability assessment.

Table ES1. Decision relevant metrics

1	Oroville Storage levels
	April 1 <sup>st</sup>
	September 1 <sup>st</sup>
2	Net Delta Outflow
	Winter
	Spring
	Summer
	Fall
3	SWP Deliveries
	Average Annual
4	System Shortages
	Average Annual

Despite a wide range of uncertainty, results of the analysis clearly show that the majority of the conditional climate probability density indicates a downward shift in mid-century system performance. By 2050, the majority of climate outcomes that might reasonably be expected lead to decreased system performance in each of the Table ES1 metrics. Only a small portion of the conditional climate probability density for each performance metric indicates improved system performance (performance better than historical). This situation is especially acute for average Oroville September storage, SWP deliveries, and spring net delta outflows, in which substantial downward shifts are identified.

The analysis shown here suggests that it is reasonable to expect that the performance of the SWP will diminish over the coming decades if nothing is done to adapt to climate change. However, there are opportunities for improved climate change planning. At the next stage of this project, refinements will be made to the methodology presented in this Inception Report, and the potential benefit of a sample of proposed DWR climate change adaptation strategies will be systematically evaluated.

## Introduction

---

Developing adaptation plans to address future climate changes is hindered by the uncertainty associated with the magnitude and character of those changes. Vulnerability-based assessments are promising for identifying where climate uncertainties are most problematic but can yield a litany of vulnerabilities with little means for prioritizing action or justifying the expenses required to address them. Given the financial constraints of the typical government water agency or municipality, vulnerabilities with unknown probabilities of their occurrence are weak priorities and long term preparedness to climate change falls prey to the pressing concerns of the present.

The goal of this project is to improve planning for the uncertain effects of climate change by integrating vulnerability-based analysis with traditional risk-based assessment methods. Risk-based approaches are typical for engineering water resources but are problematic under climate change due to their dependence on estimating probability distributions of possible climate futures. The process adopted here preserves the risk-based planning framework but reserves estimation of probabilities until the assessment of adaptation alternatives, where the consequences of any assumption are quickly realized in terms of impacts on decisions.

Water managers struggle to prioritize responses to the predicted hazards of climate change due to the uncertainty associated with projections of those hazards. This struggle is not without cause. At present decision makers face an unsavory choice relying on trusted traditional approaches that rely on statistics of the past, and thus may be ill-suited for the future, or adopting uncertain projections of the future that are known to have least skill for the most critical design variables [Hirsch, 2011]. The prevailing wisdom of “no regrets” approaches that is offered in response to this dilemma [c.f., IPCC, 2012] is hardly a rallying cry for increasing long-term preparedness to climate change.

This effort is designed to address this challenge directly. The methodology enables planning for future changes that is *informed* by the best available science on climate change while not dependent on precise prediction of future values. Instead, the process focuses on incorporating credible information on future changes within traditional risk-based planning approaches and through merging historical trends with future expectations. Those effects are delineated through a “climate stress test”, which is independent of projections of future climate. Where the effects are significant compared to other factors, the concern associated with the possible occurrence of those effects is described in accordance with the best available climate science.

Previous studies including the California Water Plan Update 2013 [California Department of Water Resources, 2013], which used a Robust Decision Making approach [Lempert et al., 2006] have identified potential adaptations through stakeholder consultation and systems analysis but have not systematically assessed the alternatives. They have also not evaluated the impacts of possible changes in climate extremes such as droughts and floods. This study uses previous planning efforts, in particular CWP 2013, as a foundation for illustrating the planning procedure for climate uncertainty described here.

## Climate Change in California

---

It has long been anticipated that anthropogenic climate change would alter the water resources of California [Gleick, 1987]. Recent observations indicate that changes to the hydro-climatology of California have begun, and that further substantial change is likely to occur throughout this century.

## Observed Trends

Mean temperature has increased 0.6 to 1.1 C since 1900 [California Department of Water Resources, 2015a], and temperature change is accelerating [LaDochy et al., 2011] with greatest rate of change in temperature minimums [California Department of Water Resources, 2015a]. Rising temperatures in the Sierra Nevada and northern California have triggered decreasing snowpack and earlier snowmelt [Cayan et al., 2010; Dettinger and Anderson, 2015; Mote et al., 2005]. Warmer temperatures also cause sea level rise, with 0.2 meters of rise recorded in San Francisco Bay in the past century [NOAA, 2016], and rates of rise now accelerating [Kopp et al., 2016], threatening the sustainability of the Sacramento-San Joaquin Delta, the heart of the California water supply system and the source of water for 25 million Californians and millions of acres of farmland.

Figure 1 shows the trend in annual mean temperature for the region of northern/central California contributing flow to the California Department of Water Resources (DWR) system, 1915-2011, and Figure 2 shows the trend by month. There is a statistically significant increasing trend in the annual mean temperature in the region, with strongest increases from August through October. Meteorological data are from Livneh et al. [2013].

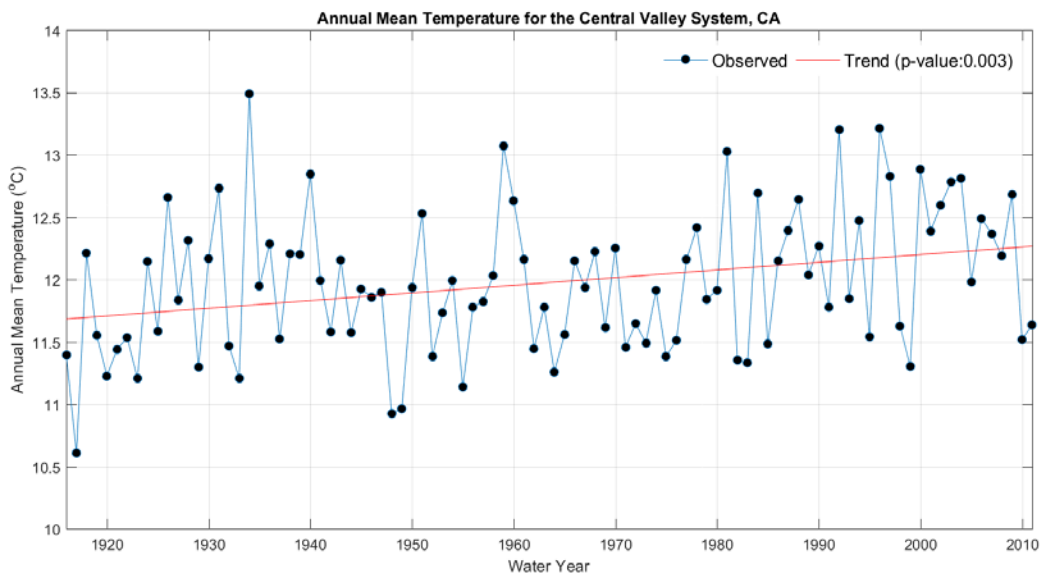


**Figure 1. Trend in annual mean temperature for the region contributing flow to the California Department of Water Resources system, 1915-2011.**

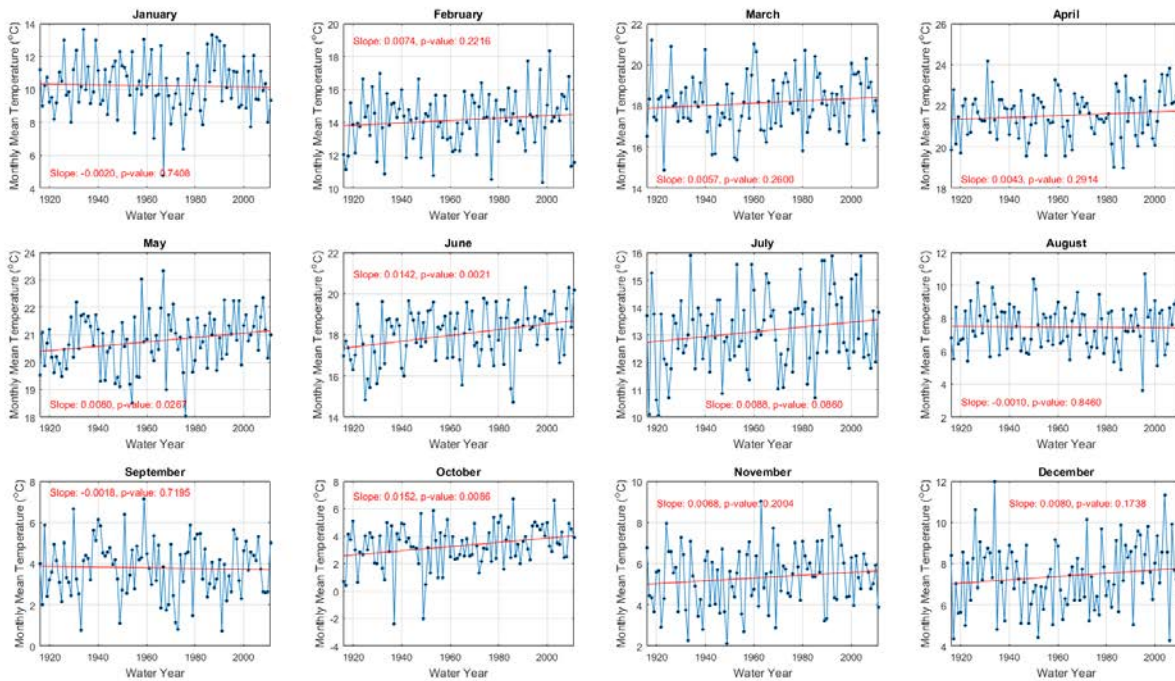


**Figure 2. Monthly trends in annual mean temperature for the region contributing flow to the DWR system, 1915-2011.**

Since 1970, California has gotten wetter in its north and dryer in its south [Killam *et al.*, 2014], though the large historical variability of precipitation in California makes it difficult to separate trend from natural variability. Higgins *et al.* [2007] found that the period 1976-2004 was substantially wetter in the western U.S. than the period 1948-1975, though the large increase in total precipitation might be partially explainable by the occurrence of the warm phase of the Pacific Decadal Oscillation (PDO), the multidecadal counterpart to the El Niño Southern Oscillation (ENSO). It may be that the warm phase of the PDO during the last quarter of the 20th century was an exceptional period (as suggested by the 1000-year tree-ring record [Swetnam and Betancourt, 1998]), and that the last 15 years marks a return to normal, pre-1977 conditions [Pavia *et al.*, 2016]. Regionally, the central and northern regions show increases in both annual totals and number of rainfall days, while southern regions show either no significant trend or some decreases since the early 1900s. A shift from light rains to heavy rains has occurred in northern CA regions [Killam *et al.*, 2014].

Figure 3 shows the trend in annual mean precipitation for the region of northern/central California contributing flow to the DWR system, 1915-2011, and Figure 4 shows the trend by month. There is a statistically significant increasing trend in the annual mean precipitation in the region. Data are from Livneh *et al.* [2013].

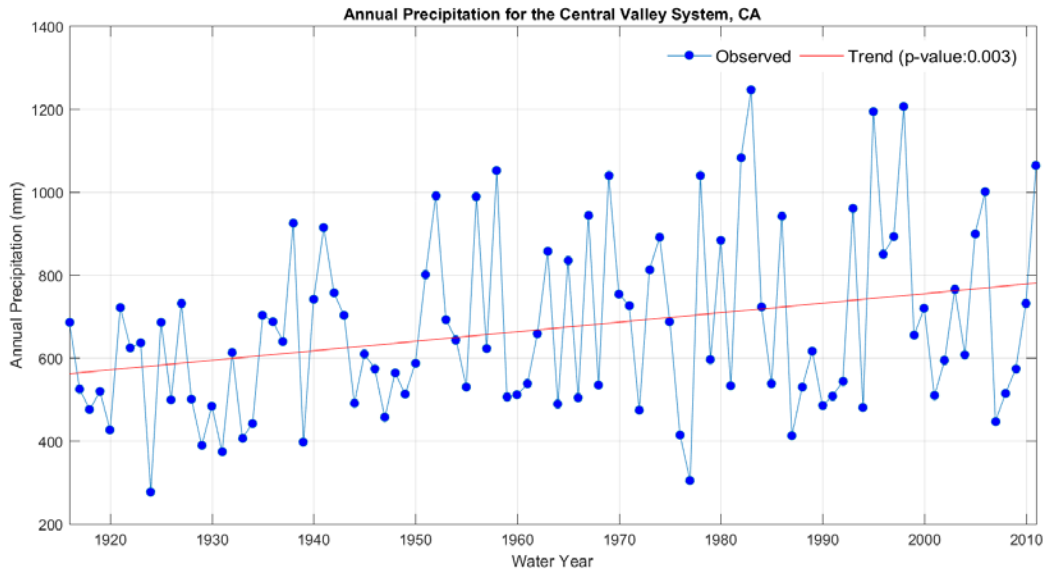


Figure 3. Trend in annual mean precipitation for the region contributing flow to the DWR system, 1915-2011.

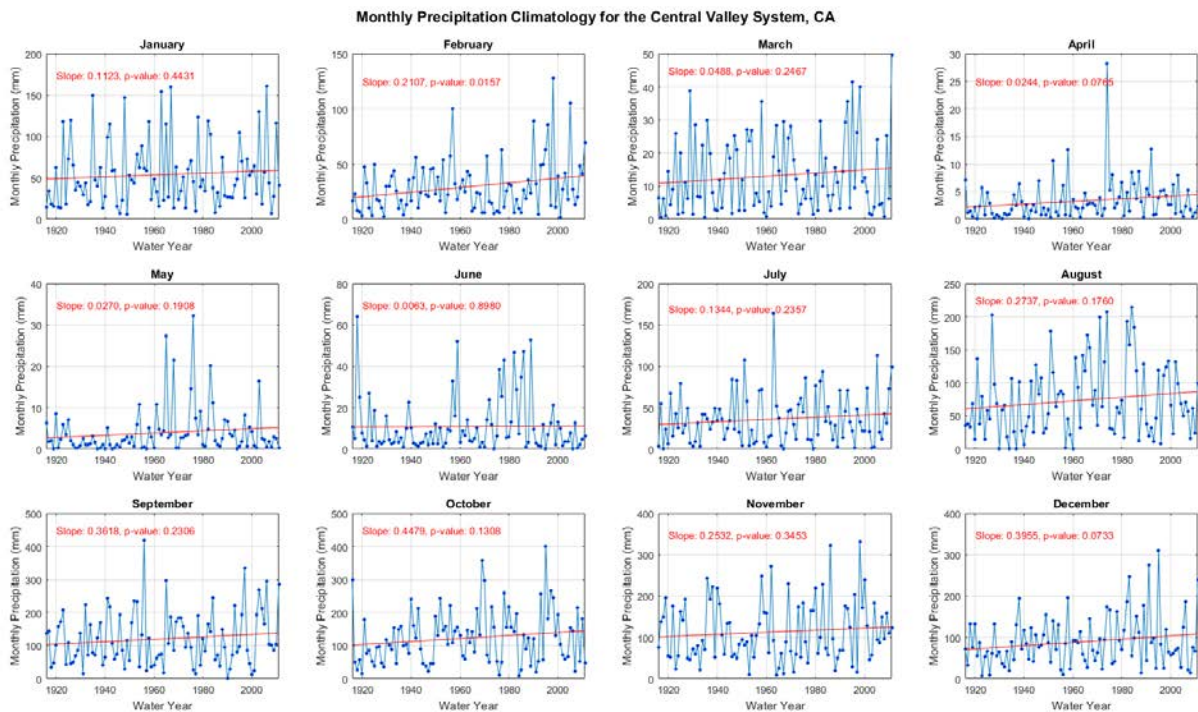


Figure 4. Monthly trend in annual mean precipitation for the region contributing flow to the DWR system, 1915-2011.

It is not yet clear that the trend observed in the past century will continue into the coming century, nor is the behavior of the PDO well-enough understood that confident forecasts can be made of its oscillations far into

the future. The global climate models do not indicate a clearly wetter or drier expectation for the region (discussed later), and there are questions regarding the quality of precipitation data for the region prior to 1950 (see Figure 5, which shows a jump in Shasta watershed precipitation at approximately 1950). We therefore exercise caution in conclusions attached to expectations of future precipitation in the region.

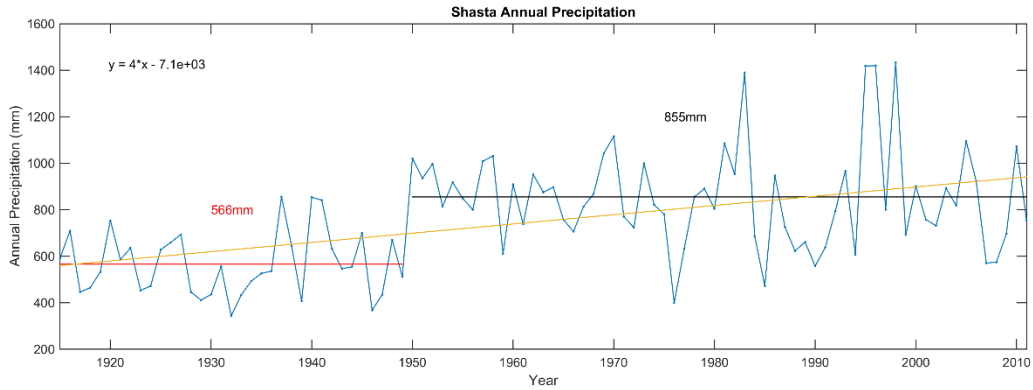
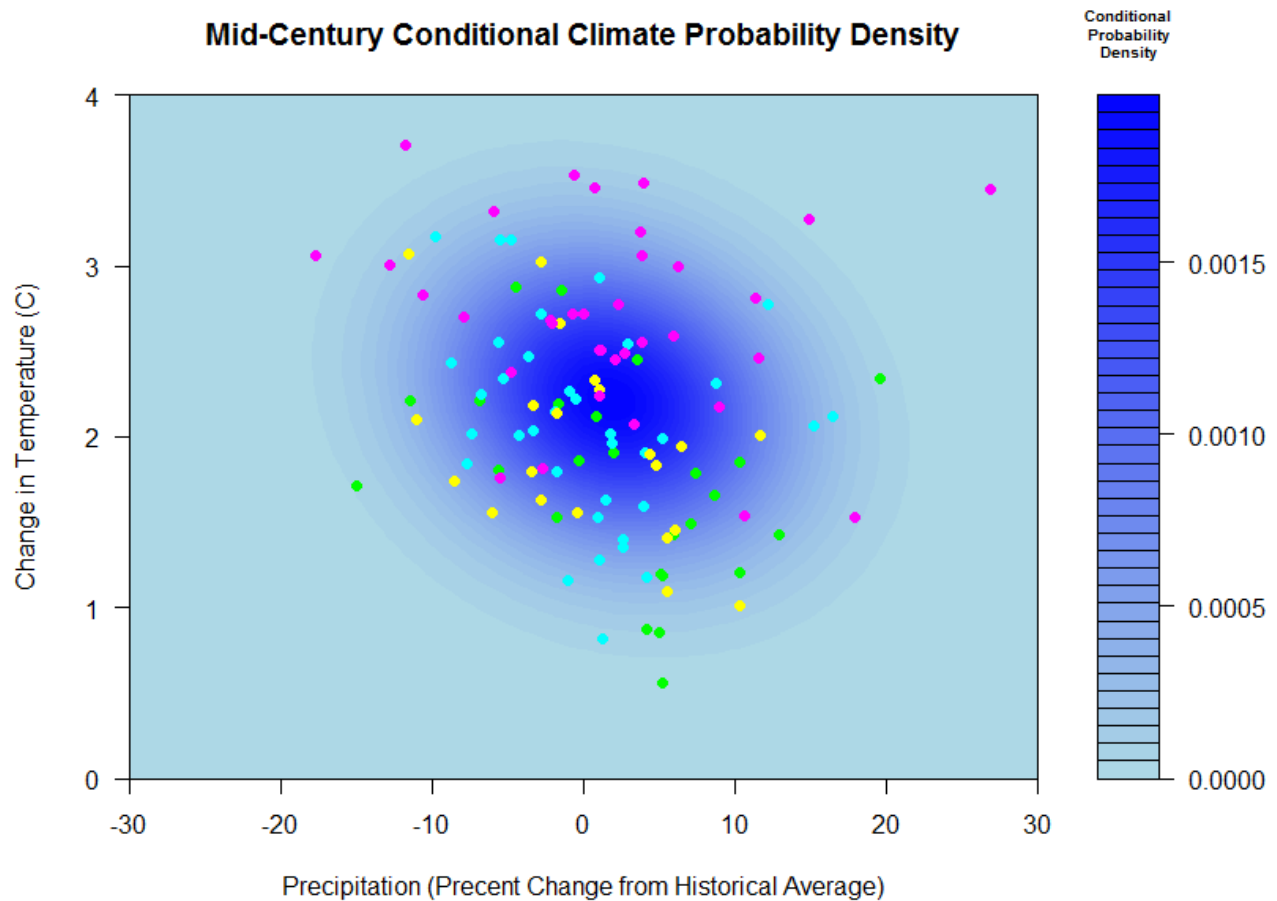


Figure 5. Precipitation in the Shasta watershed 1915-2011 from Livneh et al. [2013].

## Projections

Figure 6 shows the shift in average annual precipitation and temperature of the ensemble of general circulation models (GCMs) driven with Intergovernmental Panel on Climate Change (IPCC) Representative Concentration Pathways (RCP) scenarios 4.5 and 8.5 in the region contributing flow to the DWR system for the period 2036-2065 relative to the period 1971-2000. The probability density cloud identifies the bivariate normal distribution on the full ensemble of the Fifth Coupled Model Intercomparison Project (CMIP5) GCMs (including RCPs 2.6 and 6.0). As can be seen, there is no agreement on the direction of precipitation change (positive or negative), with some GCM runs indicating increases in precipitation of over 20% and some indicating decreases in precipitation of over 20%. Temperature increases range from almost 1C to almost 4C.



**Figure 6. Mid-Century Conditional Climate Probability Density.** Cyan dots represent GCMs run with RCP 8.5; yellow dots represent GCMs runs with RCP 6.0; turquoise dots represent GCMs run with RCP 4.5; Green dots represent GCMs runs with RCP 2.5

The projected changes in California weather patterns could exacerbate both drought and flood risks and increase challenges for water supply management. Projections of future temperature across California suggest greater increase in summer temperatures than in winter temperatures [California Department of Water Resources, 2015a], and an intensification of hot extremes [Diffenbaugh and Ashfaq, 2010]. By the end of this century, the Sierra snowpack is projected to experience a 48-65 percent loss relative to the historical April 1st average on which water supply throughout the summer and fall depends [California Department of Water Resources, 2015a; Cayan et al., 2013].

Most climate model precipitation projections for the state anticipate drier conditions in Southern California, with heavier and warmer winter precipitation in Northern California, and greater proportions of winter precipitation falling as rain instead of snow [Yoon et al., 2015]. Decrease in snowpack storage, and the concentration of streamflow in winter months would increase dry season deficits during periods of high irrigation water demand.

## Atmospheric Rivers

In California, atmospheric rivers contribute 20–50% of the state’s precipitation and streamflow [Dettinger et al., 2011], and therefore play a critical role in West Coast droughts, either by their presence or absence [Dettinger, 2013]. The atmospheric rivers delivering water to California show an increasing tendency in GCM model runs, which could reduce drought severity, but may also increase flood frequency and severity in California under projected climate changes [Dettinger et al., 2011], especially in the region of the Sierra Nevada [Das et al., 2011].

## Drought

California’s most significant droughts of the past century (by hydrologic dry-ness) were: 1929-1934, 1976-1977, and 1987-1992. The water years 2012-2014 were California’s driest three consecutive years in terms of statewide precipitation, and the drought conditions (combination of record high temperatures and near-record low precipitation) faced by California may be the worst in the last millennium [AghaKouchak et al., 2014; Griffin and Anchukaitis, 2014]. Even so, the impact of the 2012-2015 drought would be far worse if not for the slightly wet 2010 and significantly wet 2011 preceding the start of the drought [California Department of Water Resources, 2015b].

Drought conditions in California are increasing in intensity and length [Diffenbaugh et al., 2015]. Climate change is expected to amplify droughts in California, both because of rising temperatures [Cayan et al., 2010] and because of an intensification of ENSO activity [Yoon et al., 2015]. The rise in global temperatures has amplified naturally occurring drought conditions in California and has increased the chance of severe droughts in the future [Williams et al., 2015], though the main cause of intensification of California droughts so far has been natural precipitation variability, not warming [Mao et al., 2015; Seager et al., 2015]. Sea surface temperature forcing, for example (a combination of a La Niña event in 2012/2013 and a warm west-cool east tropical Pacific SST pattern from 2012-2014), sustained a high pressure ridge over the west coast that suppressed precipitation during the three winters from 2011-2014 [Seager et al., 2015; Wang and Schubert, 2014]. This recent event indicates that better understanding of the climatological causes of persistent North Pacific ridging events might be crucial in anticipating future severe drought in California [Swain et al., 2014].

California’s most recent drought began in winter 2011-2012, and intensified in winter 2013-2014, a period marked by very low winter precipitation, mountain snowpack, and spring runoff [Department of Water Resources, 2014b; U.S. Geological Survey, 2014; United States Drought Monitor, 2014]. The drought drew down reservoir storage in the state to low levels and threatened the state’s agricultural production, drinking water supply, and fisheries [California Department of Fish and Wildlife, 2014; Department of Water Resources, 2014a; U.S. Department of Agriculture, 2014]. The drought has included: 1) the lowest three-year state-wide precipitation total on record (2012-2014); 2) the most severe values of NOAA’s National Climatic Data Center drought indicators (D4, or exceptional drought, first noted across the Salinas Valley and western San Joaquin Valley in January 2014 and extending over almost 60% of the state by July 2014) [NOAA, 2014]; 3) the lowest calendar-year precipitation in the history of much of the state, including San Francisco, Sacramento and Los Angeles (2013); 4) the warmest calendar-year temperatures on record (2014); 5) the warmest winter on record (2015); 6) highest one-year (water year 2014, 9-12% above average) and three-year (water year 2012–2014, 7-9% above average<sup>1</sup>) potential evapotranspiration on record [Williams et al.,

---

<sup>1</sup> Potential evapotranspiration was calculated using gridded data of the Global Precipitation Climatology Centre (GPCC) [Schneider et al., 2014]; for some grids, potential evapotranspiration for water year 2012-2014 was second highest behind water year 2007-2009. However, it should be noted that statewide temperatures in 2015 were the

2015]; 6) lowest Palmer Modified Drought Index (PMDI) on record (July 2014, approximately -3) [Diffenbaugh et al., 2015]; 7) the lowest recorded April 1st snowpack (2015, 5% of normal) [Dettinger and Anderson, 2015]; 8) record-low water allocations for State Water Project and federal Central Valley Project contractors [California Department of Water Resources, 2015a]. The drought is responsible for an estimated \$2.2 billion in economic loss from 2013-2014 alone [Howitt et al., 2014], and \$2.7 billion from 2014-2015 [Howitt et al., 2015], and has taken a heavy toll on people and ecosystems [Swain, 2015]. Snowpack has been well below normal for each of the four years of the drought. Year 2015 snowpack is significantly less across all elevations, and shifted to higher elevations. This shift is likely driven in part by the significantly warmer temperatures, which “would lead to less snowfall and more rainfall at lower elevations, and increased accumulation season melt across all elevations (with more melt at lower elevations)” [Margulis et al., 2016].

## Previous Studies

---

### Relevant Studies Conducted to Date

Recent global (Intergovernmental Panel on Climate Change), National (National Climate Assessment), regional (National Climate Assessment for the Southwest Region), and Statewide (3<sup>rd</sup> California Climate Change Assessment) climate change assessments have all highlighted climate change driven impacts to water supply, water demand, increased flooding and drought, and changes to hydrologic processes. The State Water Project has been the focus of many studies conducted by DWR and others, a selection of which include:

- [\*Estimating Historical California Precipitation Phase Trends Using Gridded Precipitation, Precipitation Phase, and Elevation Data, DWR Memorandum Report\*](#) (July, 2014)

This exploratory study develops and describes a methodology that uses readily available research data sets to produce gridded estimates of historical rainfall as a fraction of total precipitation for areas comprising the major water-supply watersheds of California. Written by Aaron Cuthbertson (DWR), Elissa Lynn (DWR), Mike Anderson (DWR, California State Climatologist) and Kelly Redmond (Western Regional Climate Center).

- [\*Paleoclimate \(Tree-Ring\) Study\*](#) (February, 2014)

New Hydroclimate Reconstructions have been released, using updated tree-ring chronologies for these California river basins; Klamath, San Joaquin and Sacramento. The report, prepared by the University of Arizona, allows assessment of hydrologic variability over centuries to millennia, gives historic context for assessing recent droughts, and can be used in climate change research.

- [\*Hydrological Response to climate warming: the Upper Feather River Watershed\*](#), Huang, G., Kadir, T., Chung, F. Journal of Hydrology (2012)

The hydrological response and sensitivity to climate warming of the Upper Feather River Basin, a snow-dominated watershed in Northern California, were evaluated and quantified using observed changes, detrending, and specified temperature-based sensitivity simulations.

---

second-highest on record, behind only temperatures for 2014. The year 2015 was not included in Williams [2015] and would likely result in record three-year potential evapotranspiration for the period 2013-2015.

- [Isolated and integrated effects of sea level rise, seasonal runoff shifts, and annual runoff volume on California's largest water supply](#), Jianzhong Wang, Hongbing Yin, Francis Chung. Journal of Hydrology. (May, 2011)

A detailed analysis of climate change impacts on seasonal pattern shift of inflow to reservoirs, annual inflow volume change, and sea level rise on water supply in the Central Valley of California.

- [Using Future Climate Projections to Support Water Resources Decision Making in California](#), California Climate Change Center (May, 2009)

The report evaluates how climate change could affect the reliability of California's water supply. [Click Here](#) to view a Summary Factsheet.

- [Managing an Uncertain Future; Climate Change Adaptation Strategies for California's Water](#), California Department of Water Resources (October, 2008)

Focuses discussion on the need for California's water managers to adapt to impacts of climate change, some of which are already affecting our water supplies. The report proposes 10 adaptation strategies in four categories.

- [Progress on Incorporating Climate Change into Management of California's Water Resources](#), Climatic Change (March, 2008)

Published in the March 2008 special issue of **Climatic Change -California at a Crossroads: Climate Change Science Informing Policy**. This is an 18 page condensed version of the original 350 page 2006 report of the same name. Coauthored by DWR staff.

- [Sacramento-San Joaquin Basin Study](#), United States Bureau of Reclamation (2016)

## Studies and Other Efforts in Progress as of December 2015

California Water Plan Update 2018

### Academic studies of climate change impact on the water resources of California

In addition to the reports just described, an array of academic research has focused on specific aspects of climate change impacts on California's water resources. Previous exercises in hydro-system modeling have provided substantial insights for policy-making and public discussion related to water resources management in California [*Connell-Buck et al.*, 2011; *Harou et al.*, 2010; *Null et al.*, 2014; *Tanaka et al.*, 2011]. Most of these studies have shown that California's water system, while not impervious, can be quite robust to substantial climate disturbances without widespread catastrophic losses, if well managed.

*Connell-Buck et al.* [2011] used CALVIN (CALifornia Value Integrated Network), a hydro-economic optimization model of California's statewide water supply system, to compare a warmer climate scenario and a warmer-drier scenario centered on 2085 with updated 2050 water demand estimates. Because the study based its exploration on a particular run of a particular GCM (A2, model GFDL CM2.1), however, it is limited to that model's representation of a theoretical local climate future, and relies on the model's potentially unrealistic representation of natural (inter and intra annual) climate variability. The study is not able, for example, to systematically explore the vulnerability of the system to meteorological droughts of varying intensity and duration.

Other attempts at evaluating the sensitivity of the California system to climate conditions different from the past have been subject to similar limitations in the type and number of model runs. For example, *Harou et al.* [2010] tested the response of the CALVIN model to a single 72-yr synthetic hydrologic time series with half the mean historical inflow. The synthetic hydrologic time series was generated by random resampling from the 10 driest years of record (1922–1993). The random resampling does not facilitate risk assessment, which requires information on the relative likelihood of occurrence of droughts of varying return periods. *Null and Lund* [2006] used an economic engineering optimization model to evaluate the water supply feasibility of removing O’Shaughnessy Dam, located in the Hetch Hetchy Valley of Yosemite National Park, by examining alternative water storage and delivery operations for San Francisco. The model was run under historical hydrology, and a single time series of a warmer drier hydrology with water demands increased to projected year 2100 demands. Similarly, *Null et al.* [2014] used the CALVIN model to evaluate the habitat and economic consequences of removing rim dams in California’s Central Valley under historical conditions and a single warm and dry climate time series from the Geophysical Fluid Dynamics Laboratory (GFDL) CM2.1 model for the A2 emissions scenario.

*Rheinheimer et al.* [2015] explored the effect of temperature increases on reservoir operating procedures to manage downstream temperatures with climate warming of 2, 4, and 6 °C. The study altered stream temperatures only and did not adjust water quantity or flow timing.

Examples of studies that have explored a wider range of possible climate futures are *Willis et al.* [2011] and *Groves and Bloom* [2013]. In order to understand the effect of climate change on flood operations in the Sacramento Basin, *Willis et al.* [2011] ran downscaled time series from 11 GCMs (each run twice, once for CMIP3 scenario A2 and once for B1) through the Army Corps’ Hydrologic Engineering Center Reservoir Simulation (ResSim) model (after converting the climate information into reservoir inflow through application of the National Weather Service River Forecast System, NWS–RFS).

*Groves and Bloom* [2013] used a Robust Decision Making (RDM) approach applied to the Water Evaluation and Planning (WEAP) Central Valley Model modeling environment [*Joyce et al.*, 2010] to develop and compare robust water-management response packages that could ameliorate the vulnerabilities identified. The RDM approach explored the uncertainty associated with the system response to output from 6 GCMs (each run twice, once for scenario A2 and B1, as was done by *Willis et al.* [2011]). Although the ensemble of GCM projections (22, in the case of *Willis et al.* [2011] and 12 in the case of *Groves and Bloom* [2013]) widens the range of future plausible hydrologic conditions relevant to the performance of California water system beyond that considered by previous more deterministic studies, they do not necessarily capture the range of uncertainty in future climate [*Cayan et al.*, 2010], and they likely underestimate the range of future interannual variability, including the potential for multiyear droughts [*Brown and Wilby*, 2012]. Furthermore, like other studies before them, they offer no systematic exploration of system response to the types of droughts of varying intensity and duration that might be experienced in the future.

Whereas these previous studies have tested the response of some aspect of the California water system to climate traces different from the historical, the decision scaling [*Brown et al.*, 2012] approach adopted for this study allows systematic assessment of the vulnerability of the entire (interconnected and complex) DWR water system to a wide range of potential future climate conditions, and quantification of the significance of climate shift relative to natural (and climate-change-amplified) variability. The climate response function that results from the decision scaling approach identifies the range of climate change within which the performance of the system is acceptable, and the critical amount of climate change beyond which unacceptable losses of water system performance will occur. An important benefit of this approach is the

ability to assign formal probability estimates to the vulnerability space, which allows discussion of risk and opportunity (each a function of impact and likelihood) in water system investment.

## Methodology

---

DWR's vulnerability assessment for long-term and persistent hydrologic impacts of climate change focuses on impacts to the operation of the State Water Project (SWP), including ecological conditions that dictate operating rules. DWR owns and operates the SWP for flood control, maintenance of environmental and water quality conditions, water supply, hydropower, and recreation. Thus, analysis of SWP performance under climate changed conditions yields an array of impact metrics across all of these areas of concern.

Water resources system models are the essential tools for exploring the risks to water system performance of potential future hydro-climatological and socio-economic conditions [Brown *et al.*, 2015]. In order to conduct a stress test that can meaningfully inform the vulnerability of the multifaceted DWR system, a water system model is needed that can rapidly simulate the coordinated operations of the Central Valley Project (CVP) and SWP. This study has adopted CalLite 3.0, a simplified, faster version of the water system model used by DWR, which is called CalSim-II. DWR estimates that the trade-off for the faster speed of CalLite 3.0 is an approximate error of 1 percent as compared to a corresponding run of CalSim-II [Islam *et al.*, 2014]. CalLite 3.0 requires input including:

- time series of streamflow in rivers serving the Central Valley,
- status of regulatory requirements (such as Delta water quality and minimum instream flows), and
- settings for operational rules (such as water demands and delivery priorities).

As CalLite 3.0 runs, those inputs are used to calculate, at a monthly time step, the resulting system conditions, examples of which include:

- reservoir storage levels,
- flow in rivers downstream of reservoirs,
- deliveries to SWP and CVP contractors, and
- Delta water quality parameters.

CalLite 3.0 receives time series of streamflow as input; however, in order to inform the likelihood climate-change-related water system vulnerabilities, it is necessary to begin with the most fundamental factors available – those describing conditions of meteorological drought, i.e., precipitation and temperature. This study uses a weather generator to develop time series of plausible alternative precipitation and temperature, which are then sampled systematically in order to explore a wide range of climate change characteristics. An advanced hydrologic model (in this case SAC-SMA-DS, described later) translates descriptors of fundamental meteorological drought into measures of available water at Earth's surface. The estimates of available water from the hydrologic model become the key inputs to a water system model (CalLite 3.0), which simulates the complex interactions of water supply, water demand, regulatory compliance, and operational choices and produces measures of water system performance such as water deliveries, reservoir storage, and river flow volume. In the case of CalLite 3.0, a number of additional inputs, beyond river flows that could be directly provided by the hydrologic model, are required. This requirement necessitated an additional pre-processing routine (quantile mapping and water year typing) that involves incorporation of anthropogenic co-factors in the operation of water system infrastructure.

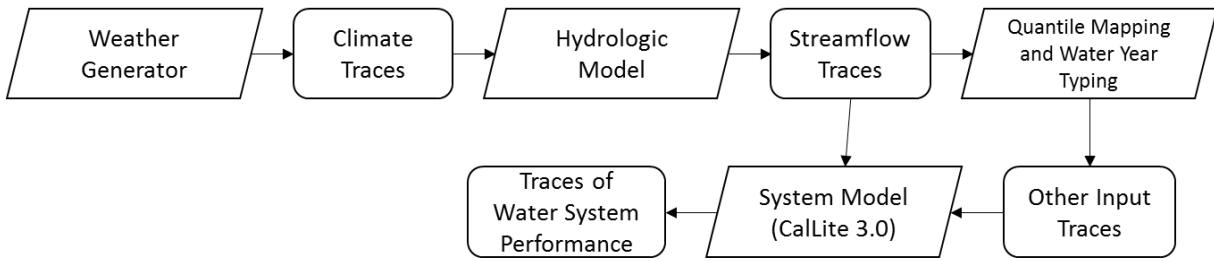


Figure 7. Modeling Workflow for Climate Change Vulnerability Assessment

When simulated repeatedly, the resulting workflow (Figure 7) allows the exploration of climate change impact in response to a wide range of meteorological input. It does this by maintaining proportionate anthropogenic response to relative scarcity of available water through propagation of probabilistic relationships.

As a first step in the approach, decision-relevant metrics are identified that can be used to characterize the adequacy of system performance. Table 1 lists the decision-relevant metrics used for the DWR climate vulnerability assessment (this is only a small subset of the information available, and can be expanded in the future to evaluate additional vulnerabilities as needed). The vulnerability of each of the metrics shown in the table was evaluated using the stress test approach (repeated simulation of the workflow shown in Figure 7).

Table 1. Decision relevant metrics

1	Oroville Storage levels
	April 1 <sup>st</sup>
	September 1 <sup>st</sup>
2	Net Delta Outflow
	Winter
	Spring
	Summer
	Fall
3	SWP Deliveries
	Average Annual
4	System Shortages
	Average Annual

System shortages occur when there is not enough water in the system (precipitation, runoff, and storage) to meet all of the water demands, regulatory requirements, and health and safety required diversions. In the modeling simulations, these shortages typically result in the relaxation of Delta water quality or outflow requirements. The shortage amount is the amount of water that would be needed to meet all the requirements. Historically, these shortages have been rare but do occur periodically (i.e. 2014 and 2015).

This analysis focuses on persistent medium and long-term conditions evaluated at a monthly time-step.

**Short-duration extreme precipitation events that cause flooding may also stress water resource management but this analysis does not explicitly evaluate flood risk.**

This methodology section describes each step of the modeling workflow, beginning with a description of the study area, and proceeding through a description of the weather generator, the hydrologic model, and the water system model.

## Description of Study Area

The catchment area of the Sacramento and San-Joaquin rivers (Figure 8) provides at least a portion of the water supply for about two-thirds of California’s population. About half of California’s average annual streamflow flows toward the Sacramento and San-Joaquin Delta, and most of California’s farmland depends on water tributary to it [Lund *et al.*, 2010]. The Delta itself is a web of channels and reclaimed islands at the confluence of the Sacramento and San Joaquin rivers. It forms the eastern portion of the wider San Francisco Estuary, which includes the San Francisco, San Pablo, and Suisun bays, and it collects water from California’s largest watershed, which encompasses roughly 45 percent of the state’s surface area [Lund *et al.*, 2010]. It is also a center for important components of California’s civil infrastructure, such as electricity, gas transmission lines, underground storage of natural gas, and transportation lines, and provides crucial habitat for many of California’s fish species that live in or migrate through it (esp., four fish that are listed as endangered or threatened pursuant to the federal Endangered Species Act [Mount and Twiss, 2005]). Not inconsequentially, the Delta is valued for its aesthetic appeal and support of recreational activities [Lund *et al.*, 2010]. The usable water resources for the California Central Valley System can be approximated as the quantity of streamflow flowing into the Central Valley from the north-east upgradient regions that are comprised of twelve large sub-basins, referred to as the rim sub-basins (Figure 8).

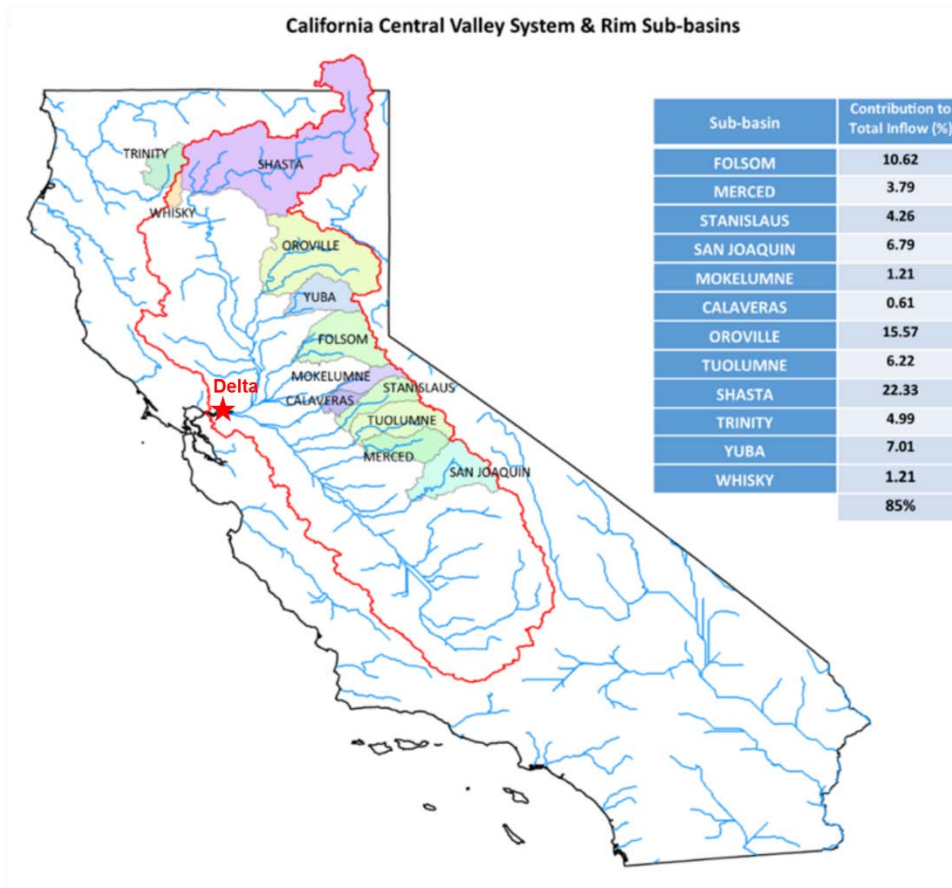


**Figure 8. California Central Valley System and Rim Sub-basins. Table inset shows the percent contribution of each river to the total delta outflow. Fifteen percent of the total delta outflow is contributed by unshaded areas within the red outline.**

The California Department of Water Resources (DWR) and the United States Bureau of Reclamation (USBR) oversee the operation of the Central Valley water systems that store and manage water supplies that flow

through the Sacramento-San Joaquin Delta, and use the Delta as a conveyance hub (see Figure 9). We therefore define the California Central Valley Water System as: *the interconnected system of natural river channels and man-made facilities that comprise the CVP, owned and operated by the United States Bureau of Reclamation (USBR) and the SWP, owned and operated by DWR.* The CVP includes more than 13 million acre-feet of storage capacity in 20 reservoirs. The CVP provides water to about 3,000,000 acres of irrigated agricultural fields, as well as municipal water uses, and rivers and wetland water releases to meet state and Federal ecological standards. The SWP includes more than 30 storage facilities, reservoirs and lakes; about 700 miles of open canals and pipelines, providing water to approximately 25 million Californians and about 750,000 acres of irrigated farmland. The SWP is not the exclusive water supplier for those it serves, as many of its customers supplement the water provided by SWP with local or other imported sources. Local water systems are outside of the jurisdiction of DWR.



Figure 9. State, Federal, and Local water infrastructure from the California Water Plan [2013] Volume 3, pg 7-6

### Description of Weather Generator

The representations of internal variability and climate change developed for this study are not driven by GCM projections. Rather, hydrologic internal variability is explored by running 13 unique hydrological sequences (described below) through the CalLite model. The potential range of climate changes are explored by increasing mean temperature in 0.5 degree Celsius (C) increments up to +4.0 degrees C and increasing and decreasing average annual precipitation in 10% increments from -30% to +30%. Sea level rise is assumed to

increase by 15 cm above 0.5 degrees C and an additional 30 cm (total 45 cm) above 1.5 degrees C.<sup>2</sup> These changes extend far enough to explore the full range of outcomes predicted by global climate models through about 2070. This was accomplished through the development of a weather generator specific to the region of DWR interest.

A weather generator has a number of advantages that distinguish it from sources of climate information that originate from global modeling efforts that serve primarily to assess the effects of greenhouse gas emissions on climate. A weather generator can be targeted specifically at the local climate characteristics, and altered systematically to explore changes to those climate characteristics that are informed by local observed changes in known climate drivers, such as atmospheric rivers and sea surface temperature correlations. It can also be adjusted to exhaustively probe systems to identify vulnerabilities. For questions of the sensitivity of the system to droughts of varying intensity and duration, the weather generator can be used to develop time series of climate metrics (e.g., precipitation and temperature) that contain exactly the type of drought characteristics of concern. Because the weather generator allows exploration of such a wide range of potential climate and natural variability impacts, it significantly reduces the possibility of under-exploring important vulnerabilities due to biases and error propagated into the analysis from downscaled GCM projections.

#### Development of New Climatological Sequences

The weather generator used for this study [Steinschneider and Brown, 2013] resamples from the Central Valley System (CVS) historic record of temperature and precipitation [Maurer et al., 2002] using an Auto-Regressive Moving Average (ARMA) model that maintains low frequency variability in the mean annual precipitation signal. Because it uses a bootstrapping technique to resample from the entire study area simultaneously, spatial correlations are maintained perfectly. There are approximately 1000 1/8<sup>th</sup> degree latitude-longitude grid cells within the study area, each of which contains daily climate data from 1950-2010. The weather generator was conditioned on annual area-averaged gridded climate data from 1950-2003 (discarding 2004-2010), as 2003 is the limit of the range of the information available for CalLite 3.0 input.

Statistically significant (90% confidence) low frequency signals occur at between approximately 12 and 16 years (Figure 10: Fourier periods 11 = 11.7 years; 12 = 13.9 years; 13 = 16.5 years). The identified 15-year periodicity in the precipitation signal is visible in the local paleo-record approximately 500 years into the past, but not before that [Dettinger and Cayan, 2014; Meko et al., 2014]. According to Meko et al. [2014]: “Cyclic variation, with an average wavelength of about 15 years, is evident in both observed and reconstructed flow series over the past 100 years, but is not a long-term feature of the hydroclimate of the basins studied. While some observed flow records have large inter-decadal swings, the near-15- year cycle in those records does not pass spectral analysis tests for statistical significance.”

---

<sup>2</sup> While sea level is expected to continue to increase above 45 cm as the earth warms, no higher sea level model compatible with CalLite 3.0 was available to simulate higher degrees of sea level rise at the time this analysis was performed. It should be noted that system performance at temperatures above 2.5 degrees is likely overly optimistic because at such temperatures sea levels would likely be substantially higher than accounted for in the model.

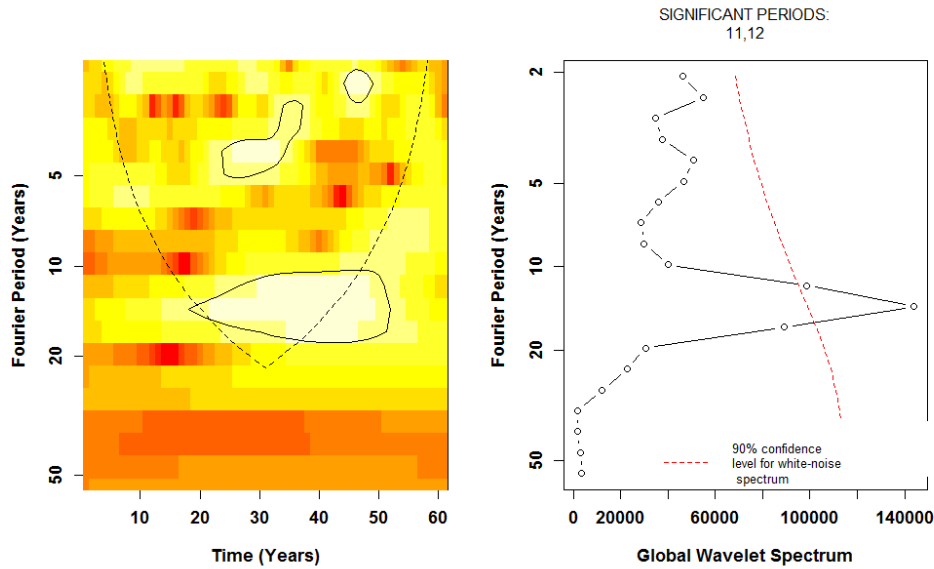


Figure 10. Wavelet power spectrum for average annual precipitation for the Central Valley catchment (1950-2003).

Because there is doubt regarding the long-term (and future) persistence of the 15-year periodicity in the precipitation of northern California, two sets of five thousand unique realizations were generated to explore the potential natural variability within the system, one with the 15-year signal, and one without. After a preliminary assessment, very little difference was found between the water system performance when forced with climate traces that maintained, and that did not maintain, the 15-year climate signal (see Appendix for comparative plots). This inception report describes the methodology used and results obtained using only those climatologic traces developed using a Wavelet Autoregressive Model (WARM), designed to maintain the 15-year climate signal; however, further exploration of this behavior is warranted, and a plan to address the uncertainty related to the system response to the natural climate variability will be described in the final section of this report.

The driest 5-year period within each of the 5,000 runs generated using the WARM, and the ensemble was arranged in order from most severe (driest) to least severe (wettest) minimum 5-year precipitation. From this ranking, 5 examples of each drought percentile were identified: 1<sup>st</sup>, 25<sup>th</sup>, 50<sup>th</sup>, and 75<sup>th</sup>. These 20 runs were then filtered for those whose mean precipitation over the 50-year period deviated more than +/- 1 percent from the historical mean. From the remaining runs, 3 from each quantile (a total of 12) were selected as representative hydrologic sequences and carried forward (Table 2). The process followed after that used by *Whateley et al.* [2016].

Table 2. Hydrologic Sequences with 15 Year Wavelet Signal

	Climate Trace
1	Historical
2-4	1 <sup>st</sup> Percentile 5 year droughts
5-7	25 <sup>th</sup> Percentile 5 year droughts
8-10	50 <sup>th</sup> Percentile 5 year droughts
11-13	75 <sup>th</sup> Percentile 5 year droughts

Each of the 13 climatological sequences provides a 50-year simulation of inter-annual climatologic variability (natural variability) within the system. These sequences provide the opportunity for an exploration of novel drought sequences that are longer and/or more severe than droughts that have been observed in the available instrumental record. In total, for each ensemble (with and without the wavelet signal) the 13 sequences provide exploration of 650 years of precipitation and temperature at California’s current climate conditions (i.e., no more climate change than has already been observed today).<sup>3</sup>

### Application of Climate Shifts

In order to explore the future effects of climate change each of the 13 sequences was warmed, and precipitation was perturbed, incrementally across a wide range of future changes as shown in Table 3. Sixty-three different combinations of temperature and precipitation change were applied to the climatological sequences. The exploration range for temperature and precipitation was informed by the range of changes projected for the CVS by the global climate models included in CMIP5 (<http://cmip-pcmdi.llnl.gov/cmip5/>).

**Table 3. Range of Temperature and Precipitation Changes Explored**

		% Δ Precipitation						
		-30	-20	-10	0	10	20	30
Degree C ΔTemperature	0							
	+0.5							
	+1.0							
	+1.5							
	+2.0							
	+2.5							
	+3.0							
	+3.5							
	+4.0							

A total of 819 different combinations of natural variability (13), temperature change (9), and precipitation change (7) were developed. Each of the 819 combinations is a 50-year time series of temperature and precipitation across the Central Valley watershed area (nearly 41,000 years of simulation). It should be made clear at this point that the application of climate shifts is probability neutral. Climate shifts are applied for the purpose of tracing out the system’s vulnerability space only (for each climate shift, the technique identifies possible future climate states that would be of concern to system performance), and do not indicate the

<sup>3</sup> What is described here is the original experimental design, which aimed to understand the system response to drought severity. Throughout the course of the preliminary work described in this inception report, it became clear that a revised climate sampling strategy is needed. At the next phase of this experiment, climate trace sampling will emphasize fidelity to the historical climate characteristics (mean, variance, 15-year low frequency variability), and give less attention to the characteristics of the worst drought in each climate trace. The revised experimental design is described in the final section of this report.

likelihood of the particular shift under consideration. Likelihood concepts are explored in later sections of this report.

### Details on Approach to Climate Change Factors

After consideration of differences in rates of climate change by season and elevation, it was decided to apply climate shifts (i.e., changes in precipitation and temperature assigned to the bootstrapped traces of historically-similar climate) uniformly across space and time. In order to represent the stronger precipitation increases in historically wetter months, precipitation change factors were applied as fractions of historic rainfall amount (% changes were applied to historical values). Changes to the precipitation are ranged from  $\pm 30\%$  of the historic average using increments of 10%. Temperature shifts are ranged from 0 to 4°C by 0.5°C increments.

Historical evidence was not strong for a differential application of precipitation shifts to low and high altitudes (i.e., an evaluation of changes in precipitation and temperature above and below 2000 m absl did not indicate systematically different rates of change at the two elevation bands). Figure 11 summarizes an exploration of differential rate of change in precipitation (left) and temperature (right) between early-mid-20<sup>th</sup> century (1920-1960) and the end of the 20<sup>th</sup> century (1980-2011) in the Central Valley system. Hollow triangles show changes in high-elevation (>2000 m above mean sea level) grid cells of the *Maurer et al.* [2002] dataset, and solid dots show changes in low-elevation (<2000 m amsl) grid cells. Temperature trends show greater scatter, and do not strongly argue for differential application of temperature changes by either altitude or season.

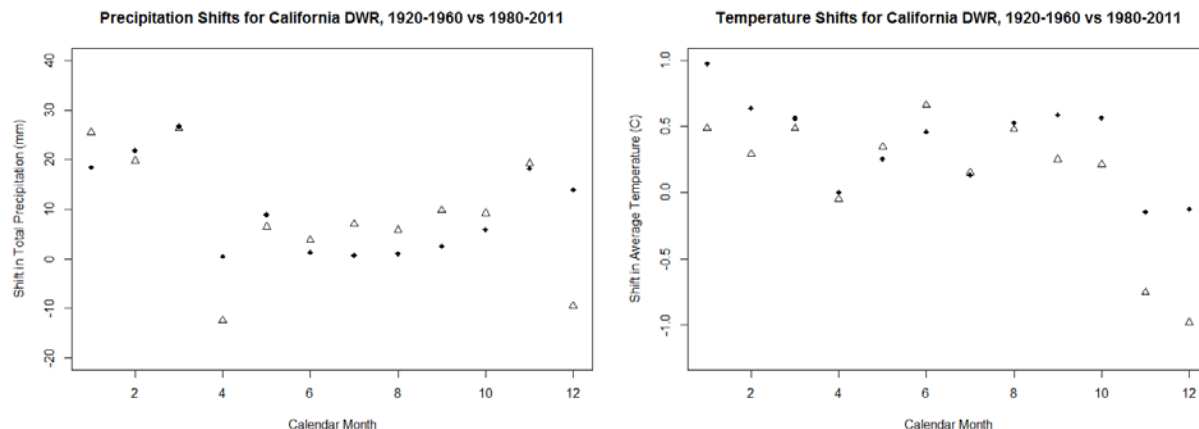


Figure 11. Exploration of differential rate of change in precipitation (left) and temperature (right) between early-mid-20<sup>th</sup> century (1920-1960) and the end of the 20<sup>th</sup> century (1980-2011). Hollow triangles show changes in high-elevation (>2000 m) grid cells of the *Maurer et al.* [2002] dataset, and solid dots show changes in low-elevation (<2000 m) grid cells.

Projected seasonal shifts by mid-century in temperature (Figure 12) and precipitation (Figure 13) in the ensemble of CMIP5 GCM runs for the Central Valley system indicate more warming in the summer than the winter (though this differential trend is not clearly mirrored in the historical data of Figure 11), and great uncertainty in magnitude (and direction) of precipitation change in historically wet months.

CMIP5 Temperature Change Projection: 1971-2000 vs 2036-2065

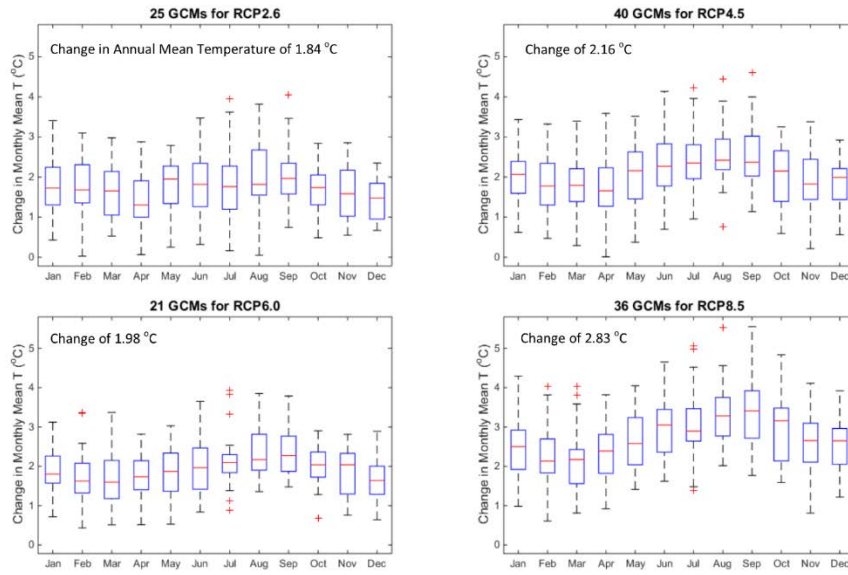


Figure 12. CMIP5 Projected temperature change: 1971-2000 vs 2036-2065

CMIP5 Precipitation Change Projection: 1971-2000 vs 2036-2065

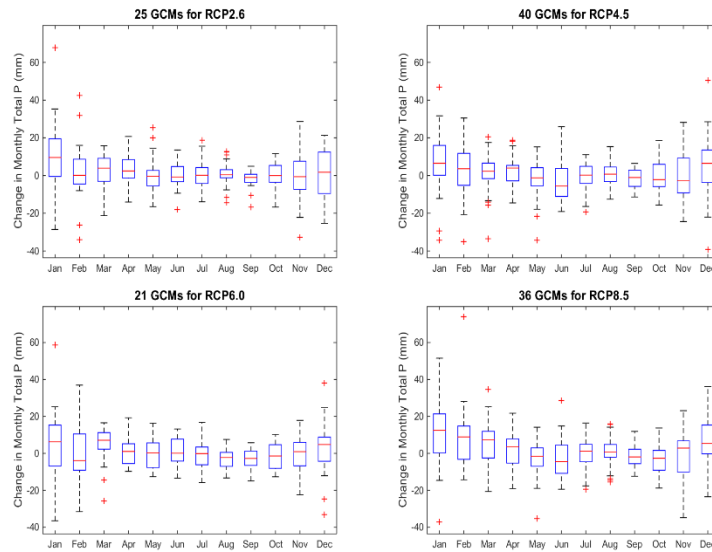


Figure 13. CMIP5 Projected precipitation change: 1971-2000 vs 2036-2065

The historical period from 2002-2011 was approximately 0.33 C warmer than the period from 1922-2001 (illustrated in Figure 1). Before assigning climate shifts to the bootstrapped traces of historically-similar climate, then, it was necessary to add 0.33 C to every year of the bootstrapped historical time series. The warmest years in the historical record remain the warmest years in the resampled set, preserving relationships between temperature and some of the more poorly understood non-hydrologic CalLite input parameters. The imposed 0.33 C shift in historical temperature allows reference to current/recent historical

conditions when developing the stress test matrix (as opposed to more abstract reference to mid-20<sup>th</sup>-century temperatures at the median of the historical timeseries).

### Description of SAC SMA Hydrologic Model

Because of its essential role in the quantification of available water on which water allocations to all water sectors are based, very high performance is required of the hydrologic model. Hydrologic model residuals propagate through the modeling chain and contribute to a cascade of uncertainty [Wilby and Dessai, 2010]. This section describes the development of a distributed, physically-based hydrologic model capable of supporting subsequent phases of the climate change vulnerability assessment workflow.

The amount of usable water for the CVS can be approximated as the quantity of streamflow in the twelve largest rivers flowing from the north-east into the Central Valley. These are referred to as the rim inflows. In order to estimate those twelve stream flows, the Sacramento Soil Moisture Accounting (SAC-SMA) model, a lumped conceptual hydrological model employed by the National Weather Service (NWS) of the National Oceanic and Atmospheric Administration (NOAA) to produce river and flash flood forecasts for the nation [McEnery et al., 2005], was coupled with a river routing model to be suitable for modeling a distributed watershed system. It is here referred to as SAC-SMA-DS, denoting the distributed version of SAC-SMA. SAC-SMA-DS (Figure 14) is composed of hydrologic process modules that represent soil moisture accounting, evapotranspiration, snow processes, and flow routing. The model operates on a daily time step and requires daily precipitation and mean temperature as input variables.

As illustrated in Figure 8, the coverage area of the hydrologic model includes all major tributaries to the northern California water system (esp., the Sacramento and San Joaquin watersheds). The contributing flow is summarized in the table insert, showing the relative importance of the Shasta and Oroville sub-basins.

SAC-SMA-DS includes the Snow 17 module [Anderson, 1976] to account for snow and ice dynamics within the 12 rim sub-basins. In this study the hydrologic modeling domains for 12 rim sub-basins are spatially disaggregated using climate input grids of 1/8° resolution and 200 m interval elevation bands corresponding to the meteorological source data [Maurer et al., 2002]. The runoff from each disaggregated area is weighted by its area fraction within the basin to obtain the total basin-wide runoff.

The overall model structure of SAC-SMA-DS is described in Figure 14. More details on the model components are provided below by focusing on the descriptions for the modules additionally introduced to develop the distributed version of SAC-SMA.

### (a) Distributed Hydrologic Model

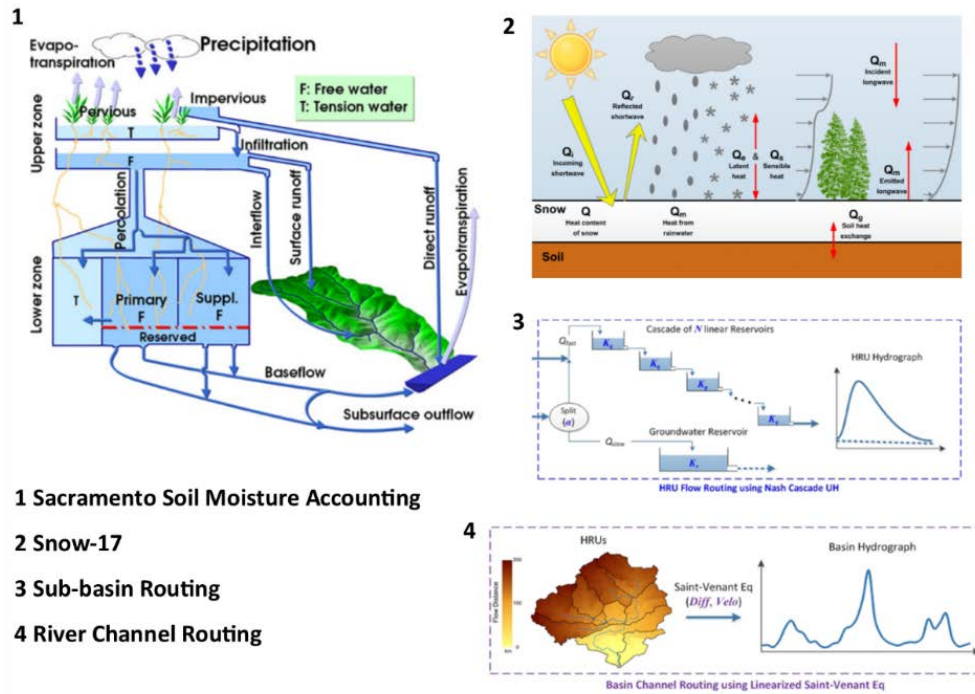


Figure 14. Schematic of distributed hydrologic model

#### Hamon Evapotranspiration Calculation

The potential evapotranspiration (PET) is derived based on the Hamon method [Hamon, 1961], in which daily PET in millimeters (mm) is computed as a function of daily mean temperature and hours of daylight:

$$PET = \text{Coeff} \cdot 29.8 \cdot L_d \cdot \frac{0.611 \cdot \exp\left(\frac{17.27 \cdot T}{T+273.3}\right)}{T+273.3} \quad (2)$$

where,  $L_d$  is the daylight hours per day,  $T$  is the daily mean air temperature ( $^{\circ}\text{C}$ ), and Coeff is a bias correction factor. The hours of daylight is calculated as a function of latitude and day of year based on the daylight length estimation model suggested by Forsythe et al. [1995].

#### In-grid Routing: Nash-Cascade Unit Hydrograph

The within-grid routing process for direct runoff is represented by an instantaneous unit hydrograph (IUH) [Nash, 1957], in which a catchment is depicted as a series of  $N$  reservoirs each having a linear relationship between storage and outflow with the storage coefficient of  $K_q$ . Mathematically, the IUH is expressed by a gamma probability distribution:

$$u(t) = \frac{K_q}{\Gamma(N)} (K_q t)^{N-1} \exp(-K_q t) \quad (3)$$

where,  $\Gamma$  is the gamma function. The within-grid groundwater routing process is simplified as a lumped linear reservoir with the storage recession coefficient of  $K_s$ .

### River Channel Routing: Linearized Saint-Venant Equation

The transport of water in the channel system is described using the diffusive wave approximation of the Saint-Venant equation [Lohmann *et al.*, 1998]:

$$\frac{\partial Q}{\partial t} + C \frac{\partial Q}{\partial x} - D \frac{\partial^2 Q}{\partial x^2} = 0 \quad (4)$$

where C and D are parameters denoting wave velocity and diffusivity, respectively.

### Water Resources System Model

CalLite 3.0 is the water resources system model used in this study to assess impacts. It is a screening level planning tool developed by DWR and USBR for analyzing CVS water management alternatives. CalLite is the faster, streamlined version of CalSIM-II [Draper *et al.*, 2004], designed to be accessible to policy and stakeholder demands for rapid and interactive policy evaluations. CalSIM-II, driven by the Water Resource Integrated Modeling System (WRIMS model engine or WRIMS) is “a generalized water resources modeling system for evaluating operational alternatives of large, complex river basins [that] integrates a simulation language for flexible operational criteria specification, a [mixed integer] linear programming solver for efficient water allocation decisions, and graphics capabilities for ease of use” [California Department of Water Resources and United States Bureau of Reclamation, 2011]. As explained by Draper *et al.* [2004], “for each time period, the solver maximizes the objective function to determine a solution that delivers or stores water according to the specified priorities and satisfies system constraints. The sequence of solved [Mixed Integer Programming] problems represents the simulation of the system over the period of analysis... [CalSim-II] also allows the user to specify objectives using a weighted goal-programming technique pioneered by Charnes and Cooper [1961].”

CalLite, a schematic of which is shown in Figure 15, represents reservoir operations, SWP and CVP operations and delivery allocation decisions, existing water sharing agreements, and Delta salinity responses to river flow and export changes on a monthly timestep. CalLite can also represent the effect on the water system of land use changes and sea level rise, features of particular use to this study. CalLite 3.0, released in 2014, has 796 input parameters, and approximately 240 additional data tables that store all relational data, such as reservoir area-elevation-capacity data, wetness-index dependent flow standards, and monthly flood control requirements [California Department of Water Resources and United States Bureau of Reclamation, 2011; Draper *et al.*, 2004]. Output includes water supply indicators, environmental indicators, and water use metrics.

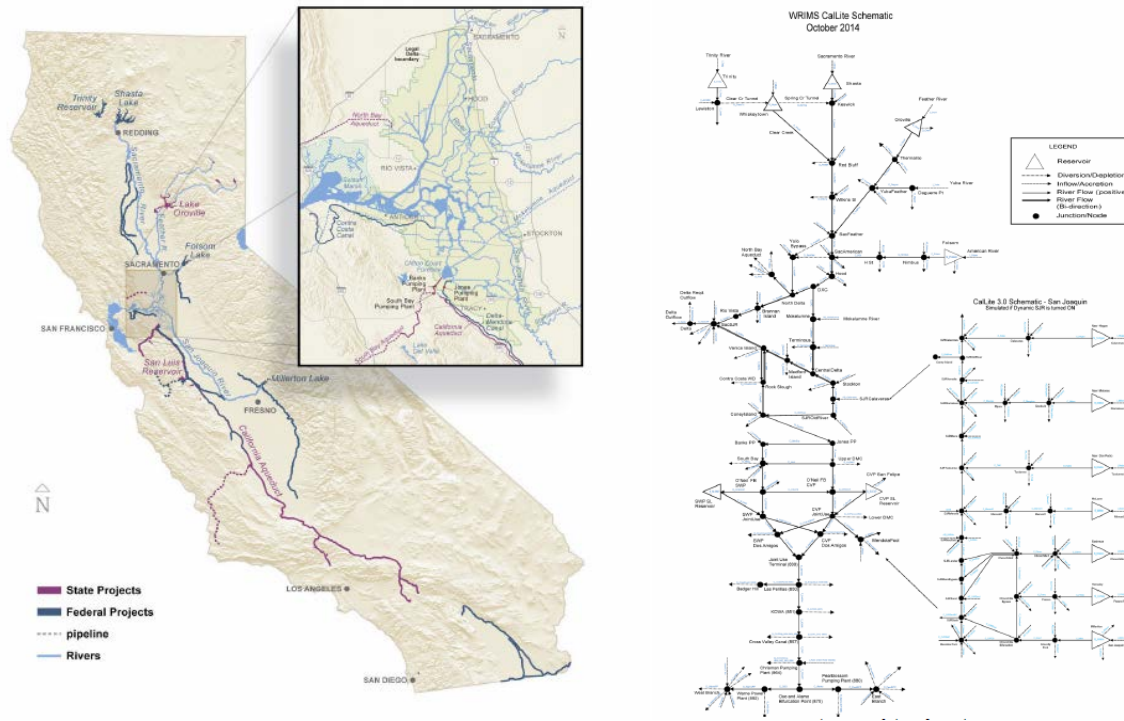


Figure 15. Callite schematic

### Generation of Inputs to Callite

Callite's 796 input parameters consist of: unimpaired inflow, impaired inflow, return flow, base flow, groundwater inflow, outflow, and pumping, water demands, evaporation rates, precipitation rates, diversion requirements, delivery patterns, release hydrographs, water quality, storage levels, withdrawals, environmental triggers, and other variables. In order to perform a climate change stress test on the system, a methodology was needed to vary the 796 input time series in an internally consistent manner.

Of the 796 Callite inputs, 39 are hydrologic inflows to the CVS. These 39 inflows consist of the 12 rim basin inflows, 9 "unimpaired" local inflows, and 18 "other" local inflows. Internal consistency in these hydrologic inflows can be maintained using the weather generator in combination with the SAC-SMA-DS hydrologic model. Further, most of the input variables were found to have a relatively small impact on model output. Of the 796 inputs, only 20 (the 12 rim basins plus 8 of the 9 unimpaired local inflows) of the 39 inflow variables and 11 of 18 accretion/depletion (AD) terms exerted strong influence on model output.

The SAC-SMA-DS hydrologic model was used to simulate inflows for the 12 rim sub-basins (Table 4, and Figure 16 left), the 9 unimpaired inflows (Figure 16 right), and the location of 11 physical stream gages related to the 12 rim inflows (Figure 16 center). These flows represent the great majority of the total inflows to the CVS. As shown in Figure 16, the locations of the 11 stream gages in SAC-SMA-DS Calibration Set II are nearly identical to the locations of the basin outlets for the 12 rim inflows in Calibration Set I. This is because the historical data for the Callite 3.0 rim inflows are derived from the 11 physical stream gages described in Calibration Set II. Because it was important to validate the workflow shown in Figure 7 relative to the baseline run of the Callite 3.0 simulation model, the SAC-SMA-DS model was calibrated directly to the streamflow in the Callite 3.0 package (Calibration Set I). This is different than calibrating to historical observations, as the streamflow pre-loaded in the Callite 3.0 package is the output of a previous (Variable

Infiltration Capacity, VIC, Model) hydrologic modeling project performed for the CVS. To evaluate the quality of the original VIC hydrologic model output, and to gain the confidence associated with validation relative to historical observations, it was necessary to calibrate the SAC-SMA-DS directly to the observations at the 11 physical gages of Calibration Set II. The results of Calibration Set II were not used as input to Callite 3.0, but were used in determination of water year type classification, as described below.

**Table 4. Twelve Major Rim Inflows to the Callite Model**

American River (into Folsom Lake)
Merced River (into Lake McClure)
Stanislaus River (into New Melones Lake)
San Joaquin River (into Millerton Lake)
Mokelumne River
Calaveras River (into New Hogan Lake)
Feather River (into Lake Oroville)
Tuolumne River into (New Don Pedro Reservoir)
Sacramento River (into Shasta Reservoir)
Trinity River (into Trinity Reservoir)
Yuba River (into New Bullards Bar)
Clear Creek (into Whiskeytown Reservoir)

Calibration Set III was developed when it was realized that Calibration Set I and Calibration Set II failed to account for a substantial portion (especially south and west) of the total CVS basin area shown bounded in red in Figure 16. The 9 unimpaired inflow basins of Calibration Set III add information on CVS sub-basins that are rain-dominated (as opposed to many of the 12 rim inflows, which are largely snow-dominated), and accounts for a substantial portion of the rain that falls within the CVS system. The 9 basins of Calibration Set III are referred to as “unimpaired inflows” as they are the result of a modeling project that estimated the runoff “that would have occurred had water flow remained unaltered in rivers and streams instead of stored in reservoirs, imported, exported, or diverted” for 24 Central Valley sub-basins and the Sacramento-San Joaquin Delta for October 1920 through September 2003 [*Bay-Delta Office, 2007*]. Whereas Calibration Set I was used as direct input to Callite 3.0 and Calibration Set II was used principally as a check on Calibration Set I and in the development of water year type classification, Calibration Set III was used principally to add information to the process for generating other, non-hydrologic inputs to Callite 3.0.

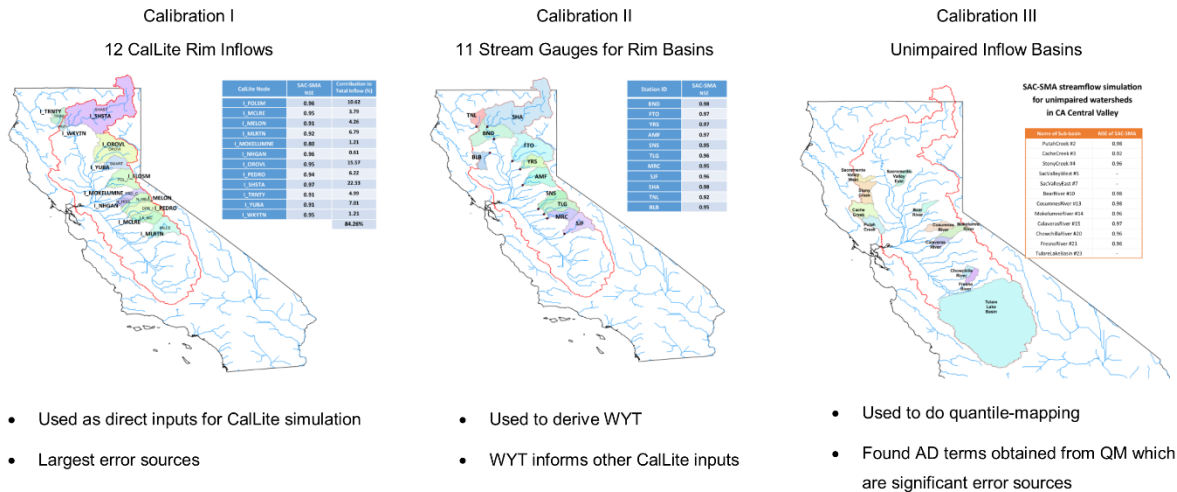


Figure 16. Maps of three calibration sets for the application of SAC-SMA-DS to the CVS

The other 27 local inflow inputs to CalLite, which make up the remaining portion of the system’s total inflows were not directly simulated, because: 1) acquisition of unimpaired natural flow for those rivers was not straightforward; and 2) the increasing computational effort was not justified by the increase in model accuracy (given the small fraction of total flow contribution). The AD terms could not be simulated using a hydrologic model because they are aggregations of hydrologic, management, and other anthropogenic behaviors that cannot be approximated as unimpaired catchment inflows.

The remaining 757 non-hydrologic time series fit into one of three categories: 1) constant value; 2) time series with several discrete steps, or recurring values; 3) or continuously varying time series. In both the discrete recurring value time series and continuously varying time series the values tended to vary as a function of hydrology (wetness or dryness of month), either directly (correlated to one of the 12 rim inflows of Calibration Set I or one of the 9 additional unimpaired inflows of Calibration Set III), or by way of one of two streamflow indices called “water year type”, developed using Calibration Set II. The Sacramento and San Joaquin Water Year Type indices classify the two major watersheds of the CVS into one of five states: “wet” classification, two “normal” classifications (above and below normal), and two “dry” classifications (dry and critical). Information regarding the DWR method of water year classification can be found at [http://cdec.water.ca.gov/cgi-progs/iodir\\_ss/wsihist](http://cdec.water.ca.gov/cgi-progs/iodir_ss/wsihist).

In order to evaluate the goodness of fit of each CalLite input parameter to the DWR water year types, 60 water year type values were computed (5 water year types x 12 months) for each of the Sacramento and San Joaquin Water Year Type Indices. The average value of each CalLite input parameter was calculated for each month of each water year type. For the purpose of exploration of correlation with the water year types, then, the raw time series of each input parameter was regressed against a discrete time series (with 60 unique values) representing the water-year-type-average in each month of each year of the historic record.

Seven hundred nineteen of the non-rim-inflows were better correlated to a water year type index (either the Sacramento or the San Joaquin index) than they were to one of the 21 particular rim/unimpaired inflow streams (Table 5). Those 719 CalLite input parameters were therefore associated with one of the two water year type indices and varied accordingly. Most of the remaining CalLite input parameters were associated with a particular rim inflow and varied in response to variations in that stream using a quantile mapping

technique. The values of a few of the CalLite input parameters were generated by way of special processes unique to those inputs. This section describes the process for quantile mapping, water year typing, and the application of “special conditions”.

**Table 5. R Squared Correlations for 31 most important inputs**

CalLite Input Parameter	Correlation Coefficient	Best Fit
I_NHGAN.FLOW.INFLOW	1	I_NHGAN
I_SHSTA.FLOW.INFLOW	1	I_SHSTA
I_FOLSM.FLOW.INFLOW	1	I_FOLSM
I_OROVL.FLOW.INFLOW	1	I_OROVL
I_MCLRE.FLOW.INFLOW	1	I_MCLRE
I_WKYTN.FLOW.INFLOW	1	I_WKYTN
I_PEDRO.FLOW.INFLOW	1	I_PEDRO
I_MLRTN.FLOW.INFLOW	1	I_MLRTN
I_LEWISTON.FLOW.INFLOW	1	I_TRNTY
I_TRNTY.FLOW.INFLOW	1	I_TRNTY
I_MELON.FLOW.INFLOW	1	I_MELON
I_YUBA.FLOW.INFLOW	1	I_YUBA
I_MOKELUMNE.FLOW.INFLOW	1	I_MOKELUMNE
I_ESTMN.FLOW.INFLOW	0.99	ChowchillaRiver
I_HNSLY.FLOW.INFLOW	0.99	FresnoRiver
AD_REDBLF.FLOW.ACCRDEPL	0.92	StonyCreek
AD_MOKELUMNE.FLOW.ACCRDEPL	0.9	CosumnesRiver
I_CALAV.FLOW.INFLOW	0.78	PutahCreek
AD_SACFEA.FLOW.ACCRDEPL	0.77	StonyCreek
AD_CALAVERAS.FLOW.ACCRDEPL	0.75	I_NHGAN
AD_YOLOBP.FLOW.ACCRDEPL	0.7	PutahCreek
AD_SJR_PULSE_V.FLOW.CHANNEL	0.65	I_MOKELUMNE
AD_SJR_V.FLOW.ACCRDEPL	0.65	I_MOKELUMNE
AD_SJR_VAMP_V.FLOW.CHANNEL	0.64	I_MOKELUMNE
AD_YUBFEA.FLOW.ACCRDEPL	0.46	CacheCreek
I_MDOTA.FLOW.INFLOW	0.39	I_MELON
I_TUOL.FLOW.INFLOW	0.27	CalaverasRiver
I_KELLYRIDGE.FLOW.INFLOW	0.26	SacWYT
I_KERN.FLOW.INFLOW	0.25	I_MLRTN
AD_WILKNS.FLOW.ACCRDEPL	0.24	SacWYT
AD_SACAME.FLOW.ACCRDEPL	0.1	SacWYT

## Creating Synthetic Time Series by Quantile Mapping Method

In parallel, each of the remaining 784 input time series were synthetically generated by quantile mapping the historical unimpaired flow time series for each of the [DWR 24 unimpaired flow basins](#) (as modeled by DWR Bay Delta Office) to the historical values of each time series in the CalLite input file.

The CalLite input parameters that correlated most closely with one of the rim inflows were paired with that inflow. For example, Figure 17 shows the correlation that two historical local inflows have (I\_BRANANIS and I\_MDOTA) with the historical inflows of the 12 rim basins and the rim inflows of I\_NHGAN and I\_MOKELUMNE are selected as the best pairs of I\_BRANANIS and I\_MDOTA respectively. The pairs of local and rim inflows determined in this way are used in the quantile mapping procedure to generate new local inflows corresponding to new rim inflows. The quantile mapping procedure is described using an example in the following section. Table 6 shows pairs of local and rim inflows determined for all local inflows. Consequently, 6 of the rim inflows are selected based on which inflows are quantile-mapped.

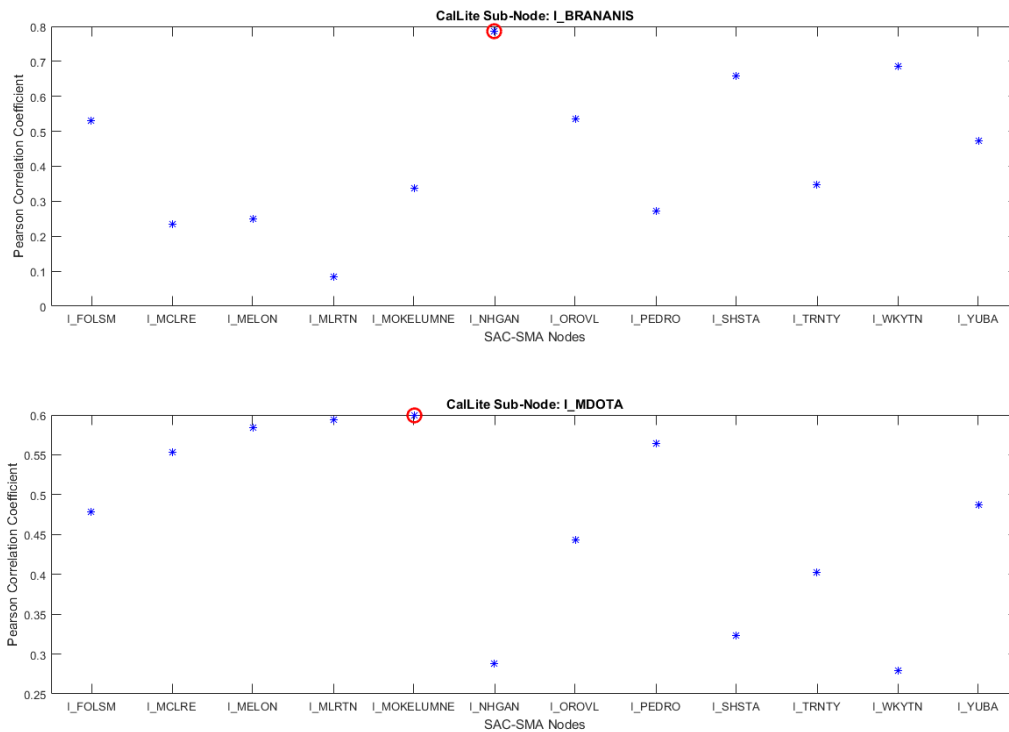


**Figure 17. Pearson correlation coefficients of two historical local inflows (I\_BRANANIS and I\_MDOTA) with historical 12 rim inflows.**

**Table 6. Pairs of rim flows and local inflows determined by correlation. Blue bold text in parentheses represent the values of Pearson’s correlation coefficient and red bold text represent contribution of local inflows to the total system inflows.**

Rim Inflow Nodes	Local Inflow Nodes
I_NHGAN	I_STANGDWN( <b>0.99</b> , <b>0.01%</b> ), I_NIMBUS( <b>0.94</b> , <b>0.03%</b> ), I_ESTMN( <b>0.91</b> , <b>0.28%</b> ), I_EASTBYP( <b>0.90</b> , <b>0.76%</b> ) I_CALAV( <b>0.87</b> , <b>0.05%</b> ), I_HNSLY( <b>0.87</b> , <b>0.33%</b> ), I_TERMINOUS( <b>0.83</b> , <b>0.22%</b> ), I_BRANANIS( <b>0.79</b> , <b>0.32%</b> ) I_STOCKTON( <b>0.77</b> , <b>0.06%</b> ), I_MEDFORDIS( <b>0.76</b> , <b>0.18%</b> ), I_HOOD( <b>0.72</b> , <b>0.05%</b> ), I_SACSJR( <b>0.72</b> , <b>0.02%</b> ), I_CONEYIS( <b>0.71</b> , <b>0.10%</b> ), I_MARSHCR( <b>0.61</b> , <b>0.13%</b> ), I_SJRMS( <b>0.57</b> , <b>0.09%</b> ), I_SJRMSA( <b>0.57</b> , <b>0.09%</b> ), I_TUOL( <b>0.42</b> , <b>0.79%</b> )
I_MELON	I_SJRMAZE ( <b>0.58</b> , <b>1.45%</b> ), I_SJRSTAN ( <b>0.58</b> , <b>0.08%</b> ), I_MERCED1B ( <b>0.51</b> , <b>0.33%</b> )
I_MLRN	I_KERN ( <b>0.49</b> , <b>0.10%</b> ), I_STANRIPN ( <b>0.32</b> , <b>0.40%</b> )
I_FOLSM	I_KELLYRIDGE ( <b>0.38</b> , <b>0.50%</b> )
I_MOKELUMNE	I_MDOTA ( <b>0.60</b> , <b>0.58%</b> )
I_TRNTY	I_LEWISTON ( <b>0.99</b> , <b>0.03%</b> )

Here, we provide a detailed description on the quantile mapping procedure with an example for the local inflow of I\_NIMBUS. For the I\_NIMBUS, the rim inflow of I\_NHGAN is selected as the best correlated inflow, with the correlation coefficient of 0.94. The quantile mapping procedure starts with fitting those two inflows to specific probability distributions. In this study, we employed two types of distributions: 1) empirical probability based on the Weibull plotting position, and 2) theoretical probability based on 2-parameter Gamma distribution. How the quantile mapping works for the I\_NIMBUS with selected rim inflow I\_NHGAN is illustrated in Figure 18. For those two inflows, both the empirical and theoretical distribution are fitted as shown in Figure 18; red line with asterisk dots represent the fit by the Weibull plotting position and blue line by the Gamma distribution. The red continuous empirical probability line is formed by doing a linear interpolation between values of asterisk dots. As shown in the figure, the new rim inflow lead us to the new local inflow value through those two quantile plots of local and rim inflows. The quantile mapping procedure is simply summarized in two steps: 1) find a quantile (i.e., non-exceedance probability) for the new rim inflow, 2) find the value of local inflow that corresponds to the quantile of the rim inflow. In our quantile mapping procedure, empirical distributions are used as long as new inflows are within historically observed range. In case the new inflows are beyond the historical range, Gamma distribution fit is used. This quantile mapping procedure is conducted on a monthly basis to take into account the seasonal variability of inflows.

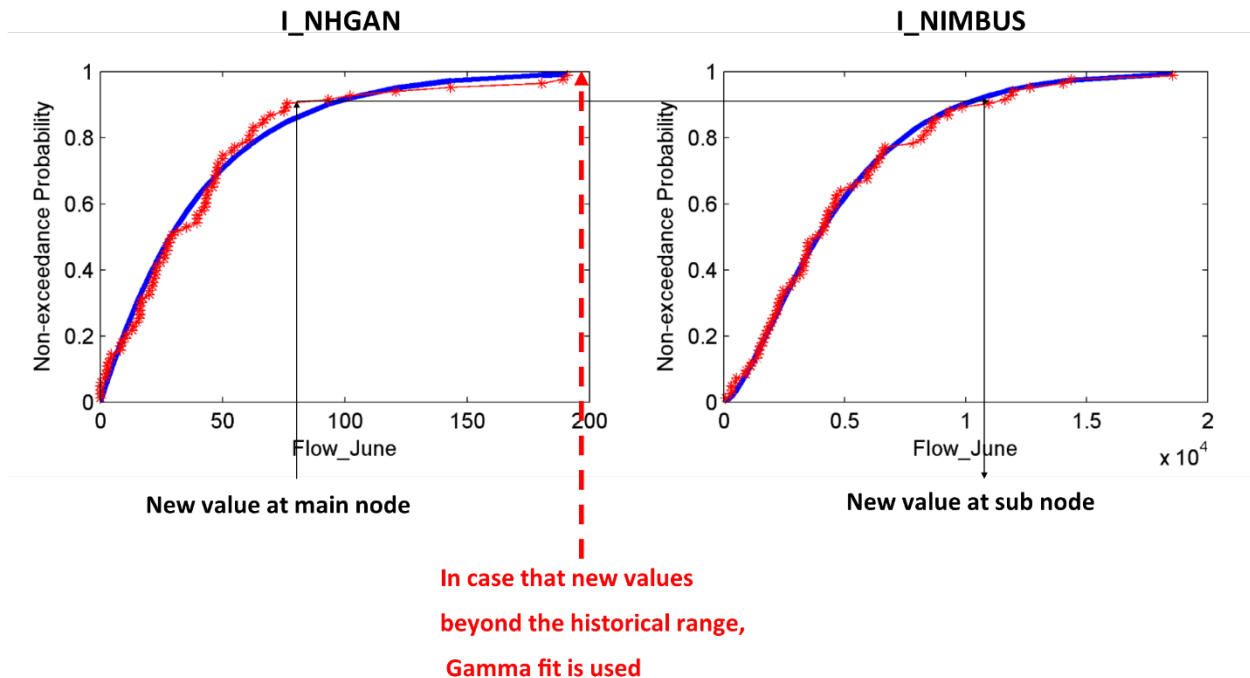


Figure 18. Quantile mapping procedure applied to example California sub-basin

#### Creating Synthetic Time Series by Water Year Type Method

For those CalLite input parameters that correlated most closely to one of the two water year type classifications (Sacramento or San Joaquin), a discrete, 60-value mapping procedure was then used.

As described by *Null and Viers [2013]*, “water year classification systems and hydrologic indices are common for water planning and management because they simplify complex hydrology into a single, numerical metric that can be used in rule-based decision making.” Water year type classification systems have been applied to development of drought indices throughout the United States [e.g., *Heim, 2002; Quiring, 2009*], and to such purposes as hydropower reservoir management in Chile [*Olivares et al., 2015*]. Explicit linking of water system operations to water year type provides the opportunity to bring water system operations in better synchronicity with the needs of aquatic ecosystems, which depend on patterns of hydrologic variability for the integrity of their lifecycles [*Richter et al., 1997*].

The sixty values for each input variable were calculated using the historical observed dataset. The historical dataset was sorted by historical water year type classification and an average value for each month-water year combination was calculated. To generate the synthetic input time series, the water year type was calculated based on the synthetic hydrologic input time series using the appropriate water year calculation methodology—which is a combination of rim inflows<sup>4</sup>. The historical calculated sixty values were then mapped into the synthetic time series input variable according to the water year type and month combination. Figure 19 shows three variables that show strong correlations with the San Joaquin Water Year Type classification.

<sup>4</sup> <http://cdec.water.ca.gov/cgi-progs/iodir/WSIHIST>

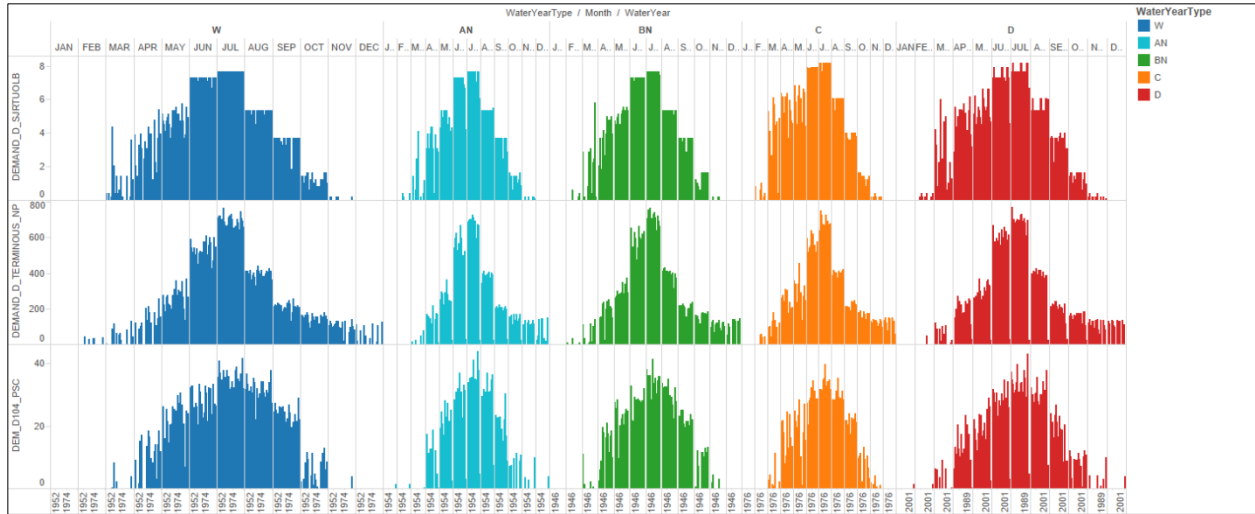


**Figure 19. Input variables with strong correlation to San Joaquin Water Year Type classification-historical observed data shown.**

#### Parameter-Specific Generation of Callite Input (i.e., Special Cases)

Two AD terms, AD-Wilkins and AD-SACAME, had a large impact on model performance and did not correlate well to rim/unimpaired inflow or water year type averages. Additional efforts were made to create new versions of these time series.

#### *AD-Wilkins*

The AD-Wilkins time series contained very large negative values. Through visual inspection this time series was identified as containing weir operations. Tisdale is likely the weir contained within the AD Wilkins time series. The design capacity of the [Tisdale weir is 38,000 cfs](#) which seems reasonable when compared to the largest negative values contained in the AD Wilkins time series (Figure 20). AD Wilkins correlated well to unimpaired flow from the Bay Delta Office’s Shasta unimpaired flow basin. When flow from the Shasta basin exceeds 13,300 cfs it was assumed that water begins to exit the Sacramento River via a weir. Two linear equations were developed for AD Wilkins: one for conditions in which Shasta flow is less than 13,300 cfs, and another when flow exceeds 13,300 cfs (Figure 20).

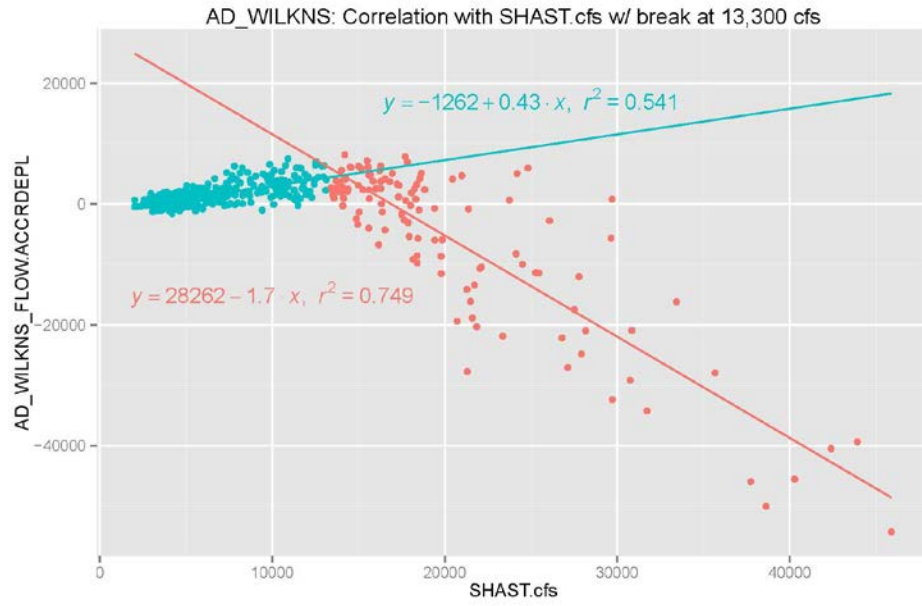


Figure 20. AD\_Wilkins: Correlation with Shasta flow

### AD-SACAME

The AD-SACAME input term did not correlate well with any of the methods described above for synthetically generating the variable time series. After an exhaustive search for a more skillful method of synthesizing the variable it was decided to use the Sacramento water year type classification average. It should be noted that the AD-SACAME time series of historical observed values contains some extremely negative values at the end of the time series (Figure 21) which call into question the assumptions used to create the CalSim terms on which the AD SACAME time series is based.

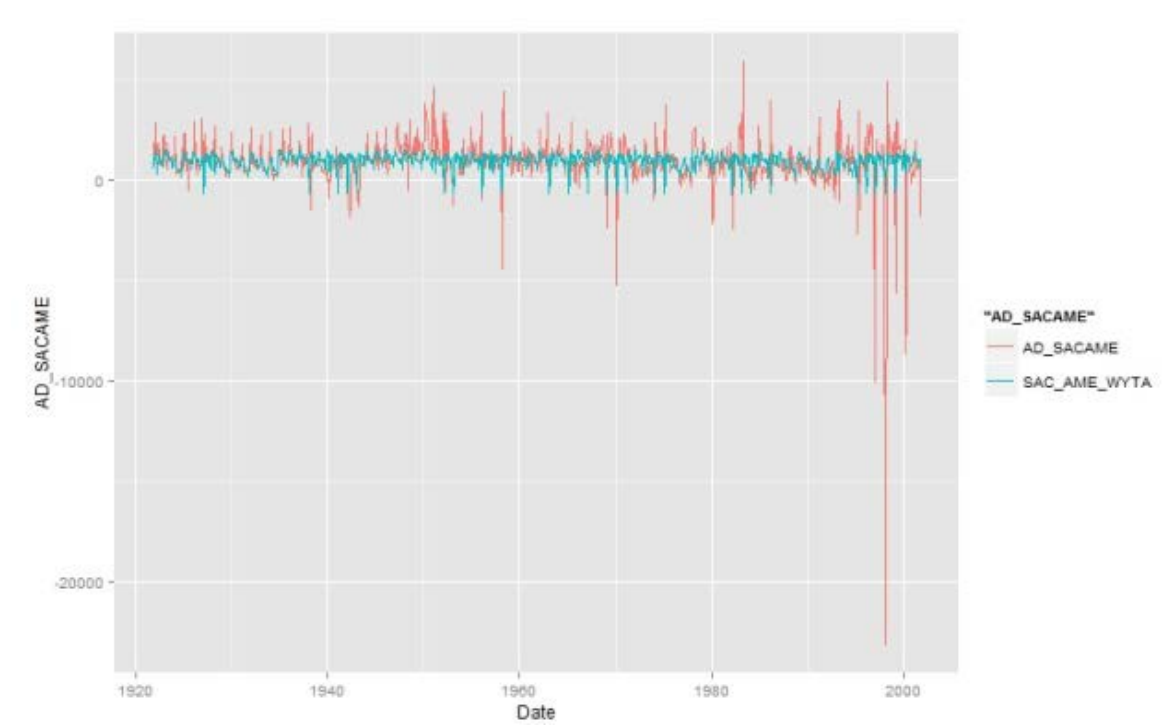


Figure 21. AD\_SACAME historical behavior

### Sea Level Rise Assignment for CalLite 3.0

At the time this project was initiated, only 3 existing sea level rise options existed within CalLite: 0 cm, 15 cm, and 45 cm. Therefore, the sea level rise implementation scheme adopted for this study made use of the available tools. Using [National Research Council, 2012], sea level rise along the California Coast south of Cape Mendocino was plotted as a function of year (Figure 22). With this relationship between future year and expected levels of sea level rise, and values for projected global temperature increases by year from Figure 11.9 of the Working Group I contribution to the Fifth Assessment Report of the Intergovernmental Panel on Climate Change [IPCC, 2014], curves were calculated for sea level rise along the California Coast south of Cape Mendocino as a function of temperature.

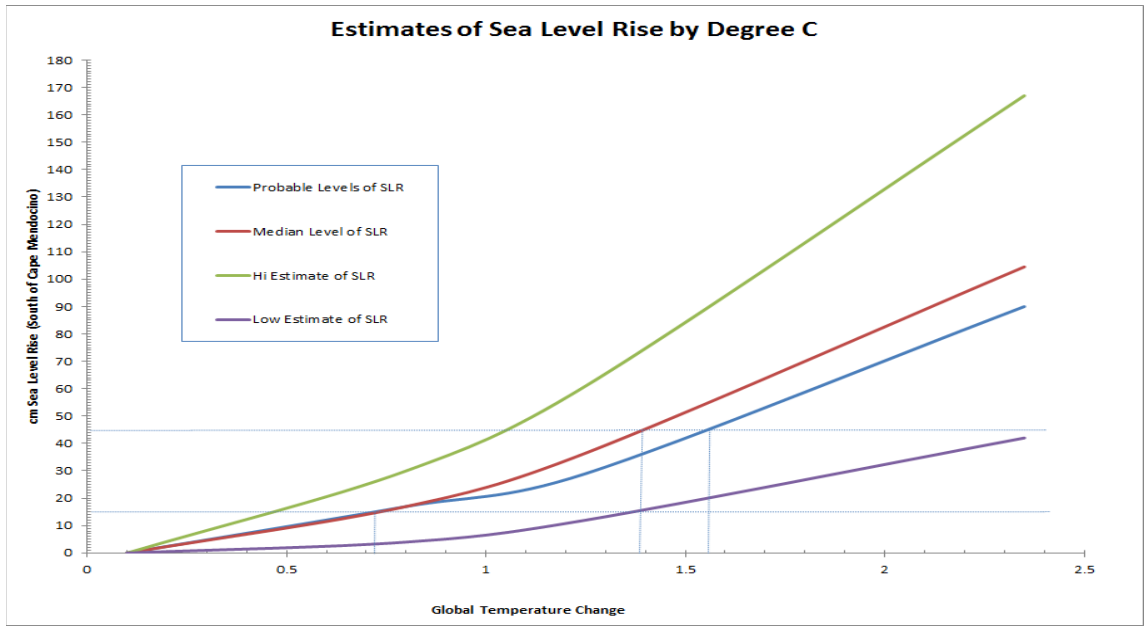


Figure 22. Estimates of Sea Level Rise by Degree C

The sea level rise assignment for Callite 3.0 was thus made according to the logic shown in Table 7, which approximates and discretizes to the three sea level rise steps available within the model our best understanding of the level of sea level rise that would be expected at each increment of temperature change. Each time a climate trace was run through Callite 3.0, the degree of temperature shift it received (as described in reference to Table 3) was noted, and the corresponding sea level rise function within the model was set according to Table 7.

Table 7. Sea Level Rise Discretization within Callite 3.0

Temperature change relative to recent historical	Sea level rise relative to recent historical
0 C	0 cm
0.5-1.0 C	15 cm
≥ 1.5 C	45 cm

## Model Verification

### Weather Generator Performance

Figure 23 summarizes the performance of the WARM weather generator in terms of its reproduction of the statistics of annual precipitation. On power spectrum, black line is observed power spectrum, the red is the 90% significance level, the blue is power mean spectrum of simulated runs, and the grey polygon block is 95% confidence interval around observed power spectrum. Figure 23 shows that the 5000 runs generated capture the signal approximately, with some of the generated runs meeting or exceeding the 90% confidence interval for power spectrum at approximately 15 years, and some falling below the historical power spectrum at 15 years. The boxplots of mean, standard deviation, and skew show that the 5000-run ensemble maintains

mean very well (red dot is mean of historic record; blue dot is ensemble mean; boxplot presents percentiles of 5000-trace ensemble), and under-represents the historic standard deviation and skew.

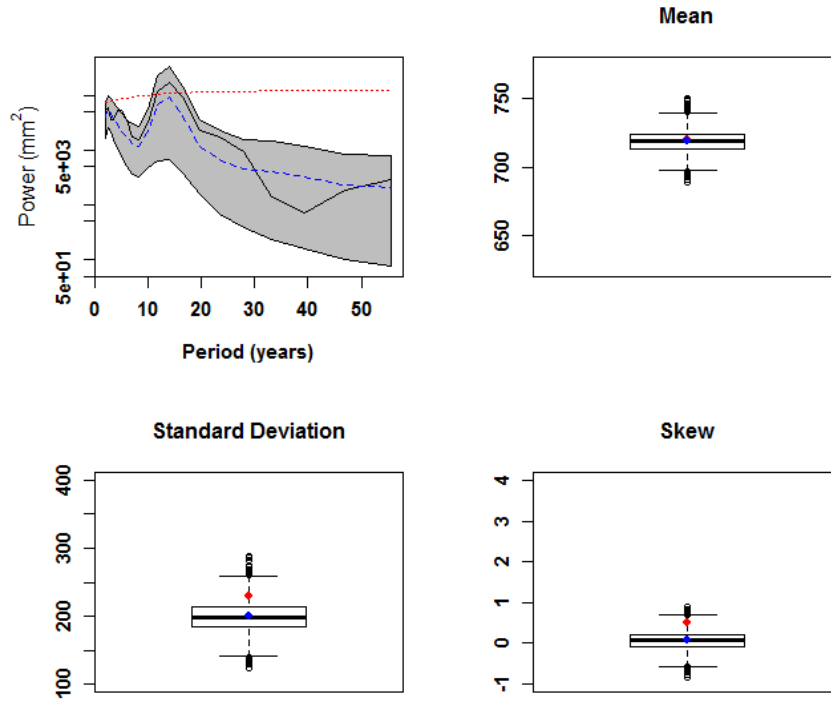


Figure 23. Performance of WARM Weather Generator WARM – Annual Precipitation

Table 8 summarizes the performance the twelve weather generator traces selected for use in this study. The twelve traces are listed in order of the increasing non-exceedance probability of the total precipitation of the worst 5-year drought contained in each. All of the selected runs reproduce historical mean annual precipitation within  $\pm 1\%$ , and historical standard deviation of annual precipitation within  $\pm 18\%$ . Half of the selected runs capture the 15-year low frequency variability, as quantified in the 90% significance level for the historical power spectrum. Generally, those selected runs that contained severe (low precipitation non-exceedance probability) droughts, also captured the 15-year low frequency climate signal.

Ideally, the standard deviation of the selected runs would be within  $\pm 5\text{-}10\%$  of the historic. This was not controlled for in the preliminary stages of this study, but will be controlled for going forward. A tight filter will not be used for skew, as skew is too noisy a metric of variability and can be dominated by a single outlier measurement. Instead, greater attention will be given to maintenance of the 15-year low frequency climate signal, and by so doing, the expectation is that skew will fall reasonably in line with the historical.

**Table 8. Statistics of the 12 WARM Weather Generator Runs Selected for Drought Characteristics**

Empirical percentile of worst 5-yr drought in trace	1 <sup>st</sup>	1 <sup>st</sup>	1 <sup>st</sup>	25 <sup>th</sup>	25 <sup>th</sup>	25 <sup>th</sup>	50 <sup>th</sup>	50 <sup>th</sup>	50 <sup>th</sup>	75 <sup>th</sup>	75 <sup>th</sup>	75 <sup>th</sup>
WG trace number	824	871	2104	1653	3075	4623	3148	3208	4038	3408	4214	4259
% dev trace mean from historic mean	-0.22	0.27	-0.78	0.99	0.59	-0.28	0.66	0.67	-0.14	0.95	0.87	0.51
% dev trace stand. dev. from historic st. dev.	-17.84	-9.90	13.85	9.22	8.53	-8.05	-1.18	-3.11	-2.29	5.68	-14.06	-13.90
15-yr Power Spectrum 90% sig?	Y	Y	Y	Y	nearly	Y	N	N	N	N	N	N

During the worst five-year drought from 1915-2010, which occurred from 1928-1932, the average annual precipitation was 453 mm/yr. During the worst five-year drought from 1950-2003, which occurred from 1986-1990, the mean annual precipitation was 510 mm/yr. The mean annual precipitation in the 1<sup>st</sup> percentile drought sampled from the ensemble of 5000 WARM runs was 383 mm/yr.

### Hydrologic Model Performance

The SAC-SMA-DS applied to reproduce historical inflows of the 12 rim sub-basins shows very good performance as shown in Table 9. The performance metrics of NSE evaluated on the monthly simulated streamflow show values of above 0.9 for all except for the sub-basin Mokelumne, for which NSE is 0.8. Considering the recommendation of *Moriasi, et al.* [2007] that model simulation can be judged as satisfactory if  $NSE > 0.50$ , these simulation results are highly satisfactory and will greatly reduce the errors stemming from the hydrology.

**Table 9. Hydrologic model performance by sub-basin**

Sub-basin	Nash Sutcliffe
<b>Folsom</b>	0.96
<b>Merced</b>	0.95
<b>Stanislaus</b>	0.91
<b>San Joaquin</b>	0.92
<b>Mokelumne</b>	0.80
<b>Calaveras</b>	0.96
<b>Oroville</b>	0.95
<b>Tuolumne</b>	0.94
<b>Shasta</b>	0.97
<b>Trinity</b>	0.91
<b>Yuba</b>	0.91
<b>Whiskytown</b>	0.95

The second test of the hydrologic model was of its ability to reproduce historical water year type classification based on the flow of rim-inflow rivers, using an algorithm designed to reproduce the water year classification system used by DWR. The combined hydrologic model and water year classification algorithm was shown to successfully match water year type for every year of the historic record to the DWR method of water year classification ([http://cdec.water.ca.gov/cgi-progs/iodir\\_ss/wsihist](http://cdec.water.ca.gov/cgi-progs/iodir_ss/wsihist)).

## System Model Performance

Figure 24 through Figure 26 show sample output of CalLite validation run selected to demonstrate the skill of the model workflow (Figure 7) in reproducing historical CalLite output for each of the decision relevant metrics described in Table 1. Figure 24 presents the validation for Total North of Delta Storage, of which Oroville reservoir storage is a part. Figure 25 presents the validation for delta outflow. Figure 26 presents the validation for SWP deliveries.

The validation is a perfect reproduction prior to 1950, as no reliable climate data were available for development of weather generator traces before that time. Weather generator traces were used to develop hydrologic traces for development of input to CalLite in the period from 1950-2003.

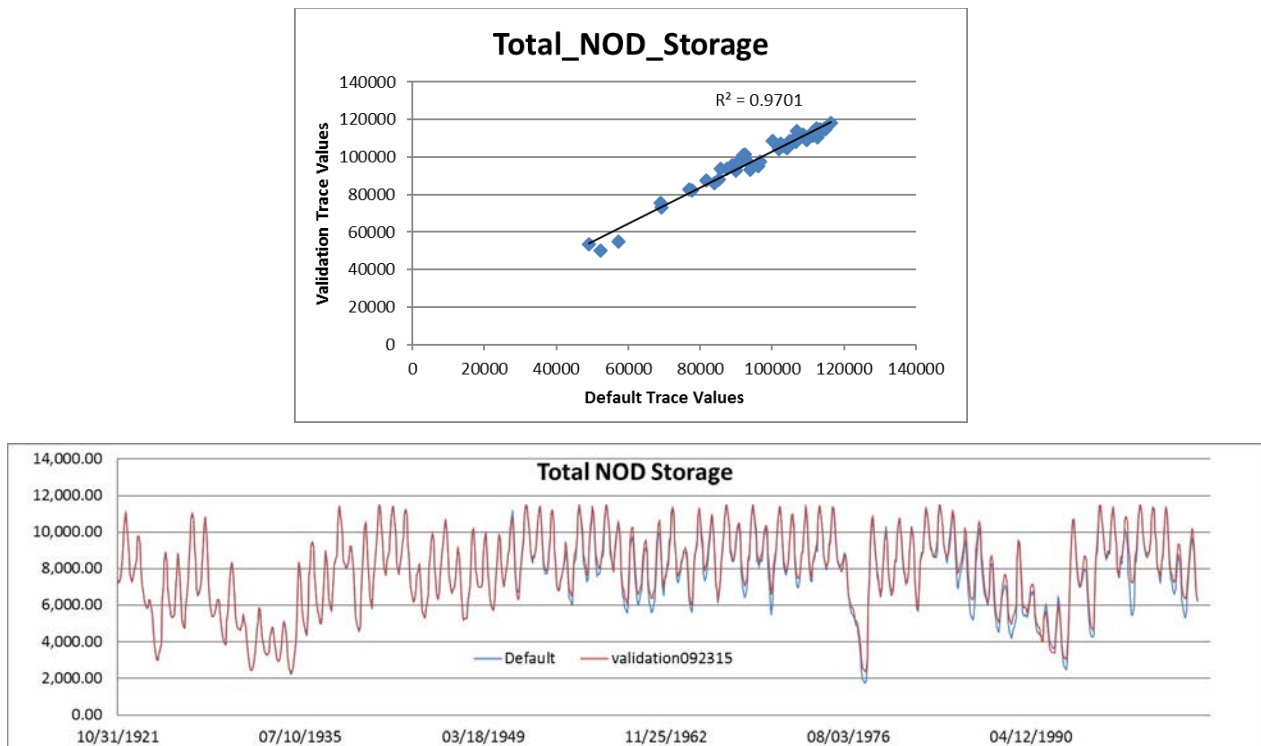


**Figure 24. Validation of CalLite stress test modeling workflow for Total North of Delta Storage. Top: Scatterplot fit of annual averaged validation trace values to default trace values. Bottom: Default (blue) and validation (red) trace monthly Total North of Delta Storage showing perfect fit before 1950 and differences after 1950.**

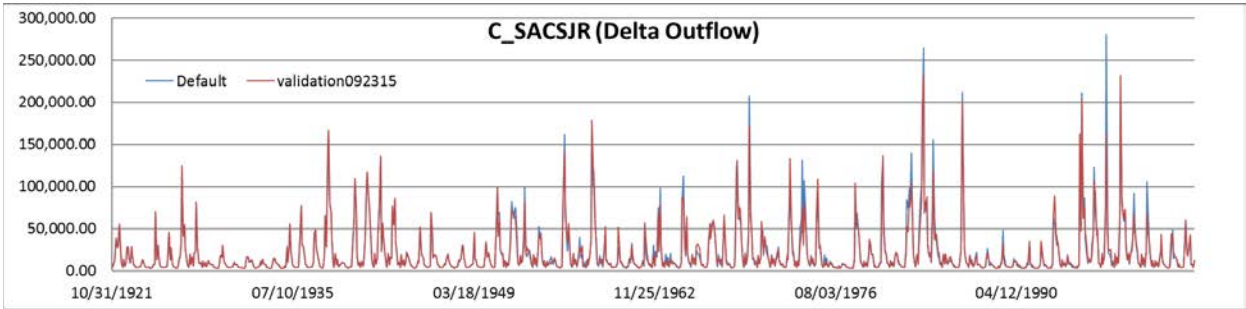
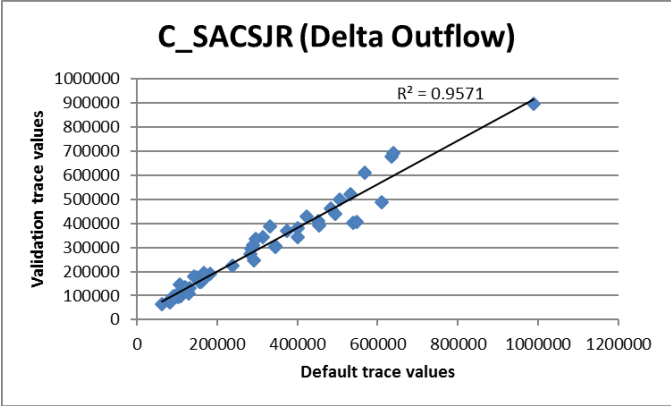
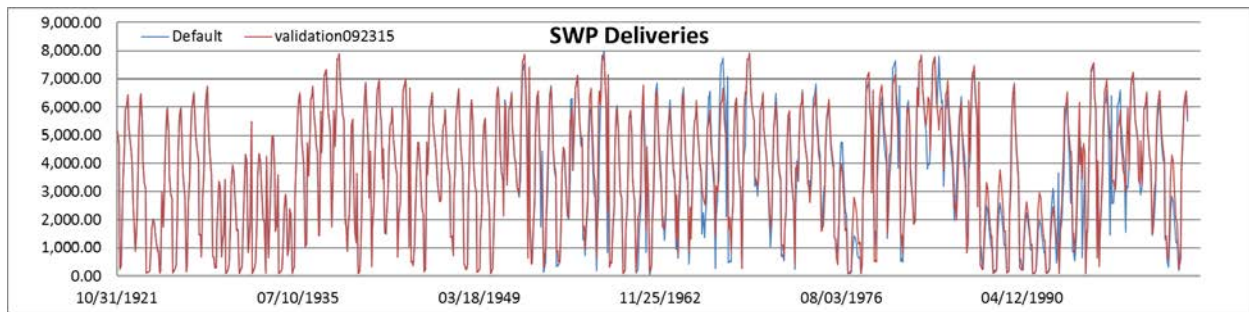
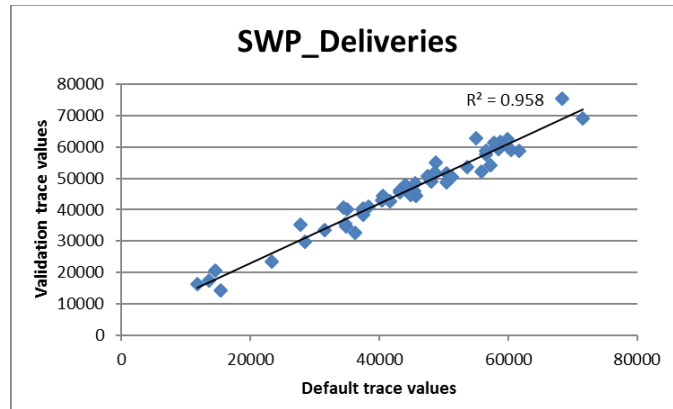


Figure 25. Validation of Callite stress test modeling workflow for Delta Outflow. Top: Scatterplot fit of annual averaged validation trace values to default trace values. Bottom: Default (blue) and validation (red) trace monthly Delta Outflow showing perfect fit before 1950 and differences after 1950.



**Figure 26. Validation of CalLite stress test modeling workflow for SWP Annual Deliveries. Top: Scatterplot fit of annual averaged validation trace values to default trace values. Bottom: Default (blue) and validation (red) trace monthly SWP deliveries showing perfect fit before 1950 and differences after 1950.**

## Risk Assessment Results

### Exposure

DWR's operation of the SWP is exposed to climate changed conditions throughout the state. In the watersheds from which water supplies originate, higher temperatures and changes in precipitation are expected to change the availability of water. In the Sacramento-San Joaquin Delta, water supplies interact with the Delta's complex hydrology, which is influenced by sea level, tides, and flows from several rivers. Throughout the SWP's service areas, demand for SWP water supplies will be affected by higher temperatures and changing precipitation.

Exposure to climate changes for these areas has been estimated using data from an ensemble of projections from the CMIP5 to develop probabilistic climate information. While the ensemble of models indicates a range of future outcomes in temperature and precipitation, we can infer conditional probabilities for temperature and precipitation change by plotting the bivariate normal distribution of the projected changes of the models. Figure 6 presented the conditional climate probability density for climate changes at 2050. By expressing the range of climate changes in the future as probabilistic possibilities a deeper understanding of the range of potential exposures is possible. In Figure 6, deeper blue colors represent higher agreement among the GCMs about future conditions, lighter blue colors represent future conditions that are predicted by fewer models, but that are still considered possible future outcomes.

## Sensitivity

The decision scaling approach described above was used to explore system performance for each of the metrics listed in Table 1. For each metric a system performance response surface was generated, which averages across the twelve climate traces described in Table 2 (the statistics of which were presented in Table 8) and the historical trace. The system performance response surfaces describe how the system performs over the range of temperature and precipitation changes. See insert box: “Understanding System Response Surfaces” for additional information on interpreting the information in these graphics.

The response surface describes the sensitivity of the SWP system to changes in climate. On the response surface, the black line represents performance at historical levels; warm colors represent performance worse than historical levels while cool colors represent performance better than historical levels. Changes in color represent sensitivity to a change in climate.

## Vulnerability and Risk

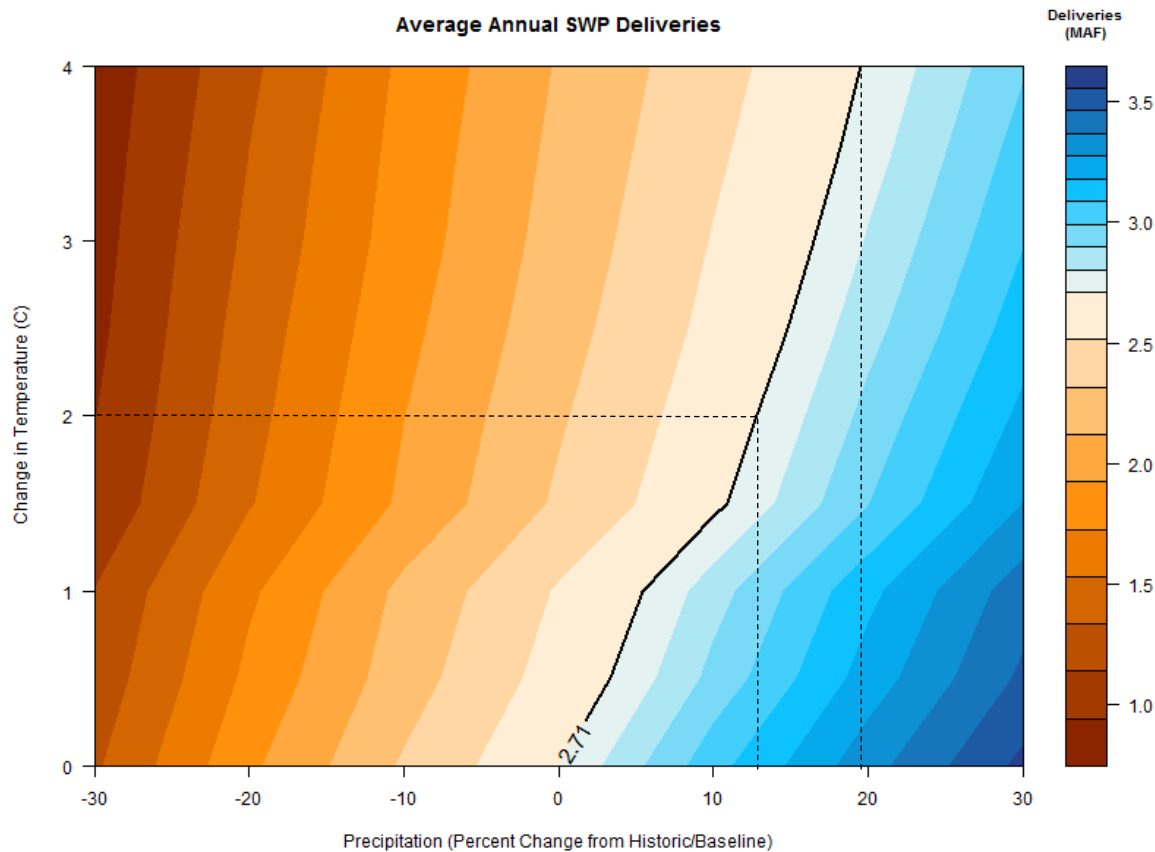
Exposure and sensitivity to climate changes have been described. By combining exposure and sensitivity with vulnerability and risk, probabilistic estimates for each of the selected performance metrics can be developed. In this step cumulative density functions (cdf’s) and probability density functions (pdf’s) are developed, which weight each run by the likelihood of its climate change space (and assuming every year within the trace to be equally likely, and a product of random internal variability represent-able as white noise). The year 2050 conditional climate probability density is summarized in Table 10. Table 10 is developed by assigning a bivariate normal distribution to the shifts in mean annual temperature and precipitation of the ensemble of CMIP5 GCM output for the years 2035-2065 relative to the same for 1970-2000.

**Table 10. Conditional Climate Probability Density of each Climate Change Shift, 1970-2000 to 2035-2065**

<b>Temp. Increase Over Histor.</b>	4	1.68E-10	7.78E-08	5.17E-06	4.92E-05	6.72E-05	1.32E-05	3.69E-07
	3.5	8.38E-09	3.15E-06	1.69E-04	1.31E-03	1.45E-03	2.30E-04	5.22E-06
	3	1.83E-07	5.58E-05	2.44E-03	1.52E-02	1.37E-02	1.76E-03	3.24E-05
	2.5	1.76E-06	4.35E-04	1.54E-02	7.79E-02	5.67E-02	5.90E-03	8.82E-05
	2	7.43E-06	1.49E-03	4.26E-02	1.75E-01	1.03E-01	8.71E-03	1.05E-04
	1.5	1.38E-05	2.23E-03	5.18E-02	1.72E-01	8.23E-02	5.63E-03	5.53E-05
	1	1.12E-05	1.47E-03	2.76E-02	7.45E-02	2.88E-02	1.60E-03	1.27E-05
	0.5	3.98E-06	4.24E-04	6.46E-03	1.41E-02	4.43E-03	1.99E-04	1.28E-06
	0	6.23E-07	5.37E-05	6.64E-04	1.18E-03	2.99E-04	1.09E-05	5.69E-08
		0.7	0.8	0.9	1	1.1	1.2	1.3
<b>Precipitation (relative to historical)</b>								

### Insert Box 5.2: Understanding the Response Surfaces.

For each performance metric, the response surface shows the performance that would be expected for various combinations of change in precipitation, warming, and sea level associated with warming. In the example below, SWP Annual Deliveries are shown. The value at 0 degrees warming and 0 change in precipitation essentially represents current conditions (i.e., the long-term average of SWP Annual Deliveries that would be expected if climate conditions remained stable at today's levels). This level of performance is referred to as the "current conditions estimate" and represents the simulated long-term average system performance over all 13, 50-year hydrological sequences with no climate warming beyond what has already occurred. A black line extends up and to the right from 0 degrees warming and 0 change in precipitation. This line represents system performance at the same level as the current conditions estimate. In other words, current performance levels can be maintained for the given metric at these combinations of warming and precipitation change. For the SWP Average Annual Deliveries metric, the current conditions estimate is 2.71 MAF. This same level of average annual deliveries could be maintained at 2 degrees C of warming coupled with about 13% higher precipitation rates or 4 degrees C warming and about 20% higher precipitation rates. Blue colors represent performance better than current conditions and orange/red colors represent performance worse than current conditions.



Each color band represents consistent system performance across a range of temperature and precipitation combinations. Bars that are more vertical indicate that the performance of the system is more sensitive to changes in average annual precipitation levels while bars that are more horizontal indicate that the system performance is more sensitive to warming temperatures.

It is important to note that the response surface does not describe performance at any given time in the future. The response surface simply illustrates how the system performs over the given range of precipitation and temperature. Also of importance is that the response surfaces presented in this report are for the current system infrastructure configuration, operations priorities, and regulations. The surfaces would change if any of these were to change in the future.

### Performance Metric 1: Oroville Storage

The response surface for Oroville April 1<sup>st</sup> Storage shows that historical simulated April 1<sup>st</sup> storage levels are approximately 3 million acre-feet (MAF), and that this metric is only moderately sensitive to changes in temperature and sea level, but is highly sensitive to changes in precipitation. A 10% increase in precipitation would be required to offset the storage losses resulting from a 2-degree C increase in temperature. This metric is less sensitive to temperature increase because it measures accumulated runoff into Oroville reservoir during the winter rainy season. Higher temperatures are likely to result in less snow fall and faster snow melting rates, with the result that a higher proportion of the winter precipitation would end up in the reservoir, and less would remain high in the watershed as snow. As this additional water enters the reservoir it increases storage levels, but leaves less water in the upper watershed to replenish the reservoir later in the season.

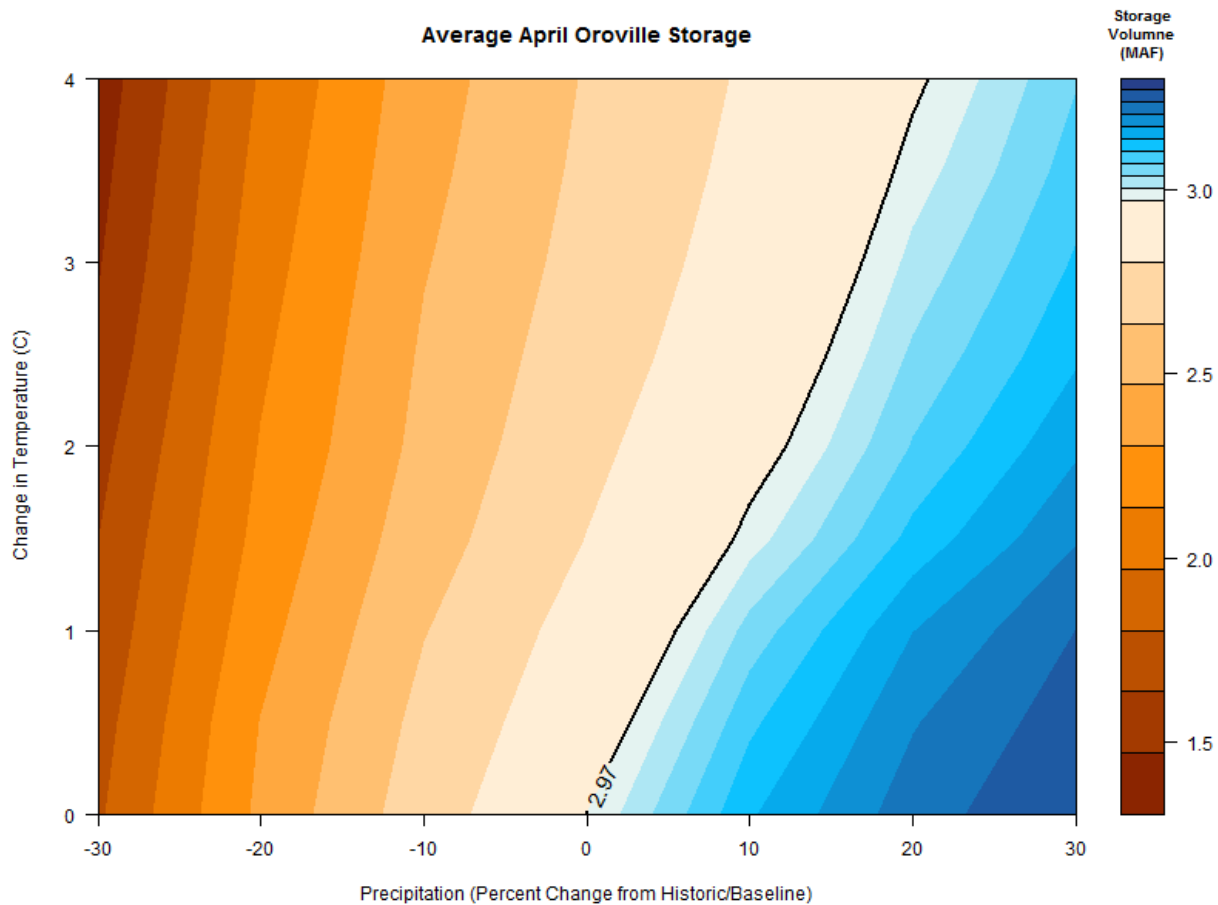
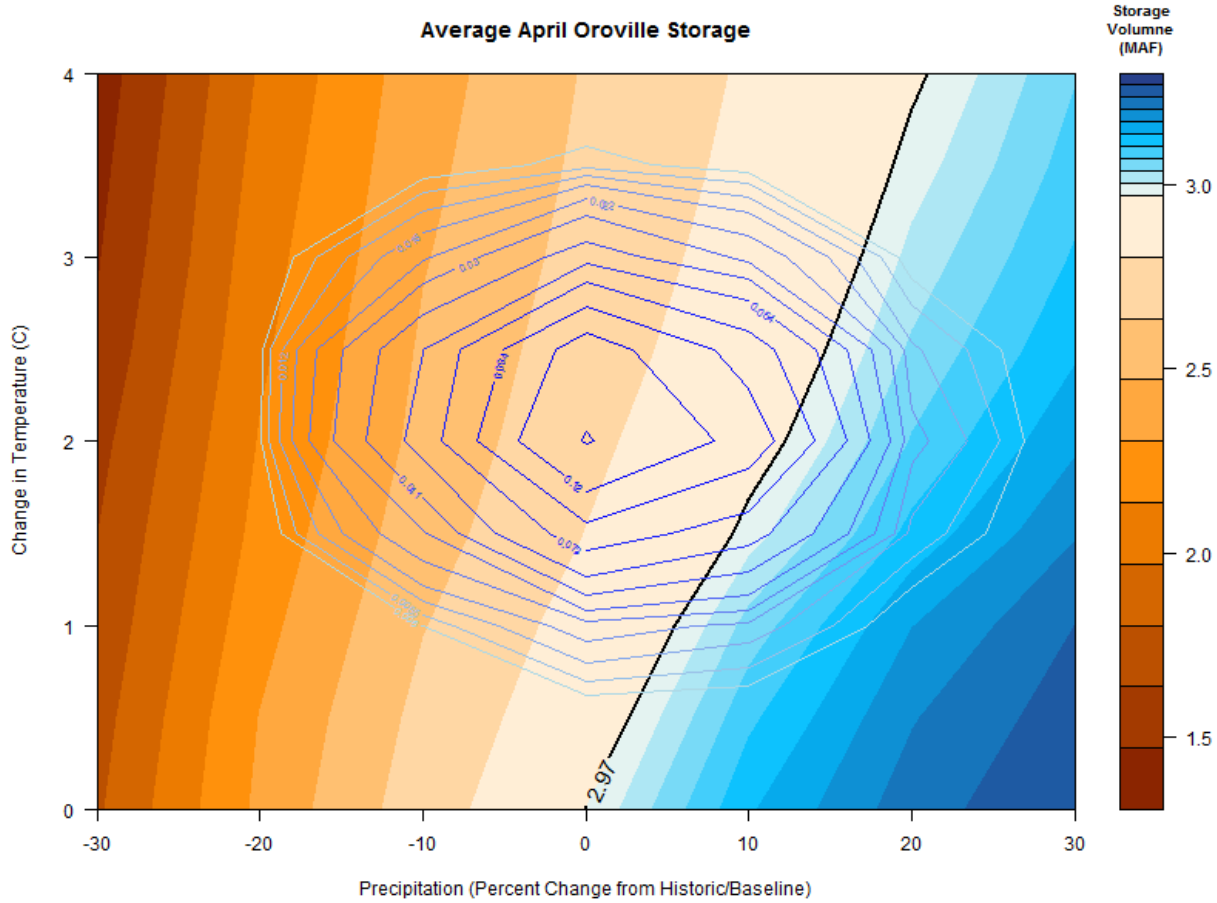
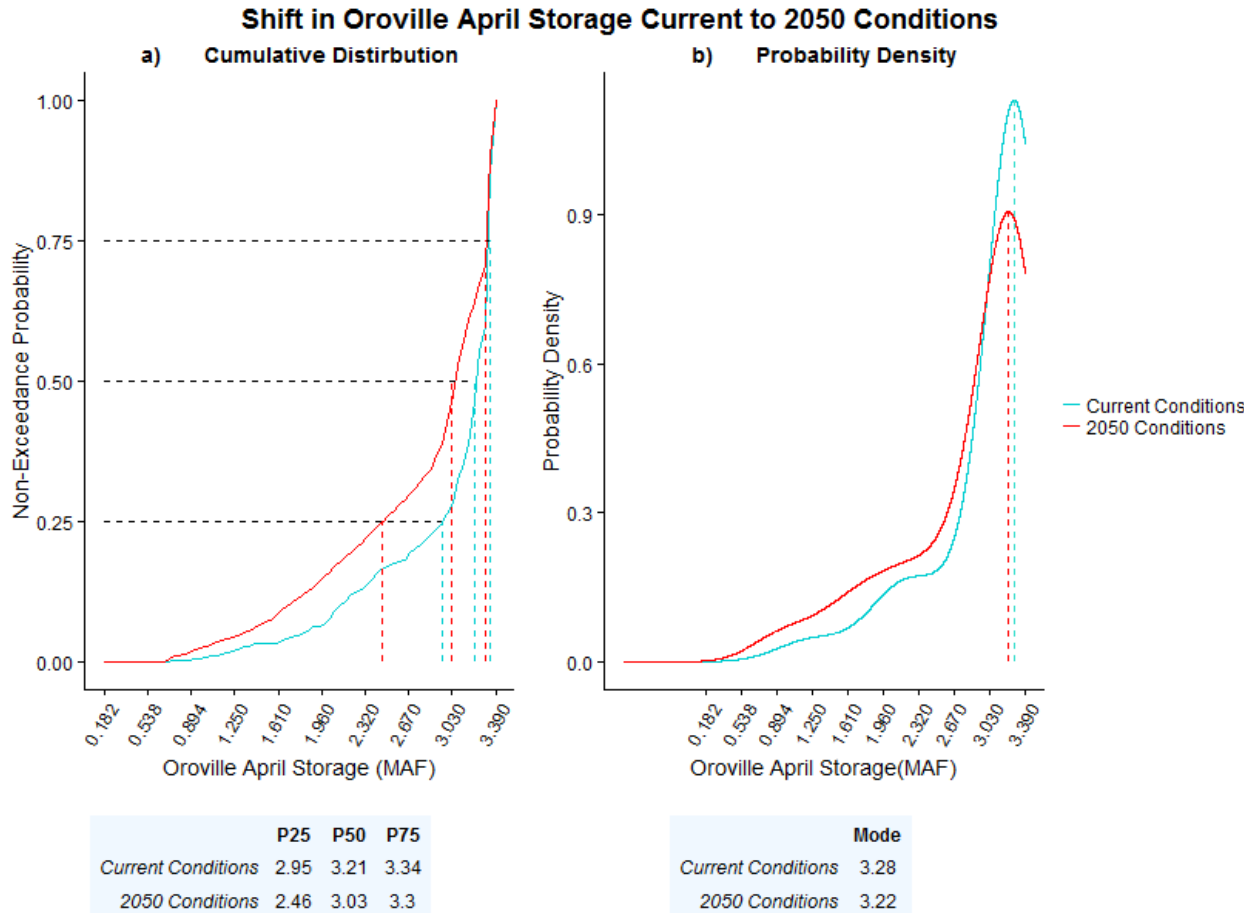


Figure 27. Response Surface – April 1<sup>st</sup> Oroville Storage

Risk is informed by the addition of the bivariate normal climate change cloud (Table 10) to Figure 27, as shown in Figure 28. The centroid of the GCM cloud is located at approximately 2 degrees of warming by mid-century, without a clear signal in precipitation change. The cloud indicates warming on the range from 1 to 3 C, with great uncertainty in future precipitation (which could be anywhere from 20% less to 28% more than recent historical). The uncertainty contained in Figure 28 makes it difficult to develop water system plans, as it is possible that April 1<sup>st</sup> Oroville Reservoir Storage might be greater (blue) or less (orange/brown) than

historical. As this stage of analysis, it is useful to evaluate probability distributions that can help to inform thinking on the likelihood of shortages in median, wet and dry climate states.





**Figure 29. Shift in April 1<sup>st</sup> Oroville storage, Current to Mid-Century Conditions**

The response surface for Oroville September 1<sup>st</sup> Storage (Figure 30) shows that historical simulated September 1<sup>st</sup> storage levels are approximately 2 MAF and that this metric is more sensitive to changes in temperature and sea level change than is April 1<sup>st</sup> Oroville reservoir storage. At temperature increases above 2.5 degrees C, even a 30% increase in average annual precipitation would not offset the loss in storage from increased temperatures. As described in reference to the April 1<sup>st</sup> Storage metric, the diminished snow reserves associated with higher temperature climate possibilities reduce the water available for later season replenishment, culminating in much lower storage levels at the end of the summer. This system response is also related to the higher sea levels assumed at higher temperature change levels. Above 1.5 degrees C, 45 cm of sea level rise are assumed, thus requiring more water to be released from storage (especially during the summer months) to repel sea water intrusion and meet delta outflow and salinity requirements. There is very little reason to believe, based on the GCM cloud superimposed on Figure 30 (right) that future Oroville Reservoir Storage will be greater than historical, and it seems likely that it will be substantially less.

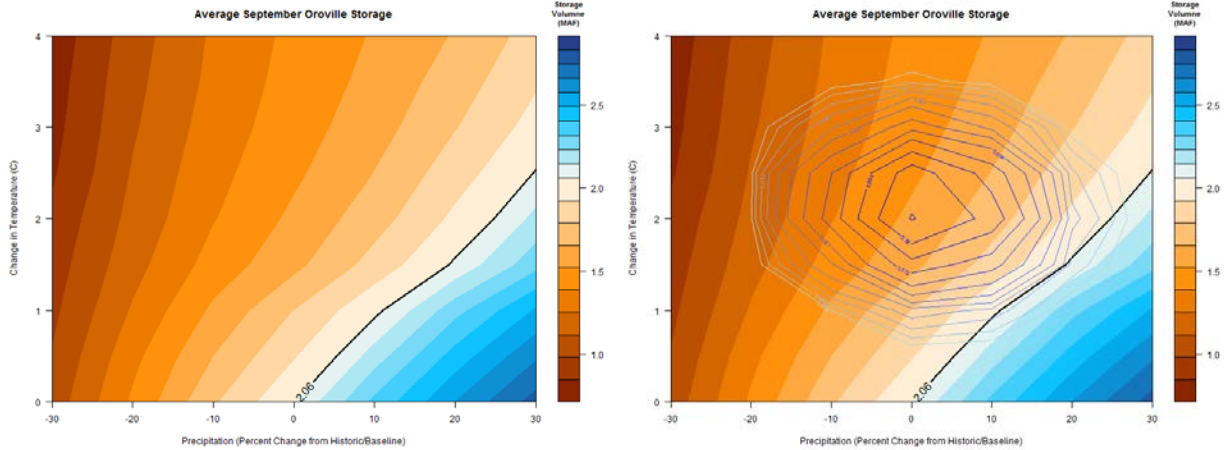
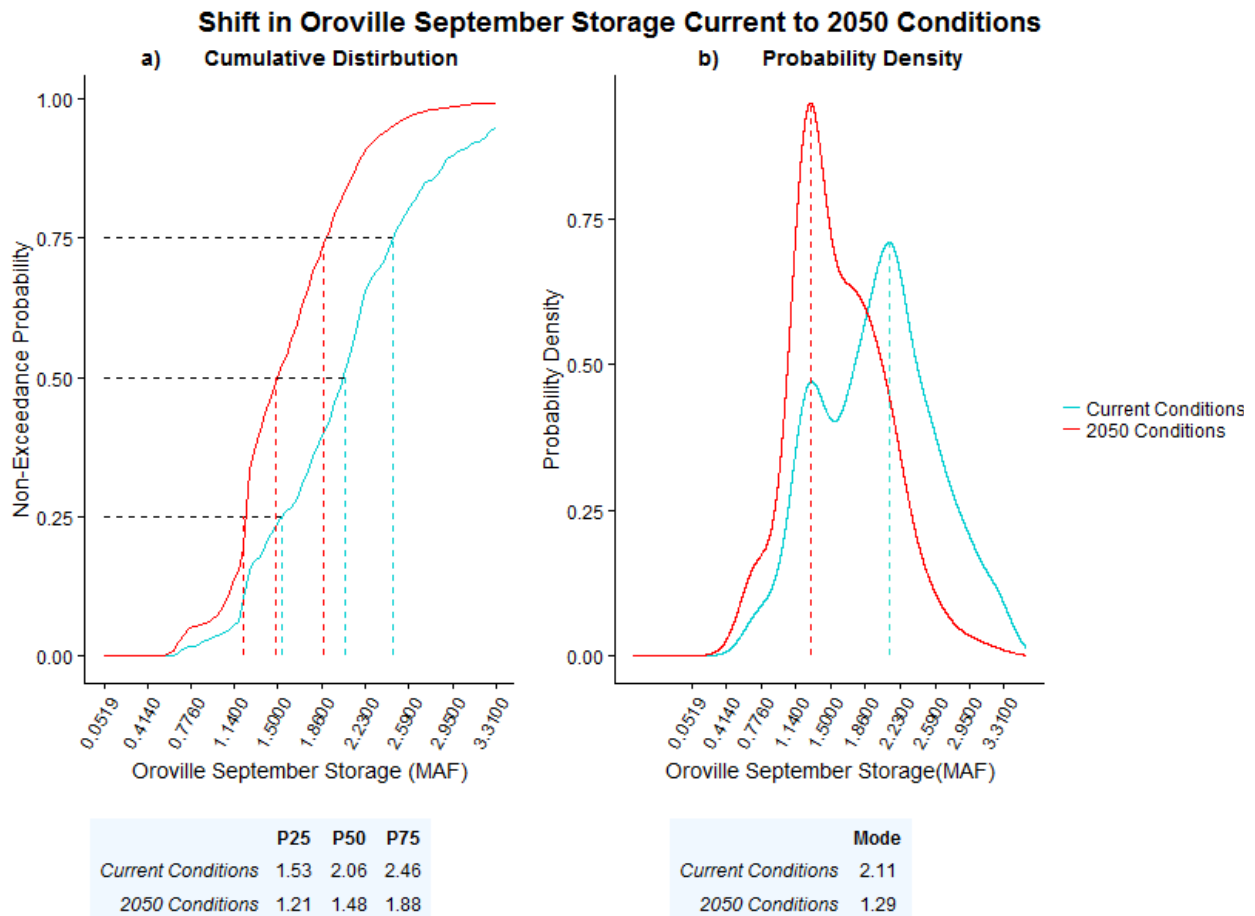


Figure 30. Response Surface – September 1<sup>st</sup> Oroville Storage without (left) and with (right) GCM “cloud”

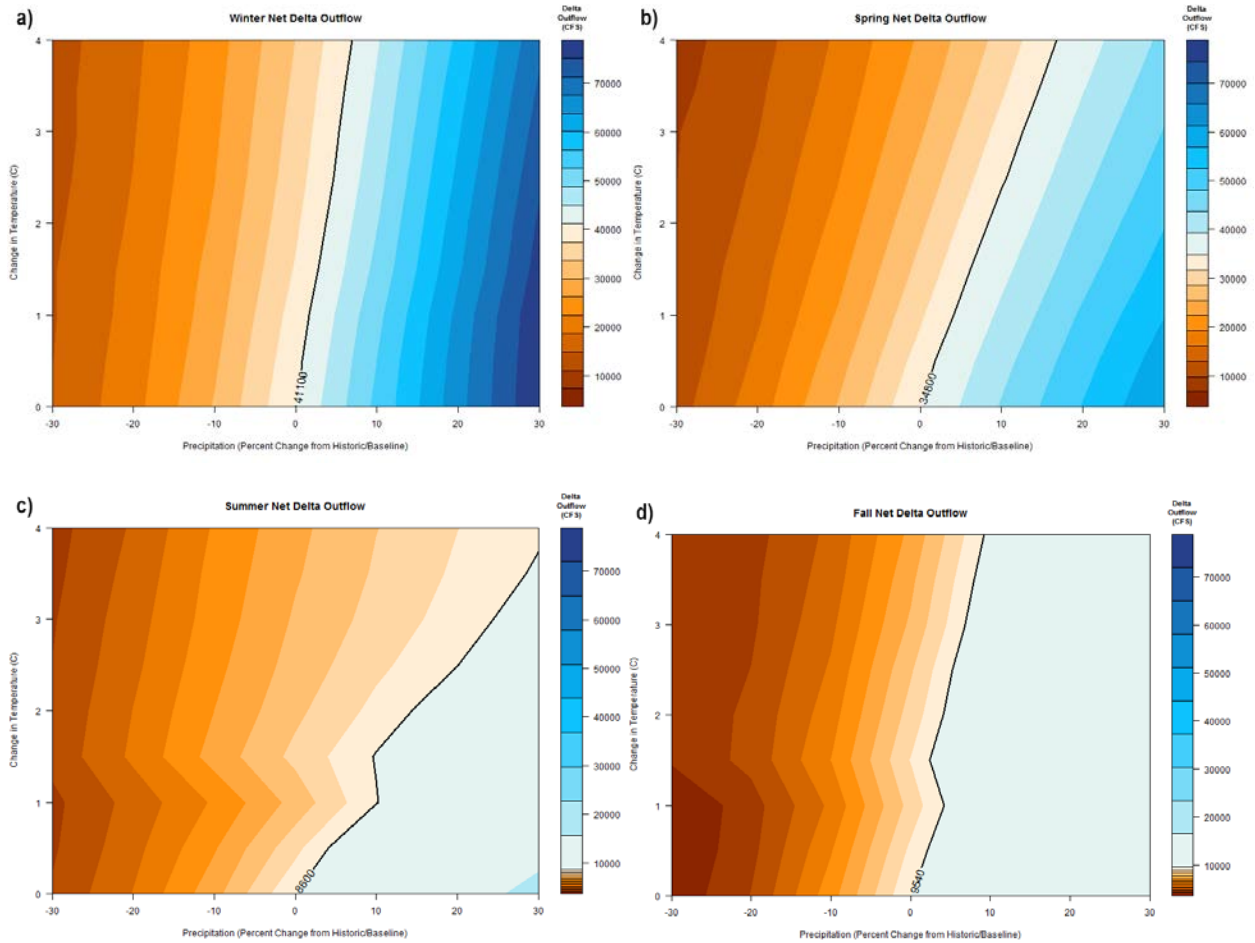
Figure 31a presents a cdf for September 1<sup>st</sup> Oroville reservoir storage. The cdf shows a downward shift of approximately 0.6 MAF (25-30%) in median September 1<sup>st</sup> Oroville storage by mid-century. The decrease in future September 1<sup>st</sup> Oroville storage is similarly significant at the 75<sup>th</sup> percentile, meaning that years that have historically been marked by high storage are likely to be disproportionately drier in the future, with less change during years of lower than average storage. Figure 31b shows a large (35-40%) downward shift in the mode of the pdf of future Oroville September storage relative to current conditions.



**Figure 31. Shift in September 1<sup>st</sup> Oroville Storage, Current to Mid-Century Conditions**

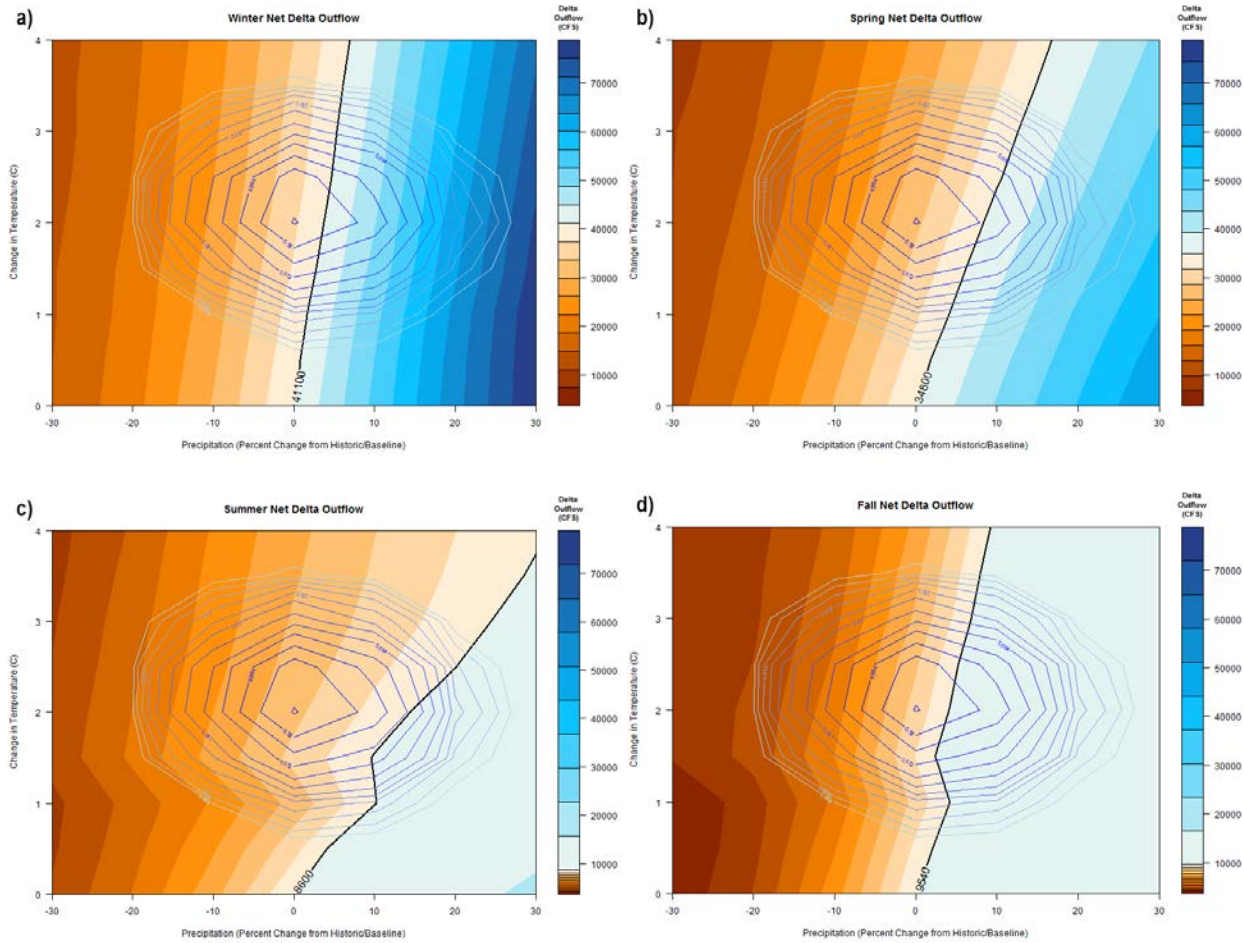
#### Performance Metric 2: Net Delta Outflow

The response surfaces for net delta outflow (Figure 32a-d) show the relative sensitivity of delta outflow in each season to precipitation change, temperature change, and sea level change. Winter delta outflow (Figure 32a) is largely insensitive to temperature change and sea level change, but highly sensitive to precipitation change, with  $\pm 10\%$  precipitation change resulting in  $\pm 25\text{-}30\%$  change in delta outflow. The response of spring delta outflow (Figure 32b) is similar, with slightly more horizontal contour lines representing a greater sensitivity to temperature change (but still no noticeable response to discrete changes in sea level rise at 1 and 1.5 C). In the case of summer and fall net delta outflow (Figure 32c-d) sea level rise pulls the contours to the left at between 1 and 1.5 C, meaning that net delta outflow is greater with the addition of sea level rise than it would be were sea level held at current levels. Greater precipitation does not appreciably increase net delta outflow in the summer or fall.



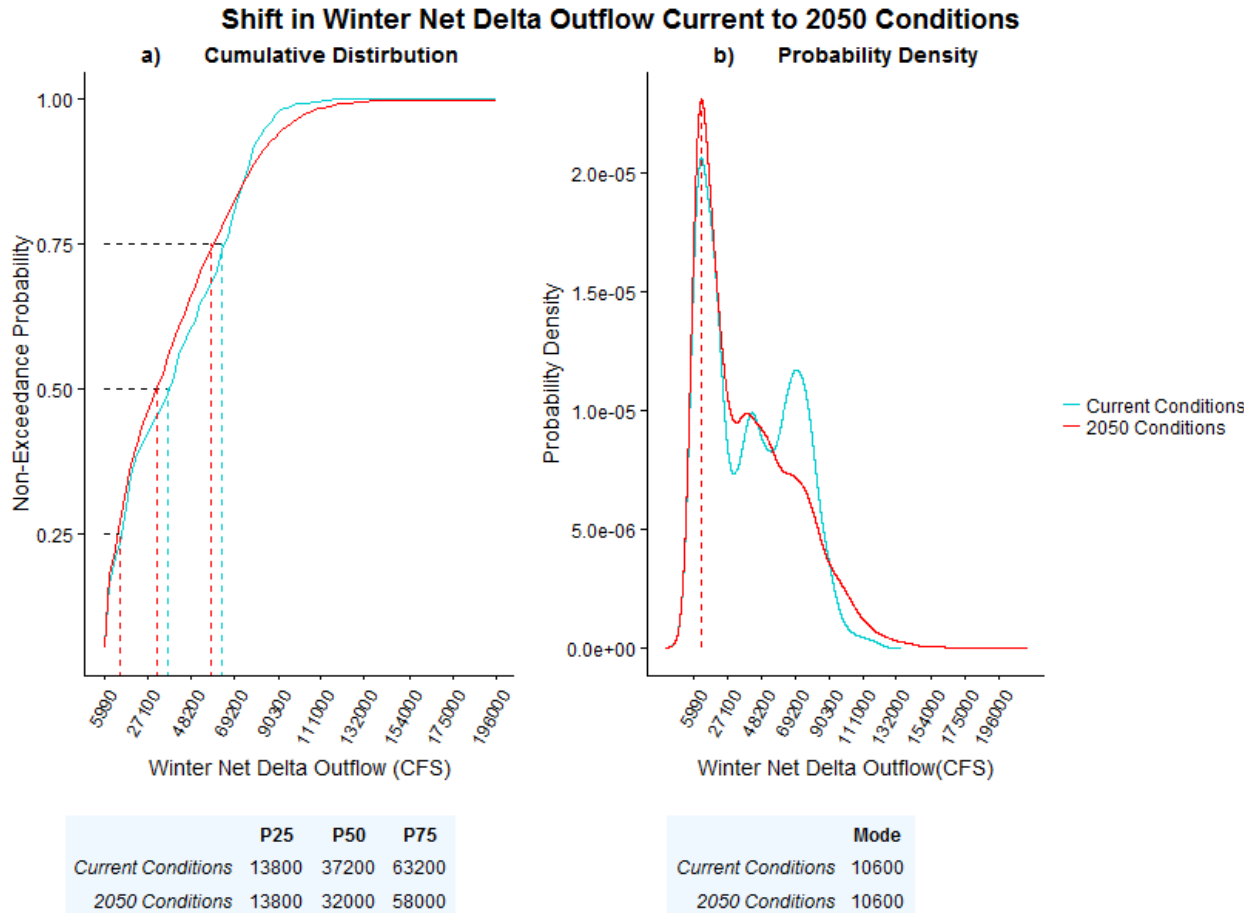
**Figure 32. Response Surfaces –Net Delta Outflow**

With the addition of the GCM “cloud” to the response surfaces for net delta outflow (Figure 33a-d), it becomes apparent that spring (b) and summer (c) net delta outflows are more likely to diminish than are winter (a) net delta outflows, which stand a fair chance of increasing (and maybe substantially). The signal is less clear when it comes to fall (d) net delta outflows, for which the GCMs indicate the reasonable possibility of small increases, or somewhat severe decreases.



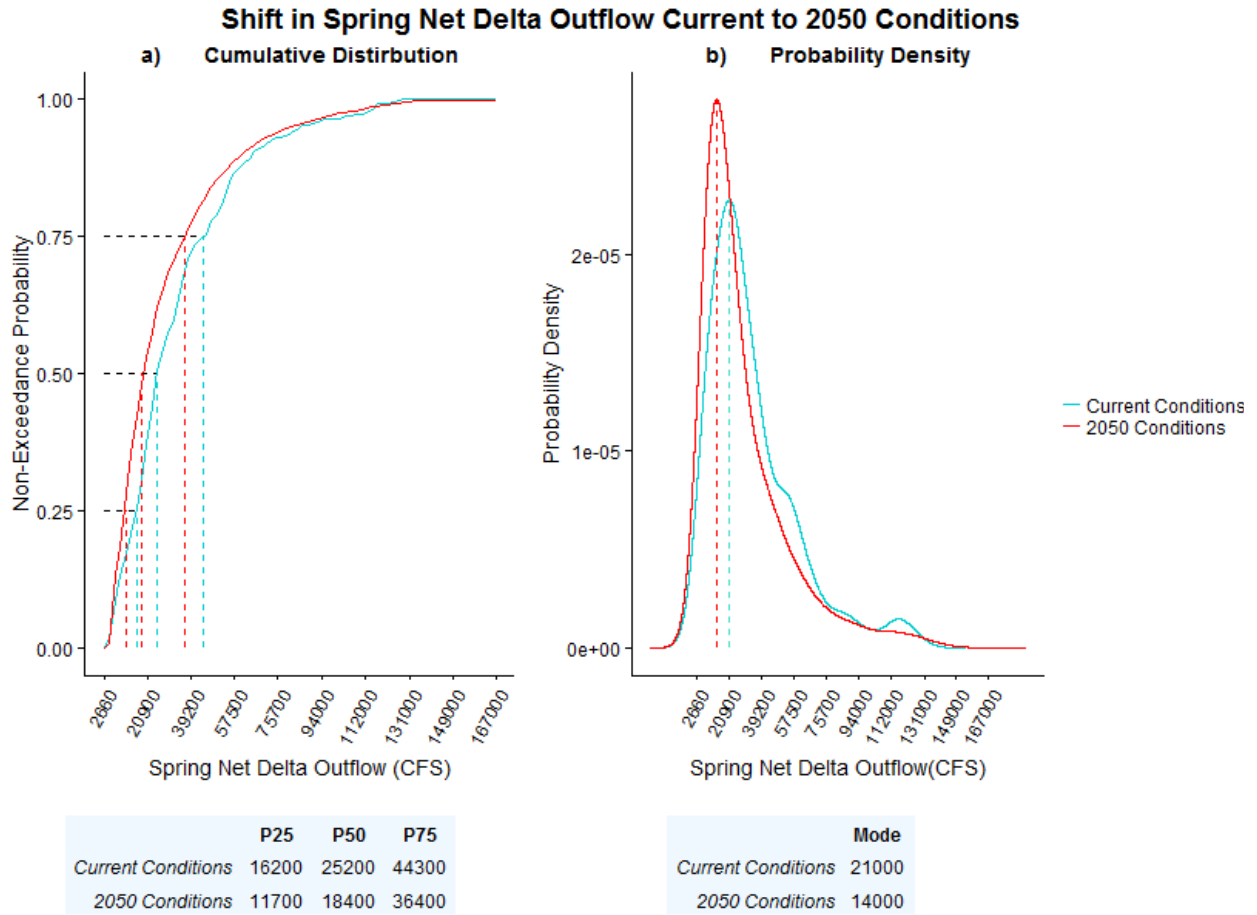
**Figure 33. Response Surfaces –Net Delta Outflow with GCM “cloud”**

Figure 34a presents a cdf for winter net delta outflow. The cdf shows a small (14%) decrease in median delta outflow, a similar decrease at the 75<sup>th</sup> percentile, and no significant change under historically low flow conditions. Of note, evaluation of the ensemble of simulations shows that, at higher flows, year 2050 winter net delta outflow could be higher than historical. Figure 34b shows no significant change in the mode of the pdf, current to future.



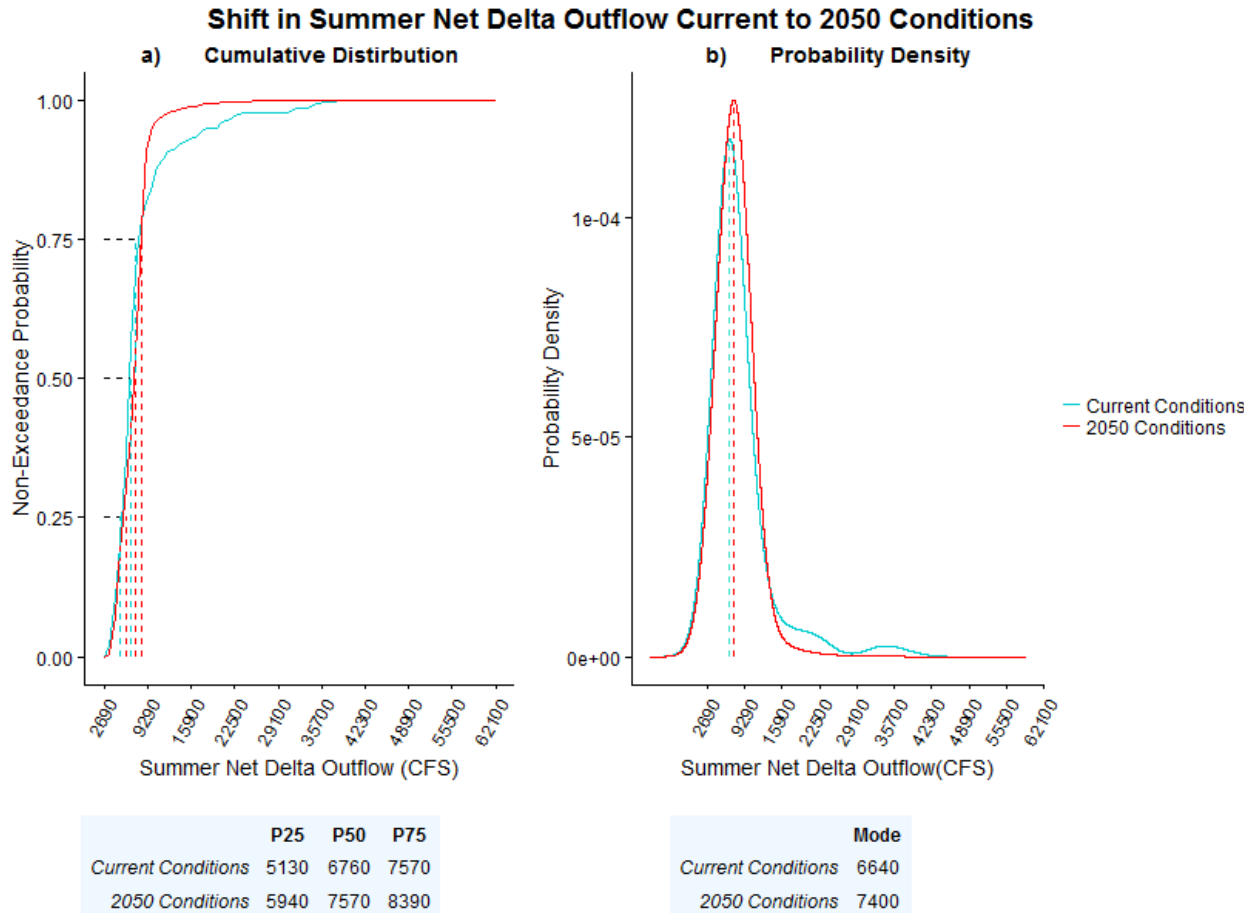
**Figure 34. Shift in Winter Net Delta Outflow, Current to Mid-Century Conditions**

Figure 35a presents a cdf for spring net delta outflow. The cdf shows a decrease in median delta outflow of 25-30%, similar (25-30%) decreases in low flow (25<sup>th</sup> percentile), and relatively smaller decreases (and 15-20%) at high flow (75<sup>th</sup> percentile) conditions. Figure 35b indicates a substantial (30-35%) decrease in the most common (mode of pdf) spring net delta outflows.



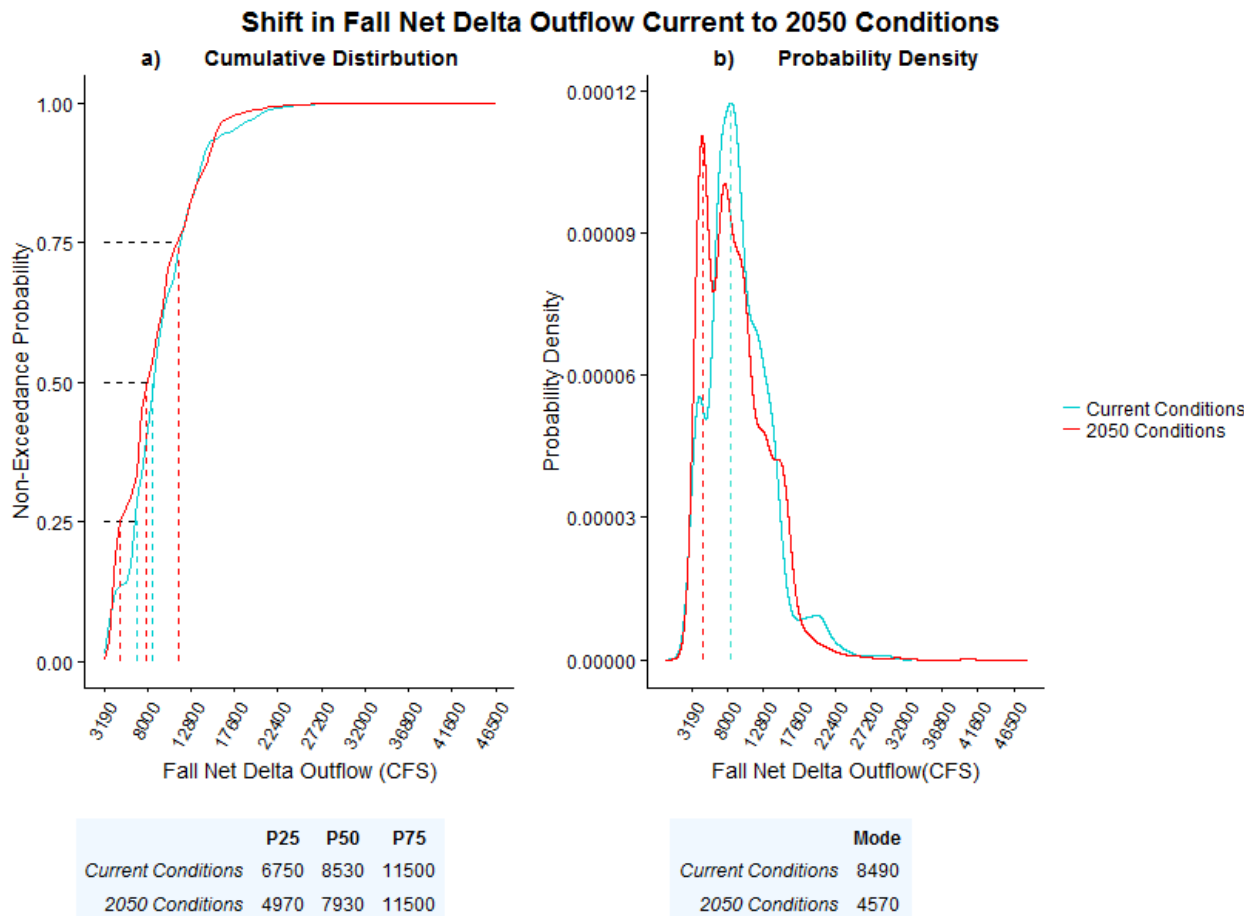
**Figure 35. Shift in Spring Net Delta Outflow, Current to Mid-Century Conditions**

Figure 36 indicates small (10-15%) increase in summer net delta outflow at every percentile (25<sup>th</sup>, 50<sup>th</sup>, 75<sup>th</sup>), and a small (10-13%) increase in the mode of the pdf.



**Figure 36. Shift in Summer Net Delta Outflow, Current to Mid-Century Conditions**

Figure 37a shows small to negligible (<10%) change in fall net delta outflow at middle-high range flows, but potentially large (25-30%) decrease in fall net delta outflow at smaller flow values. The downward shift in the mode of the pdf (Figure 37b) is substantial (45-50%).



**Figure 37. Shift in Fall Net Delta Outflow, Current to Mid-Century Conditions**

### Performance Metric 3: Annual SWP Deliveries

The response surface for average annual SWP deliveries (Figure 38) shows sensitivity to changes in temperature, precipitation, and sea level rise. Sea level rise changes (described in reference to Table 7) are clearly evident in the response surface as inflection points. It should be noted that the values on this response surface are averages across 650 years of simulation at each temperature and precipitation combination; SWP deliveries in any given years within a simulation could be much higher or lower.

At 2.0 degrees C warming, roughly the amount of warming expected for the SWP watershed area by mid-century, and no change in precipitation, average annual SWP deliveries would be expected to be approximately 400,000 AF/year less than historical, which is a nearly 15% decrease relative to current conditions.

The GCM “cloud” superimposed on Figure 38 (right) informs the likelihood of change in SWP deliveries. From the figure it appears much more likely that SWP deliveries will decrease than increase (though an increase is plausible, with more than 10% increase in average annual precipitation), and it is reasonable to expect a substantial decrease in SWP deliveries, were temperature to increase 2 C and precipitation decrease.

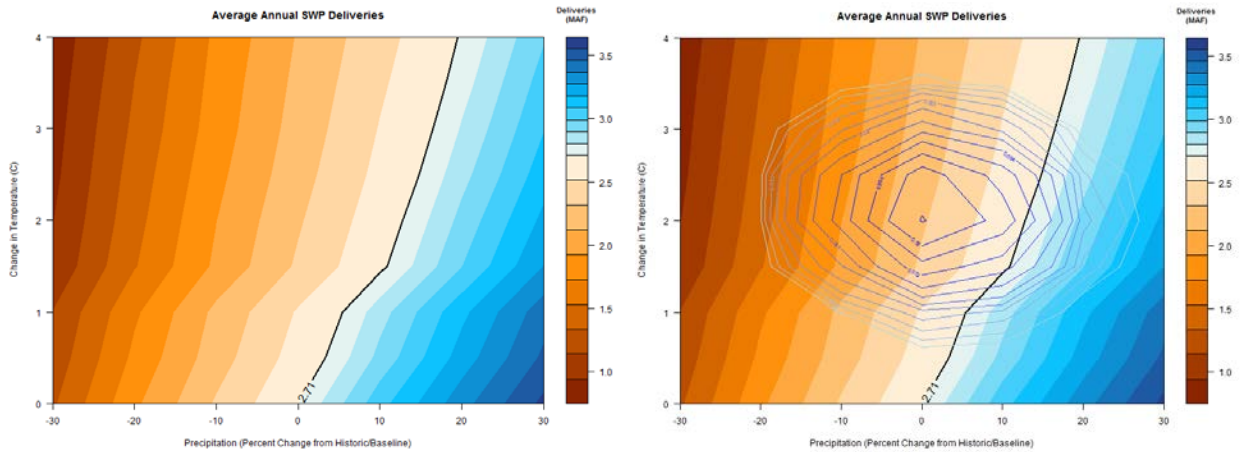


**Figure 38. Response Surface – Annual SWP Deliveries without (left) and with (right) GCM “cloud”**

Figure 39a shows a decrease in median future SWP deliveries of approximately 11% relative to current conditions, with greater (approximately 24%) decreases at low flow conditions and relatively lower (approximately 8%) decreases at high flow conditions. Figure 39b indicates a decrease in the mode of the pdf of SWP deliveries of approximately 10%.

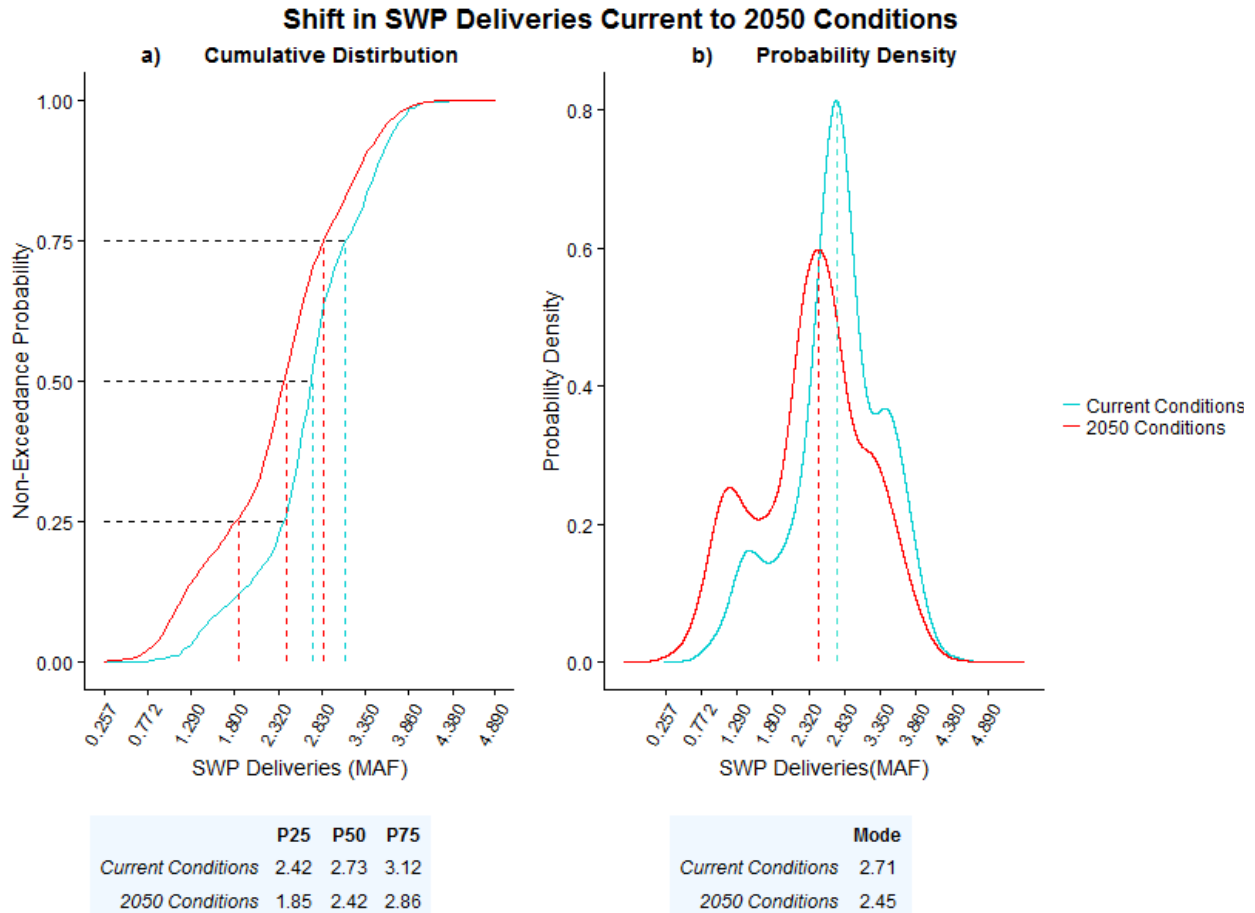


**Figure 39. Shift in SWP Annual Deliveries, Current to Mid-Century Conditions**

### Performance Metric 8: Annual SWP Delivery Shortages

The response surface for Average Annual System Shortages (Figure 40) shows that system shortages have historically been very low, averaging around 2,500 acre-feet per year. As the climate warms, system shortages increase but at a fairly slow rate, even with an increase in temperature of 4 degrees C and a loss of 10 percent of precipitation, average annual system shortages would still be expected to be less than 70 TAF per year. At higher levels of precipitation decline, annual system shortages increase more rapidly, reaching about 400 TAF per year under the most stressful conditions analyzed. The black, historical performance level line in this plot is somewhat irregular, moving diagonally to the right up at an increasing rate up to 1.5 degrees C of warming and then essentially going vertical. This behavior appears to indicate that sea level rise is the dominant factor in driving system shortages. Above 1.5 degrees C no additional sea level rise is added (beyond the 45 cm incurred at 1.5 degrees C) and no additional increase in system shortages occur. The GCM “cloud” superimposed on Figure 40 (right) indicates the likelihood of a small increase in shortages in the future.

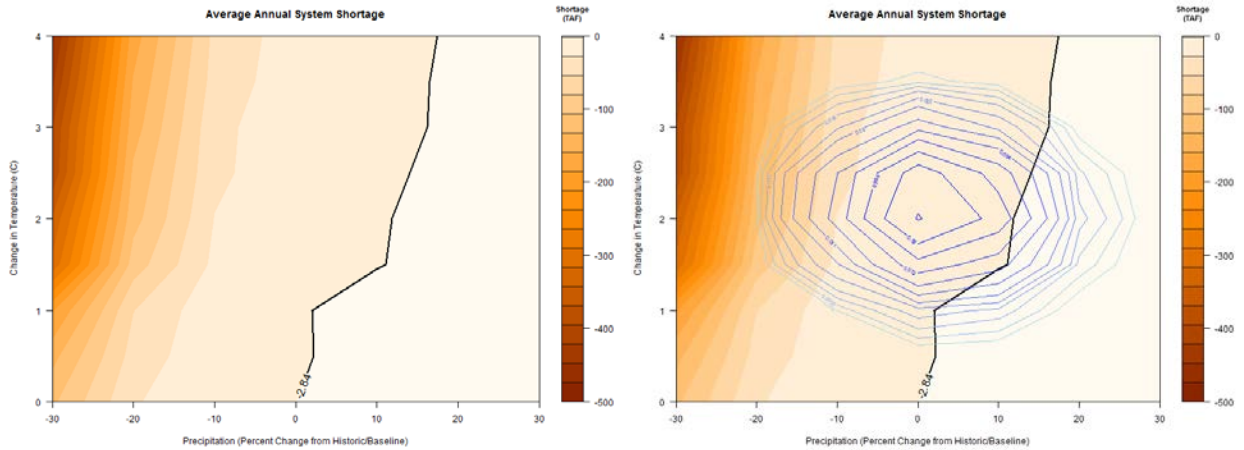
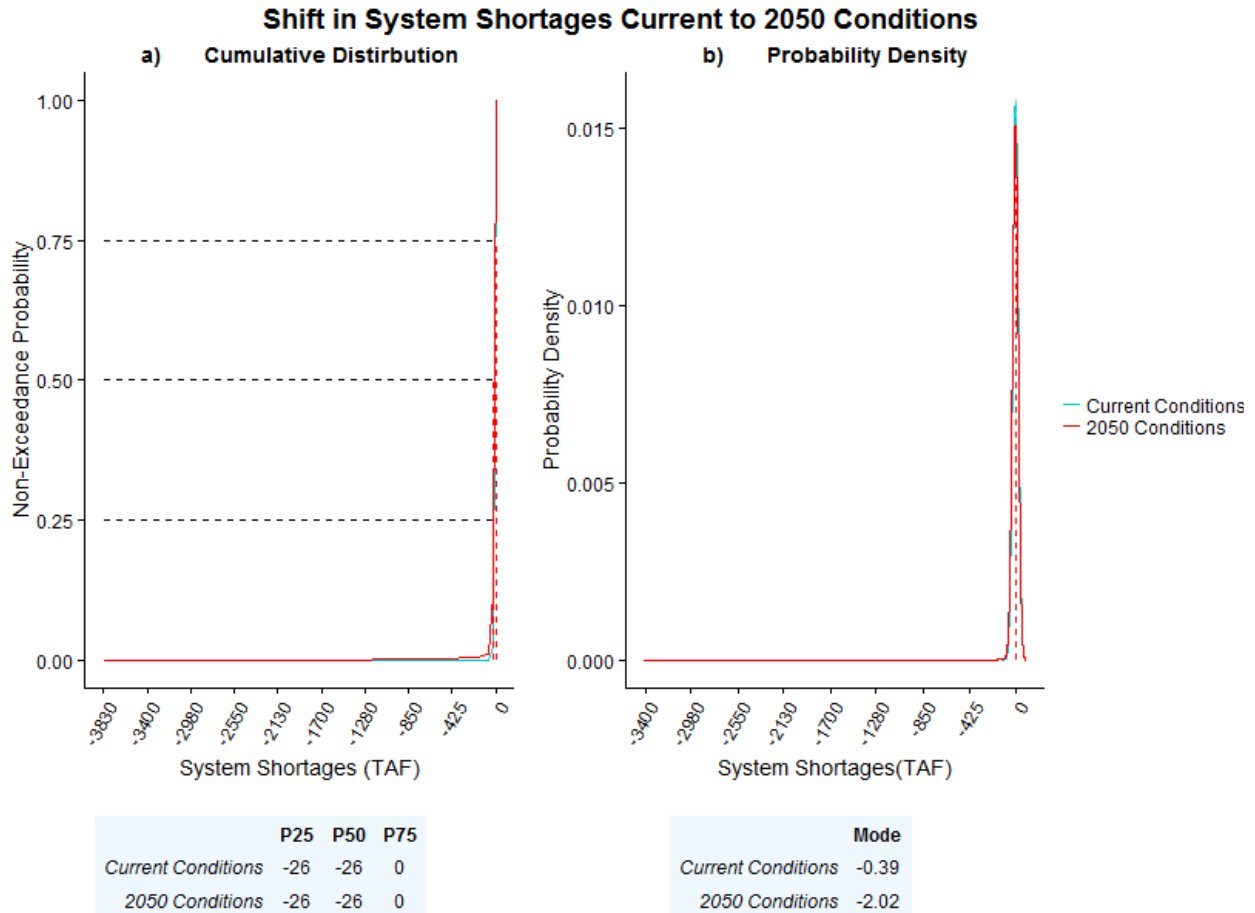


Figure 40. Response Surface – Annual SWP Delivery Shortage without (left) and with (right) GCM “cloud”

Figure 41a shows no meaningful change in shortages at any percentile of water availability (shortages are rare historically and will continue to be rare in the future), though the mode of the pdf (Figure 41b) shifts downward from -0.4 to -2 under future climate conditions, meaning that the average size of shortages (when they occur) will be larger in the future than it has been in the past.



**Figure 41. Shift in Annual SWP Delivery Shortage, Current to Mid-Century Conditions**

## Summary

Despite the wide range of uncertainty, the results of this analysis show the likelihood of a downward shift in DWR system performance by 2050. Only a small portion of the conditional climate probability density for each performance metric indicates improved system performance (performance better than historical). Decreased performance is especially acute for average Oroville September storage, SWP deliveries, and spring net delta outflows, in which substantial downward shifts are identified.

The analysis summarized here suggests that vulnerabilities to the SWP from persistent long-term changes in climate are likely to be significant. However, this approach to system evaluation and vulnerability assessment provides opportunities for improved climate change planning.

Decision scaling allows planners to quantify the risks and costs associated with both the status quo, and those of adaptation strategies. Because of the uncertainty inherent in projections of future climate conditions, planning objectives need to acknowledge and accommodate the unknown. It may not be feasible to plan for every possible climate outcome; however, with quantitative assessments of future risk such as those presented here, quantitative adaptation objectives can be established and evaluated. Climate changes will not stop at mid-century. Indeed, the impacts are expected to become increasingly severe toward the end

of the century. Thus, adaptation objectives and the strategies to achieve those objectives will need to be continually implemented into the future in response to (and ideally in anticipation of) impacts.

At the next stage of this project, refinements will be made to the methodology presented in this Inception Report, and the potential benefit of a sample of proposed DWR climate change adaptation strategies will be systematically evaluated.

## Other Considerations and Next Steps

---

The analysis presented here represents the first step in the use of decision scaling to evaluate climate vulnerabilities to the SWP. Additional analysis will be completed in the coming year to evaluate the changing likelihood of drought conditions, and DWR system vulnerabilities to those conditions. The approach described in this Inception Report will also be used to evaluate a suite of potential adaptation strategies that will be presented in DWR's forthcoming adaptation plan.

### Next Steps:

1. Revise sample strategy to filter for:
  - a.  $\pm 1\%$  historic annual precipitation mean
  - b.  $\pm 5\text{-}10\%$  historic annual precipitation standard deviation
  - c. 90% significance level for 15-year low frequency annual precipitation signal
2. Likely adaptation strategies to be explored:
  - a. 500,000 acre-feet north of delta groundwater storage
  - b. 500,000 acre-feet south of delta groundwater storage
  - c. California Water Fix
  - d. Improved multi-objective upper watershed management
  - e. Potential offstream surface storage
  - f. Improved forecasting skill

## References

---

### REFERENCES

AghaKouchak, A., L. Cheng, O. Mazdiyasni, and A. Farahmand (2014), Global warming and changes in risk of concurrent climate extremes: Insights from the 2014 California drought, *Geophys. Res. Lett.*, *41*, 8847-8852.

Anderson, E. A. (1976), A point energy and mass balance model of a snow cover, *NOAA Tech. Rep. NSW 19, Natl. Oceanic and Atmos. Admin., Silver Spring, MD.*, 1-150.

Bay-Delta Office (2007), California Central Valley Unimpaired Flow Data: 4th edition, *California Department of Water Resources*, 1-53.

Brown, C. and R. L. Wilby (2012), An alternate approach to assessing climate risks, *EOS, Transactions, American Geophysical Union*, *92*, 401-412.

Brown, C. M., J. R. Lund, X. Cai, P. M. Reed, E. A. Zagona, A. Ostfeld, J. Hall, G. W. Characklis, W. Yu, and L. Brekke (2015), The future of water resources systems analysis: Toward a scientific framework for sustainable water management, *Water Resour. Res.*, *51*, 6110-6124.

Brown, C., Y. Ghile, M. Laverty, and K. Li (2012), Decision scaling: Linking bottom-up vulnerability analysis with climate projections in the water sector, *Water Resour. Res.*, *48*, W09537.

California Department of Fish and Wildlife (2014), CDFW moves to prevent fish loss, evacuates fish at American River and Nimbus Hatcheries, *California Department of Fish and Wildlife*, 16 June, hatcheries.

California Department of Water Resources (2013), California Water Plan 2013: Investing in Innovation and Infrastructure, *Bulletin 160-13, 3 - Resource Management Strategies*, 1-858.

California Department of Water Resources (2015a), California Climate Science and Data for Water Resources Management, *California Climate Science and Data*, June 2015, 1-28.

California Department of Water Resources (2015b), California's most significant droughts: comparing historical and recent conditions, *California Department of Water Resources*.

California Department of Water Resources and United States Bureau of Reclamation (2011), *CalLite: Central Valley Water Management Screening Model (Version 2.0) Reference Manual*, vol. October 2011, 161 pp., California Department of Water Resources, Sacramento, California.

Cayan, D. R., T. Das, D. W. Pierce, T. P. Barnett, M. Tyree, and A. Gershunov (2010), Future Dryness in the Southwest US and the Hydrology of the Early 21st Century Drought, *Proceedings of the National Academy of Sciences of the United States of America*, *107*, 21271-21276.

Cayan, D. et al. (2013), Future climate: Projected average, in *Assessment of Climate Change in the Southwest United States: A Report Prepared for the National Climate Assessment.*, A report by the Southwest Climate Alliance. edn., edited by G. Garfin, A. Jardine, R. Merideth, M. Black, and S. LeRoy, pp. 101-125, Island Press, Washington, D.C., USA.

- Charnes, A. and W. W. Cooper (1961), *Management Models and Industrial Applications of Linear Programming*, Wiley, New York.
- Connell-Buck, C. R., J. Medellin-Azuara, J. R. Lund, and K. Madani (2011), Adapting California's water system to warm vs. dry climates, *Clim. Change*, *109*, 133-149.
- Das, T., M. D. Dettinger, D. R. Cayan, and H. G. Hidalgo (2011), Potential increase in floods in California's Sierra Nevada under future climate projections, *Clim. Change*, *109*, 71-94.
- Department of Water Resources (2014a), Water year 2014 ends as 3rd driest in precipitation, *California Department of Water Resources*, Available at <http://www.water.ca.gov/waterconditions/>.
- Department of Water Resources (2014b), Year's final snow survey comes up dry, *California Department of Water Resources*, 1 May, Available at <http://www.water.ca.gov/news/newsreleases/2014/050114.pdf>.
- Dettinger, M. D. and M. L. Anderson (2015), Storage in California's Reservoirs and Snowpack in this Time of Drought, *San Francisco Estuary and Watershed Science*, *13*, 1-5.
- Dettinger, M. D. and D. R. Cayan (2014), Drought and the California Delta - A Matter of Extremes, *San Francisco Estuary and Watershed Science*, *12*, 1-6.
- Dettinger, M. D. (2013), Atmospheric Rivers as Drought Busters on the US West Coast, *J. Hydrometeorol.*, *14*, 1721-1732.
- Dettinger, M. D., F. M. Ralph, T. Das, P. J. Neiman, and D. R. Cayan (2011), Atmospheric Rivers, Floods and the Water Resources of California, *Water*, *3*, 445-478.
- Diffenbaugh, N. S. and M. Ashfaq (2010), Intensification of hot extremes in the United States, *Geophys. Res. Lett.*, *37*, L15701.
- Diffenbaugh, N. S., D. L. Swain, and D. Touma (2015), Anthropogenic warming has increased drought risk in California, *Proc. Natl. Acad. Sci. U. S. A.*, *112*, 3931-3936.
- Draper, A. J., A. Munevar, S. K. Arora, E. Reyes, N. L. Parker, F. I. Chung, and L. E. Peterson (2004), CalSim: Generalized model for reservoir system analysis, *Journal of Water Resources Planning and Management-Asce*, *130*, 480-489.
- Forsythe, W. C., E. J. Rykiel Jr., R. S. Stahl, H. Wu, and R. M. Schoolfield (1995), A model comparison for daylength as a function of latitude and day of year, *Ecol. Model.*, *80*, 87-95.
- Gleick, P. H. (1987), The Development and Testing of a Water-Balance Model for Climate Impact Assessment - Modeling the Sacramento Basin, *Water Resour. Res.*, *23*, 1049-1061.
- Griffin, D. and K. J. Anchukaitis (2014), How unusual is the 2012-2014 California drought?, *Geophys. Res. Lett.*, *41*, 9017-9023.
- Groves, D. G. and E. Bloom (2013), Robust Water-Management Strategies for the California: Water Plan Update 2013 Proof-of-Concept Analysis, *RAND Corporation, California Water Plan Update 2013*, 1-72.

- Hamon, W. R. (1961), Estimating potential evapotranspiration, *J. Hydr. Eng. Div. -ASCE*, 87, 107-120.
- Harou, J. J., J. Medellin-Azuara, T. Zhu, S. K. Tanaka, J. R. Lund, S. Stine, M. A. Olivares, and M. W. Jenkins (2010), Economic consequences of optimized water management for a prolonged, severe drought in California, *Water Resour. Res.*, 46, W05522.
- Heim, R. R. (2002), A review of twentieth-century drought indices used in the United States, *Bull. Am. Meteorol. Soc.*, 83, 1149-1165.
- Higgins, R. W., V. B. S. Silva, W. Shi, and J. Larson (2007), Relationships between climate variability and fluctuations in daily precipitation over the United States, *J. Clim.*, 20, 3561-3579.
- Hirsch, R. M. (2011), A Perspective on Nonstationarity and Water Management, *J. Am. Water Resour. Assoc.*, 47, 436-446.
- Howitt, R. E., D. MacEwan, J. Medellin-Azuara, J. R. Lund, and D. A. Sumner (2015), Economic Analysis of the 2015 Drought for California Agriculture, *Center for Watershed Sciences, University of California – Davis, Davis, CA*, 1-16.
- Howitt, R. E., J. Medellin-Azuara, D. MacEwan, J. R. Lund, and D. A. Sumner (2014), Economic Analysis of the 2014 Drought for California Agriculture, *Center for Watershed Sciences, University of California – Davis, Davis, CA*, 1-16.
- IPCC (2012), *Managing the Risks of Extreme Events and Disasters to Advance Climate Change Adaptation: A Special Report of Working Groups I and II of the Intergovernmental Panel on Climate Change - Summary for Policymakers*, 1-19 pp., Cambridge University Press, Cambridge, UK, and New York, NY, USA.
- IPCC (2014), *Climate Change 2013 : The Physical Science Basis : Working Group I Contribution to the Fifth Assessment Report of the Intergovernmental Panel on Climate Change*, 1-1535 pp., Cambridge University Press, New York.
- Islam, N. et al. (2014), Central Valley Water Management Screening Model for Water Management Alternatives, International Environmental Modelling and Software Society (iEMSs) 7th Intl. Congress on Env. Modelling and Software, June 15-19.
- Joyce, B., D. Purkey, D. Yates, D. Groves, and A. Draper (2010), Integrated scenario analysis for the 2009 California water plan update, Vol. 4, , *California Dept. of Water Resources, Vol. 4*.
- Killam, D., A. Bui, S. LaDochy, P. Ramirez, J. Willis, and W. C. Patzert (2014), California Getting Wetter to the North, Drier to the South: Natural Variability or Climate Change?, *Climate*, 2, 168-180.
- Kopp, R. E., A. C. Kemp, K. Bittermann, B. P. Horton, J. P. Donnelly, W. R. Gehrels, C. C. Hay, J. X. Mitrovica, E. D. Morrow, and S. Rahmstorf (2016), Temperature-driven global sea-level variability in the Common Era, *Proc. Natl. Acad. Sci. U. S. A.*, 113, E1441.
- LaDochy, S., P. Ramirez, D. Killam, A. Bui, W. C. Patzert, and J. Willis (2011), California temperature and precipitation trends: climate variability or global warming, 91st Meeting of the American Meteorology Society 2011, Seattle, Washington, January 22-27.

Lempert, R. J., D. G. Groves, S. W. Popper, and S. C. Bankes (2006), A general, analytic method for generating robust strategies and narrative scenarios, *Management Science*, 52, 514-528.

Livneh, B., E. A. Rosenberg, C. Lin, B. Nijssen, V. Mishra, K. M. Andreadis, E. P. Maurer, and D. P. Lettenmaier (2013), A Long-Term Hydrologically Based Dataset of Land Surface Fluxes and States for the Conterminous United States: Update and Extensions, *J. Clim.*, 26, 9384-9392.

Lohmann, D., R. Raschke, B. Nijssen, and D. P. Lettenmaier (1998), Regional scale hydrology: I. Formulation of the VIC-2L model coupled to a routing model, *Hydrolog. Sci. J.*, 43, 131-141.

Lund, J. R., E. Hanak, W. E. Fleenor, W. A. Bennett, R. E. Howitt, J. F. Mount, and P. B. Moyle (2010), *Comparing Futures for the Sacramento-San Joaquin Delta*, Freshwater Ecology Series, vol. 3, 232 pp., Univ California Press, Berkeley; 2120 Berkeley Way, Berkeley, CA 94720 USA.

Mao, Y., B. Nijssen, and D. P. Lettenmaier (2015), Is climate change implicated in the 2013-2014 California drought? A hydrologic perspective, *Geophys. Res. Lett.*, 42, 2805-2813.

Margulis, S. A., G. Cortes, M. Girotto, L. S. Huning, D. Li, and M. Durand (2016), Characterizing the extreme 2015 snowpack deficit in the Sierra Nevada (USA) and the implications for drought recovery, *Geophys. Res. Lett.*, 43, 6341-6349.

Maurer, E. P., A. W. Wood, J. C. Adam, D. P. Lettenmaier, and B. Nijssen (2002), A long-term hydrologically based dataset of land surface fluxes and states for the conterminous United States, *J. Clim.*, 15, 3237-3251.

McEnery, J., J. Ingram, Q. Duan, T. Adams, and L. Anderson (2005), NOAA'S Advanced Hydrologic Prediction Service – Building pathways for Better Science in Water Forecasting, *Bulletin of the American Meteorological Society*, March, 375-385.

Meko, D. M., C. A. Woodhouse, and R. Touchan (2014), Klamath/San Joaquin/Sacramento Hydroclimatic Reconstructions from Tree Rings, *Draft Final Report to California Department of Water Resources, Agreement 4600008850*.

Moriasi, D. N., J. G. Arnold, M. W. Van Liew, R. L. Bingner, R. D. Harmel, and T. L. Veith (2007), Model evaluation guidelines for systematic quantification of accuracy in watershed simulations, *Trans. ASABE*, 50, 885-900.

Mote, P. W., A. F. Hamlet, M. P. Clark, and D. P. Lettenmaier (2005), Declining mountain snowpack in western north America, *Bull. Am. Meteorol. Soc.*, 86, 39-49.

Mount, J. and R. Twiss (2005), Subsidence, sea level rise, and seismicity in the Sacramento-SanJoaquin Delta, *San Francisco Estuary and Watershed Science*, 3.

Nash, J. E. (1957), The form of the instantaneous unit hydrograph, *International Association of Science and Hydrology*, 3, 114-121.

National Research Council (2012), Sea-Level Rise for the Coasts of California, Oregon, and Washington: Past, Present, and Future, 1-217.

NOAA (2014), California Drought: 2014 Service Assessment, *U. S. Department of Commerce and National Oceanic and Atmospheric Administration*, 1-72.

NOAA (2016), Mean Sea Level Trend 9414290 San Francisco, California, *NOAA Tides and Currents*, [https://tidesandcurrents.noaa.gov/sltrends/sltrends\\_station.shtml?stnid=9414290](https://tidesandcurrents.noaa.gov/sltrends/sltrends_station.shtml?stnid=9414290).

Null, S. E. and J. R. Lund (2006), Re-Assembling Hetch Hetchy: Water Supply Implications of Removing O'Shaughnessy Dam, *Journal of the American Water Resources Association*, 42, 395-408.

Null, S. E., J. Medellin-Azuara, A. Escrivá-Bou, M. Lent, and J. R. Lund (2014), Optimizing the dammed: Water supply losses and fish habitat gains from dam removal in California, *J. Environ. Manage.*, 136, 121-131.

Null, S. E. and J. H. Viers (2013), In bad waters: Water year classification in nonstationary climates, *Water Resour. Res.*, 49, 1137-1148.

Olivares, M. A., J. Haas, R. Palma-Behnke, and C. Benavides (2015), A framework to identify Pareto-efficient subdaily environmental flow constraints on hydropower reservoirs using a grid-wide power dispatch model, *Water Resour. Res.*, 51, 3664-3680.

Pavia, E. G., F. Graef, and R. Fuentes-Franco (2016), Recent ENSO-PDO precipitation relationships in the Mediterranean California border region, *Atmos. Sci. Lett.*, 17, 280-285.

Quiring, S. M. (2009), Developing Objective Operational Definitions for Monitoring Drought, *J. Appl. Meteorol. Climatol.*, 48, 1217-1229.

Rheinheimer, D. E., S. E. Null, and J. R. Lund (2015), Optimizing Selective Withdrawal from Reservoirs to Manage Downstream Temperatures with Climate Warming, *J. Water Resour. Plann. Manage.*, 141, 04014063.

Richter, B. D., J. V. Baumgartner, R. Wigington, and D. P. Braun (1997), How much water does a river need?, *Freshwat. Biol.*, 37, 231-249.

Schneider, U., A. Becker, P. Finger, A. Meyer-Christoffer, M. Ziese, and B. Rudolf (2014), GPCP's new land surface precipitation climatology based on quality-controlled in situ data and its role in quantifying the global water cycle, *Theor. Appl. Climatol.*, 115, 15-40.

Seager, R., M. Hoerling, S. Schubert, H. Wang, B. Lyon, A. Kumar, J. Nakamura, and N. Henderson (2015), Causes of the 2011-14 California Drought\*, *J. Clim.*, 28, 6997-7024.

Steinschneider, S. and C. Brown (2013), A semiparametric multivariate, multisite weather generator with low-frequency variability for use in climate risk assessments, *Water Resour. Res.*, 49, 7205-7220.

Swain, D. L. (2015), A tale of two California droughts: Lessons amidst record warmth and dryness in a region of complex physical and human geography, *Geophysical Research Letters*, 42, 9999-10003.

Swain, D. L., M. Tsiang, M. Haugen, D. Singh, A. Charland, B. Rajaratnam, and N. S. Diffenbaugh (2014), The Extraordinary California Drought of 2013/2014: Character, Context, and the Role of Climate Change, *Bull. Am. Meteorol. Soc.*, 95, S7.

- Swetnam, T. W. and J. L. Betancourt (1998), Mesoscale disturbance and ecological response to decadal climatic variability in the American Southwest, *J. Clim.*, *11*, 3128-3147.
- Tanaka, S. K., C. Buck, K. Madani, J. Medellin-Azuara, J. Lund, and E. Hanak (2011), Economic Costs and Adaptations for Alternative Regulations of California's Sacramento-San Joaquin Delta, *San Francisco Estuary and Watershed Science*, *9*, 28.
- U.S. Department of Agriculture (2014), California drought 2014: Farm and food impacts, *United States Department of Agriculture*, impacts.aspx.
- U.S. Geological Survey (2014), California Water Science Center, Available at <http://ca.water.usgs.gov/data/drought/surfacewater.html>.
- United States Drought Monitor (2014), California drought intensifies and U.S. drought spreads, *United States Drought Monitor*, *6 Feb*, Available at <http://droughtmonitor.unl.edu/USDMNews/NewsArchive.aspx>.
- Wang, H. and S. Schubert (2014), Causes of the Extreme Dry Conditions Over California during Early 2013, *Bull. Am. Meteorol. Soc.*, *95*, S11.
- Whateley, S., S. Steinschneider, and C. Brown (2016), Selecting stochastic climate realizations to efficiently explore a wide range of climate risk to water resources systems, *Journal of Water Resources Planning and Management*, *submitted*.
- Wilby, R. L. and S. Dessai (2010), Robust adaptation to climate change, *Weather*, *65*, 180-185.
- Williams, A. P., R. Seager, J. T. Abatzoglou, B. I. Cook, J. E. Smerdon, and E. R. Cook (2015), Contribution of anthropogenic warming to California drought during 2012-2014, *Geophys. Res. Lett.*, *42*, 6819-6828.
- Willis, A. D., J. R. Lund, E. S. Townsley, and B. Faber (2011), Climate Change and Flood Operations in the Sacramento Basin, California, *San Francisco Estuary and Watershed Science*, *9*, 18.
- Yoon, J., S. S. Wang, R. R. Gillies, B. Kravitz, L. Hipps, and P. J. Rasch (2015), Increasing water cycle extremes in California and in relation to ENSO cycle under global warming, *Nat. Commun.*, *6*, 8657.

## Appendix

This supplemental section presents figures describing in-process analysis of the effect of the inclusion of the 15-year wavelet signal in the weather generator resampling process. Figure 42 shows that weather generator traces that included the wavelet signal (purple) more closely followed the historical (CalLite source streamflow, 1922-2003) at moderately high flows, but that the weather generator traces without the wavelet signal (salmon) better matched the historical at moderately low flows. Observed historical streamflow, and both types of weather generator traces (which were conditioned on the observed record) underestimated low flows and overestimated high flows relative to the long-term paleo record.

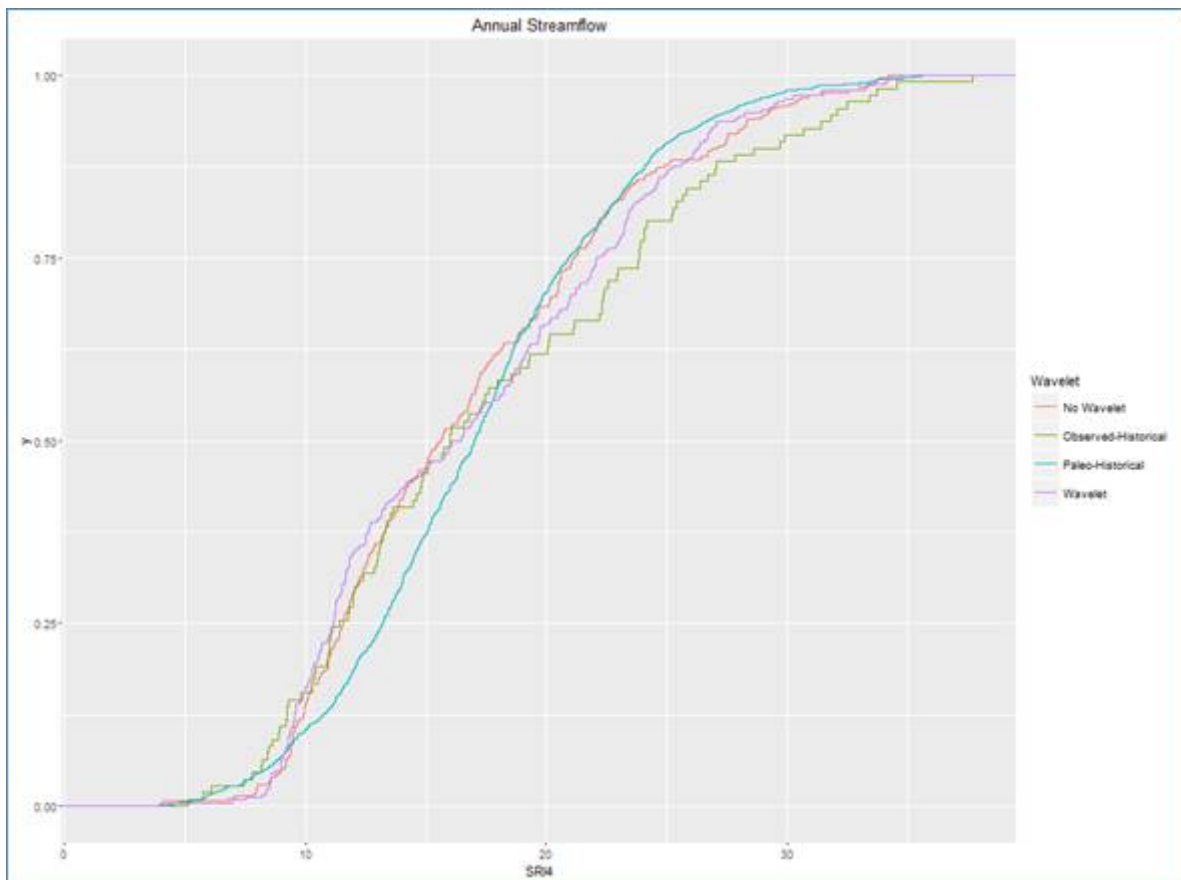


**Figure 42. CDF of annual streamflow of a subsample of wavelet (WARM) and non-wavelet (ARMA) weather-generated traces (no temp/precip change) relative to observed historical and paleo record cdfs**

Figure 43 reproduces Figure 42 but combines the weather generator traces with and without the 15 year signal into a single trace called “simulated” (blue). The combined trace follows very closely on the observed historical at low flow values, and splits the difference between the observed historical and paleo historical data at higher flows. Figure 43 argues for a redesigned sampling strategy that draws weather generator traces from both wavelet (WARM) and non-wavelet (ARMA) sampling algorithms.

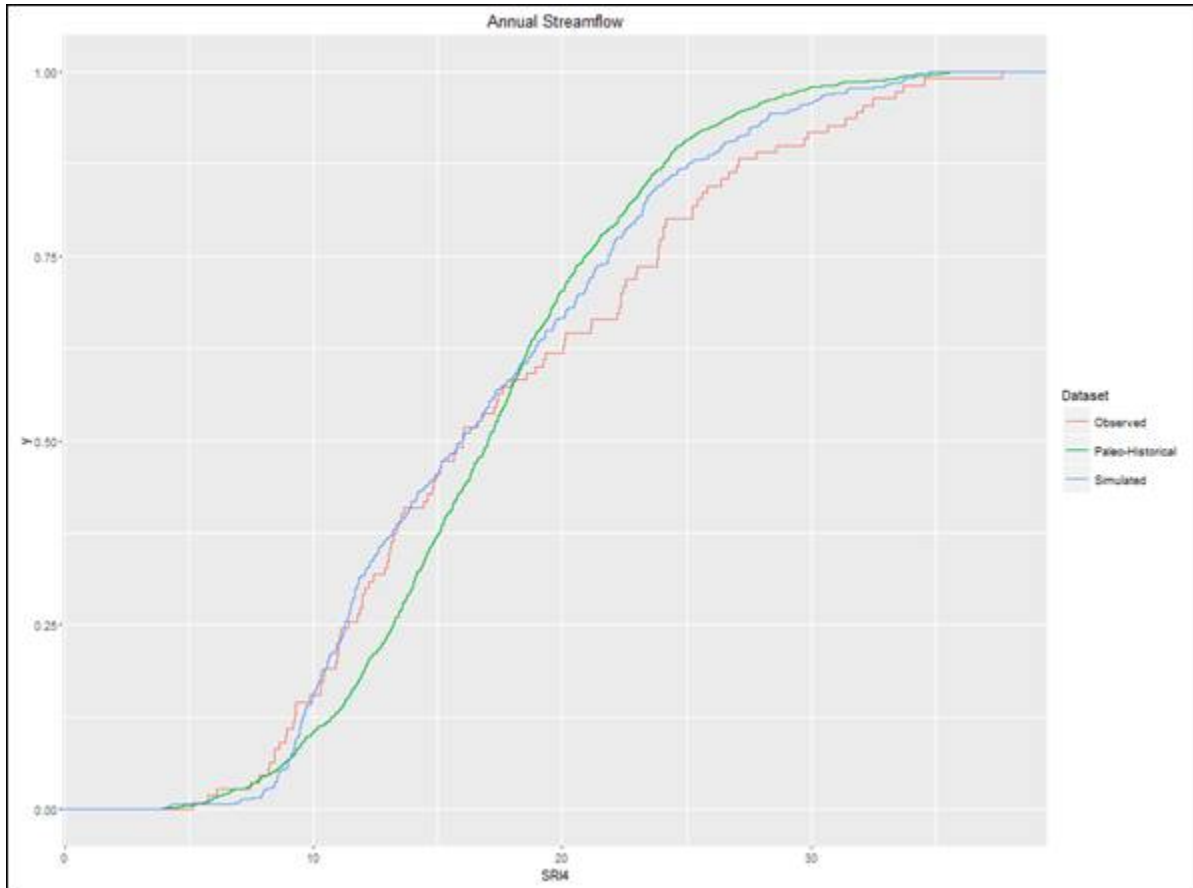


Figure 43. CDF of annual streamflow of a subsample of all weather-generated traces (no temp/precip change) relative to observed historical and paleo record cdfs